Spring 5-7-2016

Expression and Function of Inflammation-Associated MicroRNAs in Traumatic Brain Injury

Emily Harrison
University of Nebraska Medical Center

EXPRESSION AND FUNCTION OF INFLAMMATION-ASSOCIATED MICRORNAS IN TRAUMATIC BRAIN INJURY

BY

Emily Brooke Harrison

A DISSERTATION

Presented to the Faculty of
The Nebraska Graduate College
In Partial Fulfillment of the Requirements
For the Degree of Doctor of Philosophy

Pharmacology and Experimental Neuroscience
Graduate Program

Under the Supervision of Professor Howard S. Fox

University of Nebraska Medical Center

Omaha, NE

April, 2016

Supervisory Committee

Shilpa Buch, Ph.D.

Larisa Poluektova, M.D., Ph.D.

Kai Fu, M.D., Ph.D.

Tammy Kielian, Ph.D.

Acknowledgements

There are more people who have contributed to this work and my training than can be thanked on these pages. First and foremost I would like to thank my mentor Dr. Howard Fox, who has taught me how to think critically and creatively. He has afforded me the independence to make mistakes and learn from them, which has given me the confidence to pursue my own ideas and interests. You are not only an example of the type of scientist, but also the type of leader that I hope to become.

I have great admiration for my committee members who have each contributed important ideas to my understanding of biology and given me valuable career advice. Thank you to Dr. Shilpa Buch for her thoughts on the roles of microRNAs in the brain, Dr. Tammy Kielian for her understanding of the CNS immune system, Dr. Kai Fu for his views on microRNAs from an oncology perspective, and Dr. Larisa Poluektova for her expertise on animal models of CNS disease. The projects described here are clearly influenced by their suggestions and input.

Aside from my mentor and committee members, several other faculty members have been part of my graduate training as mentors and collaborators. I thank Dr. Sowmya Yelamanchili for pioneering studies of microRNAs and extracellular vesicles in our laboratory. I also greatly appreciate the personal mentoring and training she has given me. I am grateful for the opportunity to work in the field of TBI, which would not have been possible without the collaboration and training of Dr. Matthew Kelso. The electrophysiology reported was performed in the laboratory of Dr. Huangui Xiong under the guidance of Guihua Tu and Dr. Jingdong Zhang. Dr. Stephen Bonasera, Dr. Jeffrey French, and Dr. Michael Boska have been critical for work described here and ongoing projects designed to understand the chronic changes to the brain in the aftermath of traumatic brain injury. I also thank Dr. French for his ongoing mentorship and for inspiring me to pursue research as an undergraduate. Additionally, thank you to Dr. Myron Toews for helping me hone my writing and presentation skills and for having confidence in me

from the beginning of my research career. I have overwhelming gratitude for the scientific community in Nebraska for nurturing my growth as a scientist, in particular the University of Nebraska-Omaha (UNO) biology department for their encouragement of undergraduate research and the Institutional Development Award Program (IDeA) Networks of Biomedical Research Excellence (INBRE) program for their support of fledgling scientists.

The work presented in this dissertation was made possible by several members of the Fox laboratory. I would like to especially thank Kathleen Emanuel, Benjamin Lamberty, and Brenda Morsey for their assistance, training, and friendship. All three of you have spent countless hours in tissue culture hoods, microscope rooms, and at the bench with me since 2009, when I first interned in the Fox laboratory. Thank you for your patience and your sense of humor. I thank Shannon Callen for teaching me many valuable skills and for helping me to navigate the regulatory aspects of animal studies. Sorry for the incessant questions, Shannon. I have also been lucky to work with several talented rotating students, undergraduate students, and even high-school students. Thank you, Sukarn Chokkara, Colleen Hoschfelder, Lara Bergdolt, Mary Banoub, Makenzie Bates, and Megan Bosch. Your contributions are greatly appreciated. I am grateful to lab members Dr. Phillip Purnell, Dr. Amrita Datta Chaudhuri, Dr. Lance Villeneuve, and Dr. Kelly Stauch for their advice on matters of science and graduate school. Also, more importantly, I thank them for their friendship and camaraderie.

I thank my friends and family for their continuous love and support. My fiancée, Christopher Rabiola has stood by me every day for the last 10 years and is on the hook for many more to come. It is a rare and valuable thing for someone to push you to be a better and stronger person. Thank you for being my coach, my comedic relief, and the love of my life. I thank my father, Richard Harrison, for instilling in me a love of knowledge, discussion, and creativity. To my mother, Susan Harrison, thank you for teaching me about responsibility, community, and respect. I would also like to thank my siblings, Rebecca Van Ornam and Connor Harrison, for their support and interest in my career.

Finally, I would like to memorialize my grandmother, Norma Jean Harrison. My grandmother was an intelligent and outspoken woman who will always be one of my role models. Norma suffered from an undiagnosed neurodegenerative disease that caused her mental decline and likely contributed to her death in 2008. At the time of her illness I was a pre-medical student hoping to become a physician. Given my interest in the medical profession, my grandfather, Floyd Harrison, encouraged me to meet with her physicians and neurologists throughout the course of her disease. This experience had a profound impact on me and gave me a deep appreciation for the mysteries of the brain and neurological disease. I also realized the urgent need for therapies to treat these devastating conditions. My motivation to pursue a career in science and to study the brain stemmed from that realization. Therefore, I would like to dedicate my dissertation to my grandmother, Norma Jean Harrison (1938-2008), who is missed dearly.

EXPRESSION AND FUNCTION OF INFLAMMATION-ASSOCIATED MICRORNAS IN TRAUMATIC BRAIN INJURY

Emily Brooke Harrison, Ph.D.

University of Nebraska, 2016

Advisor: Dr. Howard S. Fox., M.D., Ph.D.

MicroRNAs (miRNAs) are important regulators of gene expression. Many neurological diseases, including traumatic brain injury alter expression of miRNAs in the brain. However, the function of these molecules in the context of TBI is largely unknown. Here we report multiple potential roles for miRNAs in TBI, some of which extend beyond the traditional model of post-transcriptional regulation, highlighting that these RNA molecules may have broader implications for the neurobiology of disease. We found that miR-155 plays an essential role in interferon expression after CCI and that miR-155 contributes to TBI induced anxiety, potentially through regulation of interferons. Expression of miR-155 was identified in neuronal nuclei, suggesting additional roles for miR-155 in the neuronal response to injury that may be outside of traditional gene silencing. Similarly, we found that miR-21 was also expressed in neurons. In addition, miR-21 levels were elevated in extracellular vesicles (EVs). Novel roles have recently been elucidated for miRNAs carried in EVs, including stimulation of toll-like receptor 7/8 (TLR 7/8). We identified 3 differentially expressed EV-associated miRNAs with motifs known to mediate TLR 7/8 binding. This suggests that EV-associated miRNAs may act as damage associated molecular patterns (DAMPs) in TBI. Overall, we have identified multiple potential roles for miRNA in TBI that warrant further study.

In other studies we found that neurotrophic cytokines IL-6 and CNTF could elicit both Stat3 phosphorylation and miR-21 induction in human neurons, providing a possible mechanism for miR-21 induction in many models of neuronal injury. Additionally, we identified disinhibition and hyperactivity as chronic phenotypes of a mouse model of TBI. This finding will allow for future mechanistic studies of TBI induced impulsivity.

Table of Contents

List of Figures and Tables

Figures

Chapter 1: Introduction

Chapter 3: Expression of inflammation-associated miRNA in a controlled cortical impact (CCI) model of TBI

Chapter 4: Function of miR-155 in the controlled cortical impact (CCI) model of TBI

Chapter 5: The role of miR-21 in neuronal function, injury, and repair

Tables

Chapter 1: Introduction

Chapter 2: Materials and Methods

Chapter 5: The role of miR-21 in neuronal function, injury, and repair

Chapter 6: Traumatic brain injury increases levels of miR-21 in extracellular vesicles: implications for neuroinflammation

List of Abbreviations

Abbreviations	Description
AAV	Adeno-associated virus
ADHD	Attention-deficit/hyperactivity disorder
Ago2	Argonaut 2
ALS	Amyotrophic lateral sclerosis
ANOVA	Analysis of variance
AP1	Activator protein 1
ATP	Adenosine triphosphate
Aβ	Amyloid beta
BBB	Blood brain barrier
BDNF	Brain derived neurotrophic factor
BSA	Bovine serum albumin
C/EBPβ	CCAAT/enhancer-binding protein-β
CCI	Controlled cortical impact
CCL	Chemokine (C-C Motif) ligand
CCR	Chemokine (C-C Motif) ligand receptor
CDC	Center's for Disease Control and Prevention
cDNA	Copy DNA
CHART	Craig handicap assessment and reporting technique
CIQ	Community integration questionnaire
CNPS	Composited neuropsychological score
CNS	Central nervous system
CNTF	Cilliary neurotrophic factor
CONTRA	Contralateral

CT	Computed tomography
CTE	Chronic traumatic encephalopathy
CX3CL	Chemokine (C-X3-C motif) ligand
CXCL	Chemokine (C-X-C motif) ligand
DAMPS	Damage associated molecular patterns
DAPI	4',6-diamidino-2-phenylindole
DEPC	Diethylpyrocarbonate
DG	Dentate gyrus
DNA	Deoxyribonucleic acid
dpi	Days post injury
DRS	Disability rating scale
dsRBP	Double stranded RNA binding proteins
EDC	1-Ethyl-3-(3-dimethylaminopropyl)carbodiimide
EDTA	Ethylenediaminetetraacetic acid
EGF	Epidermal growth factor
EPM	Elevated plus maze
EVs	Extracellular vesicles
EZM	Elevated zero maze
fEPSP	Field excitatory post synaptic potentials
FGF	Fibroblast growth factor
FIM	Functional independence measure
FISH	Fluorescent in situ hybridization
FJC	Fluorojade C
Flp	Flipase
FPI	Fluid percussion injury
FRT	Flp recombination target

FSE	Functional status examination
GAPDH	Glyceraldehyde 3-phosphate dehydrogenase
GCS	Glasgow comma scale
GCS	Glasgow comma scale
GFAP	Glial fibrillary acidic protein
GOS	Glasgow outcome scale
HAND	HIV associated neurocognitive disorders
HMGB1	High mobility group box protein 1
HSP	Heat shock protein
Iba1	Ionized calcium-binding adapter molecule 1
ICAM	Intercellular Adhesion Molecule
IFN	Interferon
IHC	Immunohistochemistry
IL	Interleukin
IPSI	Ipsilateral
IRAK	Interleukin-1 receptor-associated kinase
JAK	Janus kinase
KO	Knockout
LIF	Leukemia inhibitory factor
LPS	Lipopolysaccharide
Mal	MyD88-adapter-like
MAP2	Microtubule associated protein 2
MAPK	Mitogen-activated protein kinases
miRNAs	MicroRNAs
MRI	Magnetic resonance imaging
mRNA	Messenger RNA

MyD88	Myeloid Differentiation Primary Response 88
NF-κB	Nuclear factor-κB
NGF	Nerve growth factor
NMDA	N-methyl-D-aspartate
NNS	Neurological severity score
NO	Nitric oxide
NPC	Neural progenitor cell
NT3	Neurotrophin 3
OBTT	Operation Brain Trauma Therapy
PACT	Protein activator of PKR
PAMPS	Pathogen associated molecular patterns
PBS	Phosphate buffered saline
PCR	Polymerase chain reaction
PDCD4	Programmed Cell Death 4
PDGF	Platelet derived growth factor
PFA	Paraformaldehyde
PPARγ	Proliferator-activated receptor-γ
PRRs	Pattern recognition receptors
PTEN	Phosphatase and tensin homolog
PTP	Post-tetanus potentiation
qPCR	Quantitative PCR
RECK	Reversion-Inducing-Cysteine-Rich Protein With Kazal Motifs
RISC	RNA induced silencing complex
RLC	RISC loading complex
RNA	Ribonucleic acid
SDS-PAGE	Sodium dodecyl sulfate polyacrylamide gel electrophoresis

SEM	Standard error of the mean
SHIP	SH2 domain-containing inositol-5'-phosphatase
SOCS	Suppressor of cytokine signaling
SOD	Superoxide dismutase
SOX	SRY (Sex Determining Region Y)-Box
ssRNA	Single stranded RNA
SSRT	Stop-signal reaction time
STAT	Signal transducer and activator of transcription
TAB	TGF-Beta Activated Kinase
TBI	Traumatic brain injury
TBP	Tar RNA binding protein
TBS	Tris buffered saline
Tiam1	T-Cell Lymphoma Invasion And Metastasis 1
TIMP3	TIMP Metallopeptidase Inhibitor 3
TLR	Toll-like receptor
TNF	Tumor necrosis factor
TRAM	TRIF-related adaptor molecule
TRBP	TAR RNA binding protein
TRIF	TIR-domain-containing adapter-inducing interferon-β
TSA	Tyramide signal amplification
TUNEL	Terminal deoxynucleotidyl transferase dUTP nick end labeling
UTR	Untranslated region
VMP1	Vacuole membrane protein 1
WT	Wild type

Chapter 1: Introduction

The last decade has bought the eye of the public on traumatic brain injury (TBI). TBI has been called the signature injury of the wars in Iraq and Afghanistan, with millions of veterans suffering a distinctive set of symptoms caused by both penetrating and blast injuries [1, 2]. Meanwhile, a major class action lawsuit against the National Football league was prompted by the discovery of chronic traumatic encephalopathy in American football players. Together these circumstances have heightened public awareness and bought to light that even relatively mild brain injuries, such as concussions, can have severe consequences.

In the midst of all the media and public attention, many scientific advances are being made in our understanding of the brain and how it responds to injury. One element that unifies all TBI from mild to severe is the presence of neuroinflammation. As in all types of injury, inflammation plays a reparative role to clear damaged tissue and fight potential infection, but excessive inflammation can result in tissue damage and dysfunction.

This work is an investigation into the regulation of neuroinflammation in the context of traumatic brain injury. Though several molecular classes coordinate to produce an inflammatory response, we have chosen to focus on post-transcriptional regulation by microRNAs (miRNAs). Functionally, miRNAs bind to their messenger RNA targets reducing production of corresponding proteins. Translational silencing by miRNAs is accomplished by complimentary base pairing to target transcripts, typically found in the 3’ UTR. Using this mechanism a single miRNA can bind multiple targets. These targets can range in the hundreds, making miRNAs powerful regulators of the cell proteome. Recent studies in knockout mice have revealed that ablating certain miRNAs

can result in impaired or overactive immune function, showing that these molecules are critical regulators of the immune response [3]. While the importance of miRNAs in the peripheral immune response is increasing recognized, what role they play in the unique immune environment of brain injury remains largely unexplored. The overall aim of this work was to characterize the regulatory role of inflammation-associated miRNAs in the injured brain and determine their effect on brain recovery and cognitive function after TBI.

1.1 Traumatic brain injury

Traumatic brain injury is a leading cause of death and disability worldwide [4]. In 2009, the Center's for Disease Control and Prevention (CDC) estimated that 2.4 million people were diagnosed with TBI [5]. This is likely an underestimate as many TBIs, especially mild injuries, go unreported. Broadly defined TBI is any injury to the head that disrupts brain function. This includes closed head injuries where the head is struck by or against an object as well as jolts to the head that cause forward/reverse or rotating movement of the brain within the skull. Approximately 75% of TBIs are mild; concussions being included in this category [6]. Often mild TBI are left unreported and untreated. However, as is now realized with sports concussion, repeated mild TBI can cause motor and cognitive deficits. More severe forms of TBI are those that cause skull fractures or result from penetration of the brain with an object, such as a bullet. Although the most severe injuries are associated with penetration of the brain, diffuse axonal injury can also be severe and sometimes fatal.

The immediate consequences of traumatic brain injury include loss of consciousness, hemorrhage, edema, and ischemia. Surgical intervention is sometimes required and improvements in surgical techniques and more informed treatment guidelines have resulted in increasing survival rates [7]. But still, a diagnosis of TBI was

found in 30.5% of injury rated fatalities [6]. Even when patients survive a TBI, the long term effects can be disabling. It is estimated that 5.3 million people in the U.S. alone are living with TBI associated disabilities including cognitive and psychological dysfuntion [8].

The evaluation of TBI takes many forms and is highly dependent on the timing of evaluation. Severity of brain injury in the acute period is traditionally classified by the Glasgow comma scale (GCS), which takes into account impairment in speech, motor function, and loss of consciousness [9]. Several retrospective studies have called into question the reliability of the GCS, yet it is still a common tool for describing the severity of TBI [10]. Since the introduction of the GCS in 1974 [9], new technologies, such as computed tomography (CT) scans, have allowed for more physiological and reliable indicators of injury severity [11]. Other measures are more useful during the in-patient rehabilitation, also called the sub-acute phase. The functional independence measure (FIM) is most useful during this period. Scores on the FIM range from “complete independence to “total assistance” [12]. Another outcome measure with utility during the sub acute phase is the Craig handicap assessment and reporting technique (CHART) which measures physical independence, cognitive independence, mobility, social integration, occupation, and economic self sufficiency [13]. During the chronic phase after patients have been discharged the expanded Glasgow outcome scale (GOS) is the most commonly used outcome measures in clinical trials [14]. GOS is useful to determine positive or negative outcome (Table 1.1). The community integration questionnaire (CIQ) is also helpful to determine community integration after TBI [15]. One measure that can be useful to span the acute through chronic phases of TBI is the disability rating scale (DRS), which includes measures that range from “eye opening” and “motor response” to “toileting” and “employability [16].” To determine the neuropsychological impairment the composited neuropsychological score (CNPS) is

Table 1.1

Glasgow Outcome Scale (GOS)

1	Good Recovery	Return to normal life and employment. Some deficits, but lack of disability
2	Moderate Disability	Disabled, but independent. Return to work is dependent on special arrangements
3	Severe Disability	Dependent on daily support due to mental or physical disability or a combination of the two
4	Vegetative State	Unaware with only reflex responses.
5	Death	Self described

used. This test measures visuoconstruction and memory, oral fluency, sustained attention, and fine motor dexterity [17]. While many of the measures describe here show better accuracy then the GOS or measure different aspects of outcome, this is the primary measure used for research purposes and clinical trials.

The physical damage caused by a TBI can be divided into two categories the immediate mechanical damage (primary injury) and the events that occur in the wake of that primary injury (secondary injury). Primary damage can further be separated into focal damage that consists of contusion, laceration, and intracranial hemorrhage and diffuse damage resulting from acceleration/deceleration events, including diffuse axonal injury. Secondary damage includes ischemia and increased intracranial pressure as well as changes in neurochemistry, metabolism, and inflammation that can lead to neuronal cell death and dysfunction [18]. After survival of the primary insult any further decrease in neurological function or consciousness is due to secondary injury mechanisms. While eliminating or reducing primary damage is the goal of preventative efforts, once a traumatic brain injury has occurred, little can be done to reduce the primary damage. Instead therapeutic efforts are focused on the secondary damage that occurs after TBI. However, despite extensive research, there has not been any proven therapeutic treatment developed to reduce secondary damage after TBI. Many excellent reviews cover in detail the various secondary injury mechanisms [19, 20], but for our purposes here, we will focus on inflammation.

1.2.1 Neuroinflammation and TBI

After TBI there is marked elevation of activated resident glia including microglia and astrocytes. Increased cytokines and chemokine release from these resident cells in the acute time frame after TBI recruits peripheral immune cells such as neutrophils, macrophages, and T cells. Other than perivascular macrophages and resident microglia

the brain is normally free of other immune cells, however the damage caused by TBI, including disruption of the blood-brain barrier (BBB), allows the infiltration of peripheral immune cells. The multicellular response to TBI is described in figure 1.1. As in other types of injury, inflammation in TBI plays a dual role [21]. The phagocytic properties of microglia, neutrophils and macrophages helps to clear damaged tissue and these and other leukocytes reduce the risk of infection. Activated glia, including microglia and astrocytes, can also produce neuroprotective and neuroregenerative factors. However, the production of inflammatory molecules by infiltrating peripheral immune cells as well as glia, including cytokines and chemokines, nitric oxide (NO), and reactive oxygen species can also have detrimental effects on neuronal function. Even though both negative and positive components are present, generally anti-inflammatory agents improve TBI outcomes in animal models [22].

The front line of the cellular response to TBI is resident microglia. Microglia are highly sensitive to even subtle changes in the local environment. For example, microglia can be activated by molecules usually confined to the cellular compartment such as purine nucleotides [23], as well as neurotransmitters [24], and even changes in ion homeostasis [25]. First described by Rio-Hortega in 1932, resting microglia in a non-pathological brain have a small cytoplasm relative to other cells in the brain and delicate, ramified processes. Recent two-photon microscopy experiments have shown that microglial processes are constantly moving, surveying the local environment [26]. Upon activation microglial morphology rapidly changes, processes become stumpy or “bushy” and the cell body can even become amoeboid to the point were it is undistinguishable from a peripheral mononuclear cell [27].

Activation of microglia results in proliferation, migration, secretion of soluble factors and electrophysiological changes [22]. Proliferation and migration result in

Figure 1.1

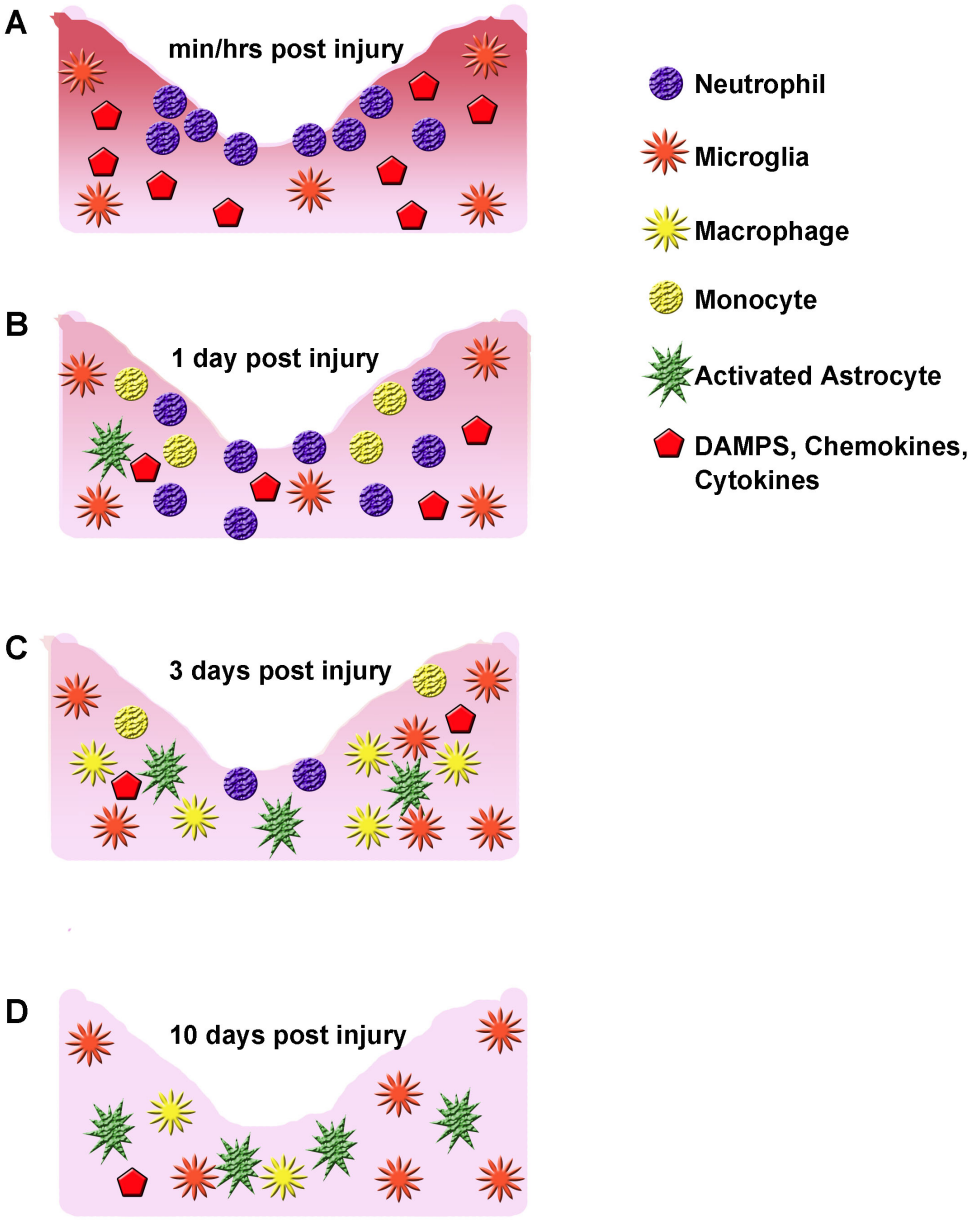
A
min/hrs post injury
B
1 day post injury
C
3 days post injury
D
10 days post injury
Neutrophil
Microglia
Macrophage
Monocyte
Activated Astrocyte
DAMPS, Chemokines, Cytokines

Figure 1.1 Inflammatory response to TBI. This figure demonstrates the time course of inflammation, activation of resident glia and recruitment of peripheral immune cells to the lesion site following TBI (A). Within minutes to hours cytokines, damps, and chemokines are released from the damaged tissue and neutrophils are recruited to the injury stie (B). By 1 day post injury (dpi) neutrophils have invaded the brain tissue and monocytes are being recruited to the brain tissue (C). By 3 dpi peripheral monocytes have begun differentiation into macrophages and activated microglia and astrocytes are present at the lesion site, but the neutrophils are now nearly undetectable (D). At 10 dpi the immune response has largely subsided, however activated astrocytes and macrophages are still present at the lesion site [28].

increased numbers of microglia at sites of injury. Factors secreted by microglia upon activation include inflammatory cytokines, proteases, free-radicals and growth factors.

Primary among microglia-secreted cytokines is IL-1β, which in turn, can induce of IL-6 and TNFα in an autocrine and paracrine manner [29]. In addition to glial cells, neurons carry receptors for IL-6, TNFα, and IL-1β, which can mediate effects in neurons [30, 31]. Although classically neurons are thought to be damaged by inflammatory cytokines [32], there is growing evidence that these same cytokines may be necessary for neuroprotective and neuroregenerative effects likely in a concentration dependent manner [33]. In addition to cytokines, free radicals such as NO are secreted by microglia and likewise cause both beneficial and detrimental effects to their neuronal neighbors [34]. To add further complexity microglia secrete neurotropic factors such as NGF, BDNF, and NT3 [35-37] in addition to proteases, which can clear the damaged extracellular matrix but can also exacerbate BBB dysfunction [38].

Overall, the interaction between neurons and microglia is complex and multi-faceted. There is no doubt that the conversation is two-sided with neurons signaling microglia, which in turn modulate neuronal function [39]. While inhibiting inflammation can improve outcomes in brain injury models, the effects of anti-inflammatory agents are not specific to microglia [22]. One clue to the balance of microglial effects in neuroinflammation is the work of Heppner *et al*. in experimental autoimmune encephalitis, a mouse model of multiple sclerosis [40]. In this study a mice were genetically altered to “paralyze” microglial activation. This microglial paralysis repressed the development of experimental autoimmune encephalitis. While similar studies are yet to be performed in studies of TBI, accumulating evidence suggests a detrimental pathological role for microglia in neuroinflammation.

Astrocytes also undergo morphological changes and activation, but they have a distinctly different role from microglia in CNS pathology. In the non-diseased CNS astrocytes control homeostasis of ions, neurotransmitters, water, and blood flow and play a role in neural circuit formation. The morphology of protoplasmic astrocytes, the type that predominates in the grey mater, consists of short, branched processes in close proximity neuronal synapses [41]. Unbranched, fibrous astrocytes are found in the white mater and function to maintain mylenated axons [42]. Astrocytes also regulate the BBB, completely ensheathing capillaries [43]. Interestingly, astrocytes do not function as indepent cells, but are connected in a vast network by gap junctions [44]. The primary pathological marker of a reactive astrocyte in neuroinflammatory conditions is the increased expression of intermediate glial fibrillary acidic protein (GFAP) [45]. Evidence points to mechanical forces as the impetus for astrocyte activation after TBI [46]. The activation of astrocytes occurs very early after injury, causing ATP release and subsequent microglial activation [47]. However, astrocytes also serve to wall-off inflamed tissue from healthy or salvageable tissue by formation of a glial scar [48]. Glial scar formation is also required for repairing the damaged BBB after TBI. As important players in the synapse, astrocytes also maintain neural circuits and promote synaptic remolding after injury [46]. This beneficial effect also has a counter-point in that through their effect on synapses after TBI, astrocytes may also promote epileptogenesis [46]. As with microglia, astrocytes have duplicitous role in TBI pathology. And again genetic studies in mouse models are beginning to elucidate whether these cell types provide net benefit or detriment. An elegant genetic study in a mouse model of TBI showed exacerbated tissue loss with ablation of reactive astrocytes [49]. All together evidence points to a net protective role for reactive astrocytes in TBI.

While activation of resident neuroglia occurs almost instantaneously after TBI, in the subsequent hours and days peripheral immune cells are also recruited to the site of injury. The recruitment of peripheral immune cells is a result of several factors, increased permeability of the BBB, secretion of cytokines and chemokines by neural cells, and increased expression of adhesion molecules. The integrity of the BBB relies on tight junctions between epithelial cells and is reinforced by astrocytic end-foot processes [50]. After TBI the BBB is damaged by both primary and secondary injury mechanisms. Mechanical forces can affect the physical integrity of the BBB and activation of astrocytes can reduce their contribution to the stability of the BBB [51]. The leakiness of the BBB allows for infiltration of peripheral immune cells and these cells are attracted to the lesion site by cytokines and chemokines secreted by brain resident cells. Primary among TBI induced chemokines are CXCL8, CCL2, CXCL12, CXCL10, CX3CL1, and CCL5, though this is not a complete list [28]. In addition to permeability and increased chememotactic agents, adhesion molecules are upregulated by TBI. Adhesion molecules, such as glycoproteins and intergrins are upregulated by cytokines IL-1β, TNFα, and IL-6 [52]. Together BBB permeability, chemoattractants and adhesion molecules result primarily in recruitment of neutrophils and mononuclear cells, though small populations of T cells and natural killer cells call also be detected after TBI [28].

Neutrophils arrive at the lesion site within 12 hours of injury [53], while peak levels of mononuclear cells are found 3 days after injury [54]. Tissue destruction after TBI is predominately due to neurotrophils and this cell type causes significant toxicity through respiratory burst [55]. However, attempts to block neutrophil accumulation have not shown any benefit in animal models of TBI [56-58]. Therefore focus has shifted to targeting monocyte recruitment. One chemokine, chemokine receptor target for intervention in monocyte infiltration into the brain is CCL2/CCR2. Early studies targeting

the CCL2/CCR2 chemokine and receptor axis have shown both histological and functional improvements in rodent models and reduced monocyte levels in the brain [59, 60]. While other chemokine and chemokine receptor systems are altered after TBI in humans and in rodent models, their functions in TBI are not well studied. Of note are CXCL10 and CCL5, which are elevated after TBI. Both CCL5 and CXCL10 are known to play a role in T-cell recruitment, but their importance for TBI pathophysiology is still unknown [28].

Taken as a whole the immune response to TBI has several distinct elements that are highly interconnected. The release of DAMPs together with mechanical shear forces disrupts brain homeostasis, this sets off the activation of resident glia which secrete a suite of cytokines, chemokines, reactive oxygen species, proteases, and growth factors. These factors, particularly chemokines, recruit peripheral immune cells to cross the damaged BBB. Once in the brain, these neutrophils, monocytes, T cells and dendritic cells assist in clearing damaged tissue and preventing infection, meanwhile releasing neurotoxic inflammatory cytokines and reactive species that further exacerbate neuronal injury. In rodent models genetically ablating or targeting different molecules or cell types within this orchestral production has a variety of effects. Reducing microglial activation generally improves outcomes, while inhibiting reactive astrocytes worsens them. Inhibiting neutrophil migration and infiltration seems to have little effect, but targeting monocyte recruitment reduces neurological deficits. It is evident that inflammation following TBI has a large impact on TBI pathophysiology. A clearer understanding of the role of individual cell types and molecules in the inflammatory response to brain injury may provide potential therapeutic targets for TBI.

1.1.2 Long-term consequences of TBI

While therapeutic strategies are currently focused on the acute period after TBI there are millions of people in the U.S. alone already living with long-term disabilities related to a TBI [8, 61]. A 2008 literature survey by the National Academy of Sciences concluded that there was a strong association between moderate to severe TBI and dementia, Parkinsonism, endocrine dysfunction, growth hormone insufficiency, depression, anxiety, aggression, and social dysfunction [62]. TBI is also associated with an increased risk of epilepsy [63]. A moderate to severe TBI increases the odds of developing a psychiatric illness 4 fold in the following 6 months [64]. Among psychiatric disorders depression is the most common, with estimates that 33% of TBI patients experience depression [65]. Moreover, TBI is often associated with aggression, social isolation, and joblessness [66, 67]. It is likely that these outcomes are linked to increased impulsivity observed in TBI patients [68]. While most of the available literature draws strong associations with severe and penetrating injuries and subsequent neuropsychological dysfunction we now know that repeated mild concussions can also produce increased aggression, motor dysfunction, and suicidality, now recognized as chronic traumatic encephalopathy (CTE) [69-71]. A handful of recent reports have also identified increased levels of Attention-deficit/hyperactivity disorder ADHD in both children [72] and adults [73]. There is no doubt that TBI can have negative life long consequences which cause great burdens to the individual, their families, and society as a whole. However, the pathophysiology behind these long-term neuropsychological changes and increased risk of neurodegeneration is only beginning to be understood.

The pathological hallmark of CTE is progressive tauopathy [71]. Many neurodegenerative diseases are considered tauopathies, most prominent among them Alzheimer's disease [74]. One marked difference between Alzheimer's pathology and that of CTE is the localization of tau tangles. While in Alzheimer's disease these pathological features are found concentrated in the hippocampus, in CTE they are found

in the sulci, superficial cortical layers, and often in a perivascular arrangement; all points of mechanical trauma. Recent work by Johnson *et al.* Identified tau and amyloid-β pathology in post-mortem brains decades after a single TBI [75]. This work suggests that tau accumulation may contribute to the cognitive dysfunction and neurodegeneration associated with a single TBI, not only repetitive mild TBI as seen in CTE. Aside from tau deposition, pathological hallmarks of long-term survivors of TBI are reactive microglia and white matter degeneration that persists for as long as 18 years after a single TBI [76]. It is unclear whether the inflammatory response causes the white matter degeneration, or vise versa and what relationship both may have to tauopathy in survivors of TBI.

Interestingly, inflammation is associated with both neuropsychological dysfunction and neurodegeneration outside the context of TBI [77]. It is generally accepted that inflammation can cause or exacerbate not only depression, but anxiety, and schizophrenia [78-81]. Early studies of the link between inflammation and depression after TBI show that inflammatory markers may be associated with risk of post-traumatic depression [82, 83]. Further mechanistic and epidemiological studies are necessary to understand the link between persistent neuroinflammation and post-traumatic neuropsychiatric dysfunction.

1.1.3 Modeling of TBI in rodents

To date there are no drugs proven in clinical trials to ameliorate the effects of TBI. In order to discover novel drug targets and test the efficacy of therapeutic approaches pre-clinical models are necessary. While some models in large mammals such as pigs are being developed to better replicate the mechanical features of the human brain, most pre-clinical studies are performed in rodents. In general, rodent models replicate pathological features of human TBI including reactive glia, peripheral cell infiltration,

contusion, edema, hemorrhage, and white matter damage. Rodent models of TBI can also recapitulate some of the behavioral and cognitive changes observed in TBI patients. One difficulty in any clinical study of TBI is the heterogeneity of injuries found in patients. Injuries can be caused by different types of impact with differing amounts of force and be localized to different areas of the brain. To represent these diverse injury types a large number of animal models have been developed.

While subtle variations of each model exist four primary models are prominent in the field. These are the fluid percussion injury (FPI), controlled cortical impact (CCI), weight-drop, and blast models [84]. For the FPI model a craniotomy is performed to expose the dura and then a fluid reservoir is placed into the opening and struck with a pendulum [85]. The CCI model also employs a craniotomy, but is followed by a mechanical impact driven pneumatically or electromagnetically [86]. Relative to the FPI, CCI offers more control of injury parameters and thus injury severity. The depth, dwell time, and speed of the impact can be controlled with a CCI injury, while only the height of the pendulum can be adjusted in the FPI model. One commonality of FPI and CCI is the use of both unilateral and bilateral injury models. Interestingly, unilateral injury models tend to consistently injure the left hemisphere, most often in the parietal sensory/motor cortex. While there does not seem to be any compelling reason for this practice, it is standard in the field. Our studies utilized the CCI model to create a unilateral injury to the parietal cortex (Fig 1.2) In contrast to FPI and CCI, the weight drop model can be either an open or closed head injury. One draw back of this model is its use of a gravity driven weight dropped down a guide. Therefore, the mechanical parameters can only be altered by changing the height at which the weight is dropped. One advantage of this method is the ability to model closed head injury in human patients and produce varying degrees of diffuse axonal injury. Blast injury models are

Figure 1.2

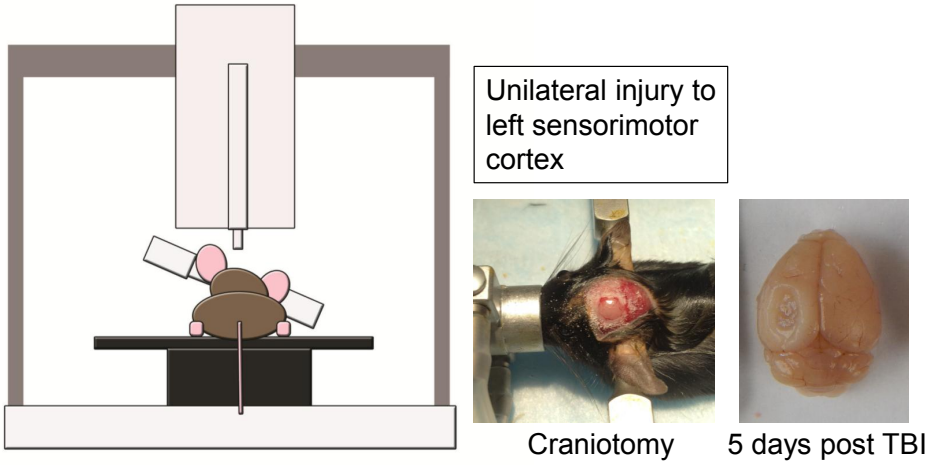
Unilateral injury to left sensorimotor cortex
Craniotomy
5 days post TBI

Figure 1.2 Description of controlled cortical impact (CCI) model of TBI. Mice are anesthetized and placed in a sterotactic frame. A craniotomy is performed exposing the intact dura. A piston driven by either air pressure or electromagnetic force is used to impact the brain. The speed, depth, and dwell time of the piston can be adjusted to create different severities of injury. This injury can be either unilateral of bilateral depending on placement of the craniotomy. Depending on injury severity CCI causes cortical or cortical and hippocampal tissue loss, shown here at 5 days after injury.

growing in popularity as these are able to mimic the diffuse axonal injury, changes and intracranial pressure, and cognitive deficits seen in human blast trauma [87, 88].

Although these are the primary models, several lesser-used variations are worth noting. The penetrating ballistic-like brain injury is designed to have similar pathology to a gunshot wound or other projectiles with high energy and a leading shockwave [89]. Additionally a number of mild repetitive injury models have also been devised. One such model modified a closed-head weight drop approach, but used repeated mild impacts. Even this relatively mild trauma showed both histological and behavioral signs of brain damage [90]. The incredible diversity of human TBI is reflected in the many animal models of TBI. However, this diversity of models is also problematic for the field. Conducting reproducible animal behavior experiments across labs is already difficult [91], and in TBI research this issue is compounded by the fact that many labs have their own unique injury model. Differences in species and strain, gender, and age all add up to a large degree of variation in TBI outcomes. Therefore, finding a pharmacological or therapeutic approach that is effective across multiple models presents a high bar for pre-clinical testing. The benefit of this high diversity is that it more accurately models the human condition and will hopefully lead to development of new agents that will prove effective in clinical trials. This is the goal of Operation Brain Trauma Therapy (OBTT), a consortium consisting of multiple TBI preclinical groups. The goal of this consortium is to test the efficacy of agents that have shown promise in pre-clinical testing across a large number of models and institutions to identify the most promising candidates for clinical trials [92].

In addition to a large diversity of injury models, there are also a myriad of outcome measures used by various laboratories. The main themes among these measures are lesion size, motor dysfunction, and cognitive dysfunction (Fig 1.3). Several of the injury models mentioned above result in brain tissue loss that can be measured

Figure 1.3

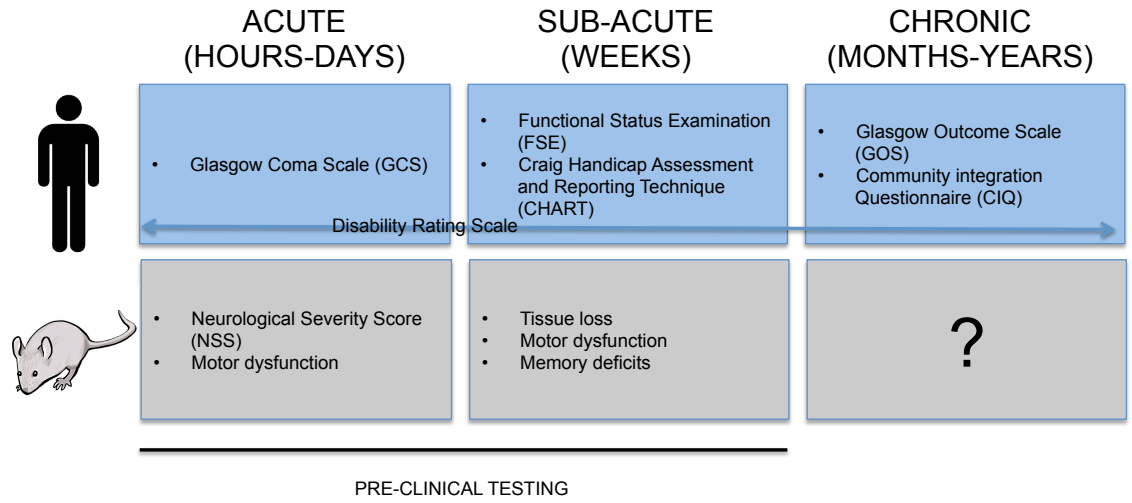
ACUTE
(HOURS-DAYS)
SUB-ACUTE
(WEEKS)
CHRONIC
(MONTHS-YEARS)
Glasgow Coma Scale (GCS)
Functional Status Examination (FSE)
Craig Handicap Assessment and Reporting Technique (CHART)
Glasgow Outcome Scale (GOS)
Community integration Questionnaire (CIQ)
Disability Rating Scale
Neurological Severity Score (NSS)
Motor dysfunction
Tissue loss
Motor dysfunction
Memory deficits
?
PRE-CLINICAL TESTING

Figure 1.3. Outcome measures for clinical and pre-clinical testing at different phases after TBI. Several outcome measures are available to measure deficits in patients after TBI. However, the Glagow Outcome Scale is by far the most common for clinical trials. In rodent models of TBI outcome is measured primarily during the acute (hours to days) and sub acute (weeks) phases and relies heavily on motor function. Both human clinical trials and mouse pre-clinical trials have struggled to show any improvement in TBI outcomes. One possible cause is the lack of sensitive outcome measures. In rodents, preclinical modeling of the chronic phase is still underdeveloped. Developing meaningful outcome measure for chronic TBI in rodents may provide a more representative model for the human condition.

histologically or by magnetic resonance imaging (MRI). Tissue loss, or lesions, are found in the FPI and CCI models and some versions of the weight-drop model, but are absent in blast injury. Tissue loss is a result of apoptosis and necrosis of brain tissue as well as destruction of tissue by immune cells. In these models, lesion size correlates to behavioral deficits [93, 94].

Behavior assessment can occur anytime spanning the acute, sub acute, and chronic phases of TBI and most measures change dynamically within this time frame. The neurological severity score or NSS was developed as a counterpart to the Glasgow outcome scale, and has several iterations. Generally this is a mix of various motor skills, such as the ability to walk on various size beams, startle response, ambulation, hemi-paresis. Other motor behaviors often used in the literature include beam walking tasks and rotarod testing [95]. The most common cognitive test used in TBI models is the Morris water maze, though novel-object testing and Barnes maze have also been used [96]. While there is a wealth of literature on lesion size, motor, and cognitive function in the acute (< 7 d) and sub-acute (7 d-28 d) time period, relatively little is know about the persistence of chronic (> 28 d) deficits in rodent models. Also, considering that neuropsychiatric dysfunction is linked to TBI, little is known about the presence of neuropsychological changes in TBI models, especially in the chronic period. Identification of depression, anxiety, impulsivity, or aggressive phenotypes in TBI models could not only provide a tool for testing treatment strategies, it would also provide insight into the pathophysiology of these conditions. For example, is inflammation related to post-traumatic depression? Does white matter degeneration contribute to neuropsychiatric dysfunction? Clearly, given the personal and economic burden of TBI associated personality changes and neuropsychiatric dysfunction this is an area demanding further research.

1.2 The biology of miRNAs

The 1990s brought about several landmark discoveries regarding non-coding, but functional RNA. Xist RNA was shown to regulate X chromosome inactivation [97] and the first long non-coding RNA, murine H19 was discovered [98]. During this time, work in *C. elegans* uncovered that a crucial developmental gene, lin4, encoded a 22bp RNA that was responsible for post-transcriptional regulation of mRNA transcripts. Soon after several genes exhibiting this pattern emerged and were named microRNA (miRNA) for their small size. Lin-4, the first miRNA discovered, shows many features that we now understand to be typical of miRNA. Lin-4 regulates lin-14 through anti-sense sequences in the 3' UTR of lin-14, but does not decrease levels of Lin-14 transcript, suggesting that it prevents translation without causing mRNA degradation. Also, there are long (60 nt) and short (22 nt) gene products, which correspond to different stages of microRNA processing. Since this initial publication more than 28,500 miRNA have been discovered in a wide variety of species (miRNbase.org) many, like let-4, are involved in development; however, miRNAs are known to regulate many diverse physiological processes. The essential nature of miRNAs is highlighted by the fact that mice lacking the Dicer enzyme necessary for processing miRNA die at embryonic day 7.5 [99].

The transcription and processing of miRNA is complex, and can be regulated at many levels. Some miRNA genes are found within non-coding regions of host-genes, while others carry their own promoter sequences. RNA polymerase II is the primary polymerase for miRNA transcription. Once a miRNA is transcribed, the primary miRNA forms a stem-loop structure, which is cleaved within the nucleus by a multiunit complex containing Pasha and Drosha to form an ~70 nt pre-miRNA product [100]. Once exported from the nucleus, the pre-miRNA is further processed into its mature form by the enzyme Dicer as part of the RNA-induced silencing complex (RISC) loading complex (RLC). Aside from Dicer the RLC includes Tar RNA binding protein (TBP), protein

activator of of PKR (PACT) and Argonaut 2 (Ago2). After cleavage occurs and the mature miRNA is formed Dicer, TBP, and PACT dissociate from the RLC, leaving the active RISC, which mediates gene silencing [101]. RISC stabilizes the miRNA and helps guide it to complimentary sequences on target mRNA molecules. Once bound to its mRNA target miRNA induces either degradation or sequestration of the target transcript causing a reduction in protein production [102]. A single microRNA is capable of targeting hundreds of mRNA and a single mRNA can be targeted by multiple miRNA. This creates a highly complex system for regulating the proteome of the cell [103]. While this scenario represents the canonical view of miRNA function, the picture becomes increasingly complex with further investigation. Reports of miRNA increasing protein translation in certain circumstances [104] and regulating transcription in the nucleus [105] open the possibility for many nontraditional functions for these molecules.

The expression of mature miRNA molecules can be regulated transcriptionally or at the stage of processing. Transcriptionally, miRNA can be regulated by the promoter sequences that control the host gene, or by independent promoters. Often miRNA are regulated temporally by negative feedback loops where the transcription factor inducing miRNA expression is also targeted by the miRNA. It is increasingly evident that post-transcription regulation is essential to miRNA biology. Many molecules are known to both positively and negatively regulate Drosha, Dicer, and RISC complexes. For example, double stranded RNA binding proteins (dsRBP) such as DGCR8 and TRBP associate with these complexes and their levels affect the rate of miRNA processing. The stability of the miRNA is also regulated. Therefore, some stimuli and developmental processes can affect the levels of many microRNA simultaneously [100].

Levels of miRNA expression are highly dependent on cell type, creating a type of miRNA signature. When a cell transitions from one state to another is also shifts its miRNA profile. For example, shifts from a multipotent to a differentiated state are

accompanied by corresponding shifts in miRNA levels [106]. The same is true for changes in cells as they shift from healthy to diseased, from normal to cancerous [107], or from a resting to activated state [108]. In these cases miRNA may be acting to effectively shut off protein production of targets that are no longer beneficial for the new state of the cell [103]. In this way, one can conceptualize miRNA as important mediators of change in the biological world.

1.2.1 Inflammation and miRNAs

In the immune system, miRNAs are critical regulators of both immune system development and activation. Studies of miRNA knock-out mice have revealed roles for miRNA in the development of specific immune cell subsets [109]. Additionally inflammatory stimuli induce a specific subset of miRNA that can play pro or anti-inflammatory roles by acting on cytokine signaling pathways. Disturbing the delicate balance between these pro and anti-inflammatory functions can on one side disable the immune system leaving the organism open to infection or on the other side create excessive inflammation leading to autoimmunity. We will cover the relevant inflammatory signaling pathways, then delve into their regulation by miRNAs. Subsequent sections will discuss the role of miRNAs in the regulation of neuroinflammation.

The first phase of the innate immune response is recognizing possible pathogens. This is accomplished through the use of pattern-recognition receptors (PRRs) that recognize unique molecular motifs present in pathogens such as bacterial lipopolysaccharides. These molecular motifs are called pathogen associated molecular patterns (PAMPS). When PRRs bind PAMPs they alert innate immune cells such as macrophages and dendritic cells, inducing an inflammatory response. The most well characterized class of PRRs are the Toll-like receptors (TLRs) named after the Toll protein of drosophila. TLRs that are expressed both on the surface (TLR1-6 and TLR10)

of the cell and in the interior compartment of the endosome (TLR3 and TLR7-9). There is a large family of TLRs that can be subdivided into categories based on the type of PAMPS they recognize. TLR 1, TLR2, TLR4, and TLR 6 recognize lipids, while TLR3, TLR7, TLR8, and TLR9 recognize nucleic acids. Therefore one pathogen can stimulate multiple TLRs depending on which PAMPs it expresses. For example a virus expresses glycoproteins that can be recognized by TLR2 and TLR4, but also DNA, which stimulates TLR9 or RNA, which stimulates TLR3, TLR7, and TLR8. This diverse array of PRR/PAMP pairings ensures that there is a robust inflammatory response to a pathogen [110]. However, when tissue damage occurs, cells release components that are normally sequestered, these are termed damage associated molecular patterns (DAMPs) and they can also bind to TLRs. Intracellular protein, DNA, RNA, and nucleotides can all serve as DAMPs [111]. This system is the reason that tissue damage causes an inflammatory response strikingly similar to a pathogen. Practically speaking tissue damage, such as a cut, is often accompanied by an increased risk of infection. This association may be the underlying evolutionary reason for ability of PRRs to recognize DAMPs. The ability of DAMPs to elicit an immune response is not without drawbacks. Recently associations have been made between chronic inflammatory conditions and DAMPs. A small list includes arthritis [112], psoriasis [113], atherosclerosis, and systemic lupus erythematosus [114], though others are being added with increasing frequency. As discussed here, TLR signaling was first characterized in the peripheral immune system, but these receptors and signaling pathways are also present in nervous system infection and damage [115]. In TBI specifically, TLRs are expressed on both resident and invading immune cells, which respond to DAMPs such as heat shock protein 70 (HSP70) released from neurons and other damaged cells in the brain [116]. Laird *et al.* showed that the DAMP high mobility group box protein-1 (HMGB1)

exacerbates TBI associated edema [117]. Therefore, TLRs and TLR signaling pathways show promise as therapeutic targets for TBI.

Once a DAMP or PAMP binds to a TLR, one or more adaptor proteins is recruited to the intracellular portion of the TLR. The four know adapters are MyD88, TRIF, TRAM and Mal. All TLRs are capable of interacting with MyD88, the first adapter discovered. Down stream of these adaptor proteins are pro-inflammatory transcription factors, primarily NF-κB. MyD88 dependent signaling from TLR2, TLR4, and TLR5 results in pro-inflammatory gene expression, while TLR7 and TLR9 MyD88 dependent signaling specifically induces type I IFN production [110].

Profiling studies of miRNA during the immune response has shown that many miRNAs are induced by TLR signaling. The primary miRNA induced by TLR signaling are miR155, miR-146, and miR-21, but several others have also been cited [118]. The expression of these miRNAs seems highly dependent of NF-κB, but changes in miRNA processing may be an additional layer of regulation [119]. Once miRNAs are induced by TLR signaling they target various levels of the pathway. miRNAs can target TLR signaling proteins, transcription factors, regulators, downstream cytokine products, and even TLRs themselves. Generally speaking the role of several miRNAs in TLR signaling is to provide feed-back inhibition. TLRs stimulate NF-κB, which induces mRNA expression. Mature miRNA bind to the mRNA of signaling proteins and transcription factors involved in TLR signaling. As proteins are turned over, without active translation of target miRNA levels gradually decrease, thereby contributing to the resolution of inflammation. Two signaling molecules, IRAK1 and TRAF6, involved in MyD88 dependent responses are directly targeted by miR-146. Therefore miR-146 expression reduces MyD88 dependent TLR signaling [120]. Similarly miR-155 directly targets TAB2, an important downstream signaling molecule of TLRs that induces the MAPK pathway [121]. Several important downstream transcription factors of TLRs are also targeted by

miRNA. CCAAT/enhancer-binding protein-β (C/EBPβ) is a target of miR-155 [122, 123]. Alternatively, induction of miR-27b by NF-κB, leads to decreased levels of target proliferator-activated receptor-γ (PPARγ). PPARγ is anti-inflammatory and targeting by miR-27b would increase inflammatory signaling [124]. Additionally, the transcriptional co-activator p300 is a target of miR-132 and is required for the induction of anti-viral genes [125]. While the general trend is for miRNAs induced by TLR signaling to provide feed-back inhibition, there are some notable exceptions. Src homology 2 (SH2) domain-containing inositol-5'-phosphatase1 (SHIP1) is a negative regulator of TLRs and also a target of miR-155, a TLR induced gene [126] [127]. Another important target of miR-155 is suppressor of cytokine signaling 1 (SOCS1). SOCS1 inhibits the function of STAT1 an important transcription factor for type I, type II, and type III interferons. The complex nature of miRNA regulation of TLR signaling suggests that effects may be cell-type and context dependent. A summary of some of the targets and associated signaling pathways is shown in figure 1.4. *In vivo* studies using miRNA knockout mice are beginning to show the balance of pro and anti-inflammatory effects in TLR responses. Mice deficient in miR-146a have excessive pro-inflammatory responses to LPS causing a severe increase in lethality of an intraperitoneal injection of LPS and an autoimmune phenotype [128]. Alternatively, miR-155 knockout mice have diminished immune responses, which make them more susceptible to various infections [129, 130], but causes reduced tissue damage in injury models [131, 132]. Together studies on miR-155 and miR-146 knockout mice herald a growing appreciation for the importance of miRNAs in the innate immune response. What role inflammation-associated miRNAs have in the regulation of immune responses in the brain is still being discovered and the expression and function of inflammation-associated miRNAs in TBI has not been characterized.

1.2.2 Neuroinflammation and miRNAs

Figure 1.4

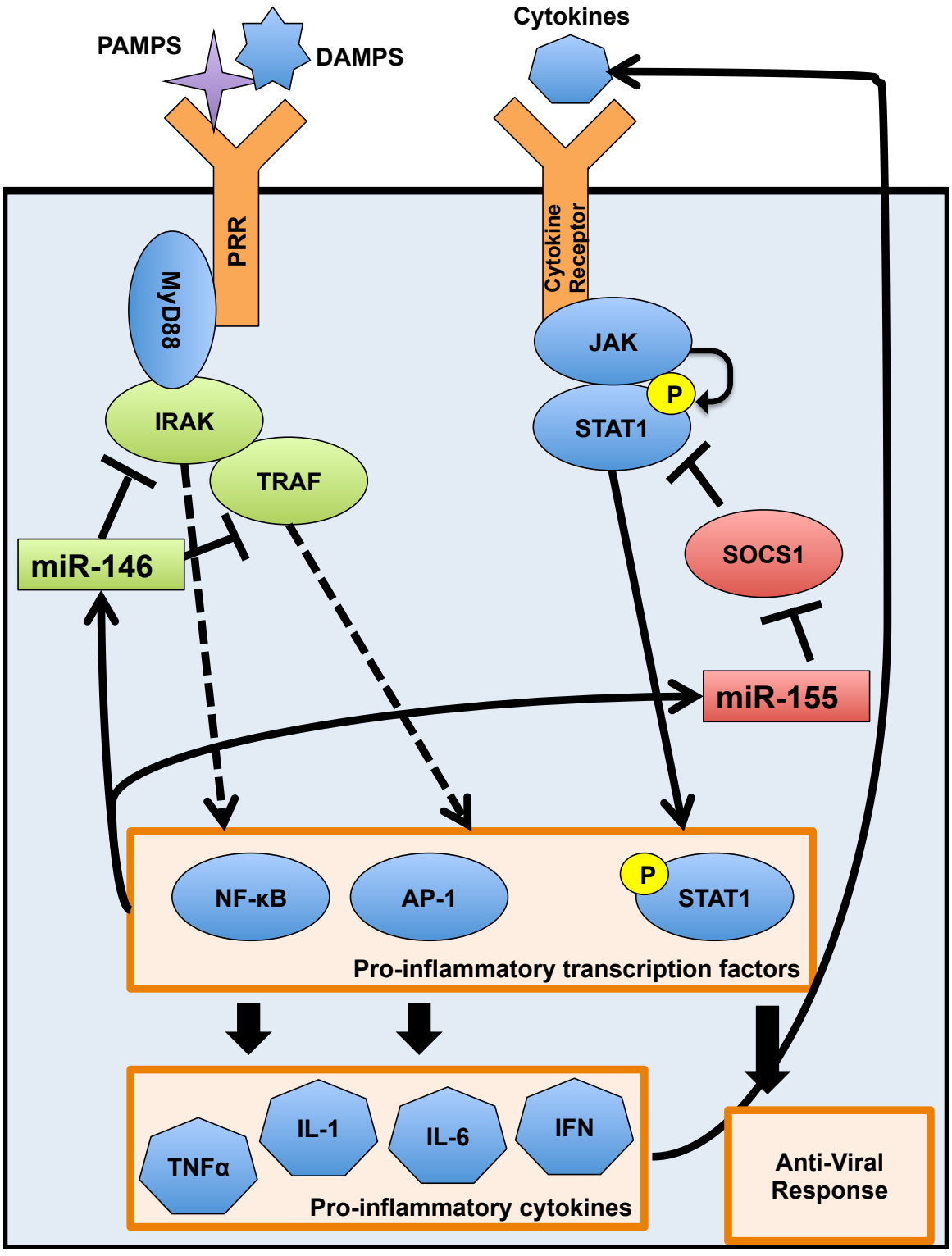
PAMPS
DAMPS
Cytokines
PRR
MyD88
Cytokine Receptor
JAK
P
STAT1
IRAK
TRAF
SOCS1
miR-146
miR-155
NF-κB
AP-1
P
STAT1
Pro-inflammatory transcription factors
TNFα
IL-1
IL-6
IFN
Pro-inflammatory cytokines
Anti-Viral Response

Figure 1.4 Roles for miRNAs in inflammatory signaling pathways.

A limited diagram of the pattern recognition receptor (PRR) signaling and cytokine signaling pathways highlighting the role of miR-155 and miR-146 in modulating the immune response. Shown in green are miR-146 and its targets and shown in red are miR-155 and its target. Pathogen associated molecular patterns (PAMPs) and damage associated molecular patterns (DAMPs) bind to PRRs including the TLR family. TLR signaling is dependent on Myeloid differentiation primary response gene 88 (MyD88), interleukin-1 receptor-associated kinases (IRAKs), and TNF receptor associated factors (TRAFs). Eventually the cascade initiated by the binding to the PRR induces activation of pro-inflammatory transcription factors such as nuclear factor kappa-light-chain-enhancer of activated B cells (NF-κB) and adaptor protein 1 (AP-1). Activation of pro-inflammatory transcription factors causes increased gene expression of pro-inflammatory cytokines and other genes involved in the immune response. Cytokines can then bind to their cognate cytokine receptors and induce further signaling cascades. Many cytokines receptors are receptor tyrosine kinases which rely on janus kinase (JAK) and signal transducer and activator of transcription (STAT) for signal transduction. The expression of miR-146 and miR-155 is also induced by NF-κB. IRAK and TRAF molecules are targeted by miR-146 leading to feed back inhibition of the PRR response. Alternatively miR-155 inhibits suppressor of cytokine 1 (SOCS1), an inhibitor of STAT1 activation. Therefore miR-155 promotes the antiviral response induced by STAT1. P represents phosphorylation events. IFN, interferon; IL, interleukin; TNF, tumor necrosis factor.

Considering the widening base of literature on miRNAs in inflammation, comparatively less is know about the role miRNAs might play in the unique immune environment of the brain. Few reports have highlighted a role for miRNAs both in the activation of resident glia calls and the recruitment of immune cells to the brain. Cardoso *et al*. found that miR-155 is induced by LPS in microglia [133], similar to what had been shown in macrophages [134]. They also validated that SOCS1 was a target of miR-155 in microglia and that miR-155 inhibition decreased levels of pro-inflammatory cytokines secreted by microglia. Additionally miR-155 increased levels of iNOS and contributed to the toxicity of microglial supernatants on cultured neurons. *In vivo* experiments on the superoxide dismutase 1 (SOD1) model of amyotrophic lateral sclerosis (ALS) ablating miR-155 restored aberrant microglia and prolonged survival [135]. Interestingly, Alzheimer's 3x transgenic model showed upregulation of miR-155. Furthermore, induction of miR-155 in astrocytes and microglia treated with Aβ fibrils was mediated by C-Jun. Increased miR-155 in transgenic mice also correlated with a decrease in SOCS1 levels [136]. Yet another study on alcohol induced neuroinflammation showed increased levels of miR-155 in the brain; in TLR4 knockout mice miR-155 was not induced. In miR-155 knockout mice alcohol induced TNFα, CCL2, and Pro-1L-1β were decreased. In another report of miR-155 in neuoroinflammation, miR-155 was shown to regulate the alpha synuclein induced inflammatory response in a model of Parkinson's disease [137]. Together these studies suggest a pro-inflammatory role for miR-155 in neuroinflammation, likely through inhibition of SOCS1 in microglia. Interestingly miR-155 is important for inflammation induced deficits in neurogenesis. Microglial activation is balanced by two miRNAs. Expression of miR-155 polarizes microglia to an activated phenotype, while miR-124 promotes a resting phenotype. The expression of miR-124 is brain specific. Ponomarev *et al.* showed that in experimental autoimmune encephalitis,

an animal model of multiple sclerosis, miR-124 levles were decreased. Additionally, inhibiting miR-124 in microglia resulted in an activated phenotype [138]. However, studies in post-mortem brains from multiple sclerosis patients found increased levels of miR-124 in demyelinating hippocampi which targeted AMPA receptors. More functional studies are needed to understand the role of miRNA in regulation of microglial activation. It is possible that miRNAs like miR-124 may play alternative roles in different neural cell types, complicating the understanding of their overall role in the brain. Interestingly, although miR-155 is a known regulator of the peripheral immune response, miR-124 is brain specific, highlighting the fact that there may be important differences between miRNA regulation of the peripheral immune system and neuroinflammation.

Although microglia are the primary immune cells of the brain, astrocytes also become activated by an immune challenge. In astrocytes miR-146 is induced by pro-inflammatory cytokines and serves as a negative feedback mechanism to lower the levels of pro-inflammatory cytokines. Levels of miR-146 correlated negatively with protein expression of IRAK-1 [139]. Work by Tarassishin *et al*. also points to a role for miR-155 in astrocyte responses [140]. As in most other cell types, miR-155 in astrocytes is pro-inflammatory and causes down regulation of SOCS1. In summary, both miR-146 and miR-155 have roles in regulating the inflammatory response to astrocytes and these roles reflect their function in the peripheral immune response. Interestingly, miR-21 is also involved in the astrocytic response to injury, promoting hypertrophy after spinal cord injury [141]. The body of research on miRNA regulation of the astrocytic response to injury is still very small. Whether additional research will identify unique miRNA involved in the astrocytic response remains to be seen.

In addition to regulating the inflammatory response of glial cells, a small number of reports have also identified roles for miRNAs in the recruitment of peripheral immune cells. In one study TNFα induced expression of miR-17 and miR-126. These miRNAs

targeted adhesion molecules E-selectin and ICAM1 respectively. Reduction in E-selectin and ICAM1 by miR-17 and miR-126 lead to decreased endothelial adhesion of neutrophils [142]. This suggests an interesting feedback loop that self-limits the recruitment of neutrophils to sites of injury or inflammation. Neutrophils are recruited to the brain after TBI [28], so miRNAs that regulate this process may be relevant to TBI. In the periphery it has been shown that CCL2 is also target for miR-126, affecting macrophage recruitment [143]. If miR-126 regulated CCL2 in the brain, it may be a mechanism for reducing monocyte recruitment and subsequent inflammation. Overall, it is clear that miRNAs do have roles in neuroinflammation. As in the peripheral immune response miR-155 acts as a proinflammatory miRNA, while miR-146 has an anti-inflammatory effect. However, the neural immune response is not identical to that of the periphery and involves additional players, such as miR-124. While knowledge about miRNA regulation of neuroinflammation is still sparse, it is a growing area of research that holds promise for enhancing our understanding of neuroinflammation.

1.3 TBI and miRNAs

At this time, 6 miRNA profiling experiments have been performed in animal models of TBI [144-149]. While all of these studies identified changes in miRNA after TBI, the specific model and time course of each study varied. Consequently there was very little agreement on miRNA expression between the studies. Additionally, most did not perform any functional studies of miRNA in TBI. One notable exception has been the emerging functional role for miR-21 in TBI. Elevated expression of miR-21 was found in four of the profiling experiments [144, 145, 147, 148]. Redell *et al.* showed that levels of miR-21 targets PDCD4 and Tiam1 showed an inverse relationship with miR-21 expression after TBI [150]. In an *in vitro* model of TBI, primary cortical neurons exposed to scratch injury exhibited elevated levels of miR-21, which had a neuroprotective effect.

Increasing miR-21 decreased PTEN, a negative regulator of the Akt cell survival pathway [151]. Additionally, increasing levels of miR-21 in TBI using an miR-21 agomir improved motor and cognitive function as well as reducing lesion size. Increasing miR-21 reduced apoptosis and increased angiogenesis likely through regulation of the Akt pathway [152]. Expression of miR-21 also increased BBB integrity [153]. These studies point to a critical neuroprotective role for miR-21 in TBI. Interestingly, both exercise and aging affected the expression of miR-21 after TBI. For example, aged mice show decreased induction of miR-21 and increased levels of targets PTEN, PDCD4, TIMP3, and RECK [154]. This suggests that decreased miR-21 induction during aging may contribute to worse prognosis for TBI recovery with increasing age. Conversely exercise improves TBI outcomes, which is associated with increased levels of miR-21. Altogether miR-21 seems to be a promising target for improving TBI recovery. However, the delivery and pharmacokinetic properties of miRNA remain challenging, so future work on miR-21 in TBI will need to take into account these factors.

While the function of other miRNAs in TBI has not yet been evaluated, some factors do alter miRNA expression after experimental TBI. For example hypothermia increases levels of miR-874 and miR-451 [155]. Given that hypothermia is protective after TBI [156, 157], these temperature sensitive miRNA may play a role in the beneficial effect of hypothermia on TBI outcomes. Interestingly, two miRNAs are upregulated in mitochondria after TBI. These were miR-223 and miR-155, both of which have known roles in inflammation [158].

Another area of active research regarding miRNA and TBI is the search for biomarkers. The TBI field is still in need of novel biomarkers, preferably ones that are unique to TBIs, which are commonly accompanied by peripheral injuries, and can predict TBI outcomes [159]. Early studies indicate that serum levels of miR-16, miR-92a, an miR-765 can predict both mild and severe TBI in human patients [160]. Studies in a rat

model of blast induced TBI identified increased levels of let-7i in both the CSF and in serum, suggesting that let-7i is a likely candidate for further biomarker studies in blast induced TBI.

Though the functional roles of miRNA in TBI are just beginning to be uncovered, miR-21 is a striking example of a miRNA that can alter TBI outcomes. Profiling experiments have shown that miRNA levels are altered by TBI in mouse models, but the function of these miRNAs in TBI is largely unknown. Functional experiments on miRNA in TBI could lead to a better understanding, not only of the pathophysiology of TBI, but also the importance of miRNAs in neurological disorders.

1.4 Overview

TBI is a prominent health concern, with a large burden on society. The effects of TBI on an individual can be devastating and life long. Even in the absence of physical or cognitive disability, neuropsychological impairment can result in social exclusion and joblessness. Many recent advances in trauma care have improved survival and TBI outcomes. However, despite significant efforts in TBI research, no pharmacological strategies have been proven to provide therapeutic benefit after TBI. There is an urgent need for identification of new drug targets that could alter TBI outcomes.

Inflammation plays a critical role in TBI pathophysiology. The activation of resident glia by DAMP released from damaged tissue and the recruitment of peripheral immune cells to the brain provides many possible levels of therapeutic interventions. One class of molecules that has an important regulatory role in both neuroinflammation and peripheral immune responses are miRNAs. These post-transcriptional regulators can serve to augment or restrict the inflammatory response. Levels of miRNAs are altered following TBI and at least one miRNA has been shown to alter TBI outcomes in animal models. Further studies on the role of miRNAs, and inflammation-associated

miRNAs in particular, will further our understanding of TBI, neuroinflammation, and miRNA function and could provide novel therapeutic targets for TBI.

Chapter 2: Materials and Methods

2.1 Animals: Mouse strains used are described in Table 2.1. Mice were fed ad libitum and housed with a 12 hour light-dark cycle. All procedures and protocols were approved by the Institutional Animal Care and Use Committee of the University of Nebraska Medical Center and conducted in accordance with the National Institutes of Health Guide for the Care and Use of Laboratory Animals.

2.2 Controlled cortical impact (CCI): CCI surgery was similar to previous reports [161, 162]. For all experiments seven to nine week-old male mice were anesthetized using inhaled isofluorane. For long term behavioral studies (Chapter 7) mice were injected IP with 3 μg buprenorphine for analgesia before surgery. For all experiments mice were given 3.75 μg bupivacaine SC at the incision site prior to surgery for analgesia. Once anesthetized the head of the animal was shaved and placed in a Kopf stereotactic head frame. During surgery anesthesia was maintained with 2% inhaled isofluorane. An incision was made in the scalp and a 4-mm trephine was used to mark the skull 1 mm from the midline midway between lambda and bregma on the left side. A drill was then used to create a craniotomy. The impact was delivered by a Precision Systems and Instrumentation TBI-0310 (Fairfax Station, VA) at a 45° angle from the midline. For all injuries the speed was set to 3.5 m/s with a dwell time of 200 ms. In order to represent different injury severities different depths of injury were used 0.5 mm (moderate) or 1.0 mm severe. After injury a 4 mm square of Surgicel (Johnson & Johnson, Dallas) was placed over the injury site, the removed skull was replaced and adhered with dental cement. The wound was closed with tissue clips and mice were placed on a warming pad until they regained sternal decumbency. For sham controls craniotomy was performed, but no impact was delivered. Naïve animals were not exposed to surgery,

Table 2.1 Information regarding mouse stains

Mouse	Strain	Supplier	Background	Controls	Origin
Wild type	C57Bl/6	Charles River, Wilmington	C57Bl/6	Na	Na
miR-155 KO	B6.Cg-Mir155tm1.1Rsky/J	Jackson Laboratory, Bar Harbor	C57Bl/6	C57Bl/6	Rajewsky [163]
miR-21 KO	129S6-Mir21tm1Yoli/J	Jackson Laboratory, Bar Harbor	C57Bl/6 and 129S	WT littermates or offspring of WT littermates	Li [164]
miR-21 knock-out first	$Mir21a^{tm1Mtm}$	Jackson Laboratory, Bar Harbor	Mixed	Na	McManus [165]
FLP	ROSA26::FLPe knock in	Jackson Laboratory, Bar Harbor	C57Bl/6	Na	Raines and Wilson [166]

drugs, or anesthesia. For long-term experiments (Chapter 3) sham, moderate, and severe animals were administered 3 µg buprenorphine every 8-12 hours for 48 hours post surgery. Animals were randomly chosen for each condition.

2.3 Collection of hippocampal tissue for RNA and protein isolation: Animals were sacrificed at the indicated times by isofluorane overdose followed by decapitation. Brains were removed from the skull and the left and right hippocampi dissected. Samples were frozen in liquid nitrogen and stored at -80°C until RNA isolation was performed. One mL Trizol (Life Technologies, Carlsbad) was added to each hippocampus and samples were homogenized at RT for 5 sec. RNA and protein were then purified as described below.

2.4 RNA and protein isolation: Tissue or cells were homogenized in Trizol (Life Technologies, Carlsbad), followed by addition of 200 µL of chloroform to each sample. Samples were shaken and incubated at RT for 2 min, and centrifuged for 15 min at 12,000 x g at 4°C. The aqueous phase was removed and RNA was precipitated with isopropanol. To pellet RNA samples were centrifuged for 10 min at 12,000 x g at 4°C. The supernatant was removed and pellets were washed with 75% EtOH. After air drying the RNA pellet was resuspended in RNase free water and analyzed by NanoDrop 8000 (Thermo, Waltham) to determine purity and concentration. To isolate protein the phenol phase above was used. First 300 µL of 100% EtOH was added to precipitate DNA and sample was centrifuged 5 min at 7,500 x g and 4°C. The supernatant was then removed and stored at -80°C until protein isolation was performed. 2 mL of 0.3 M GuHCl in 95% EtOH was added and the sample and incubated fro 20 min at RT then centrifuged at 7,500 x g for 5 min at 4°C. The protein pellet was washed three times in GuHCL and once with 100% EtOH then air dried and resuspended in 4% SDS, 100 mM Tris/HCL, 0.1 M DTT pH = 7.6. Samples were sonicated and centrifuged at 10,000 x g for 10 min

at 4°C. Protein samples were stored at -80°C. Protein quantification was performed with Pierce 660 nm protein assay (Thermo, Waltham) according to manufacturers directions.

2.5 cDNA synthesis and real time PCR: For miRNA qPCR TaqMan MicroRNA and Gene Expression Assays (Thermo, Waltham) were used for cDNA synthesis and real time PCR according to manufacturers instructions. For mRNA cDNA synthesis SuperScript III Reverse Transcriptase (Life Technologies, Carlsbad) was used according to manufacturers directions. TaqMan Gene Expression Assays (Thermo, Waltham) were used for qPCR fro mRNA. To normalize gene expression snRNA U6 and GAPDH were used for miRNA and mRNA analyses respectively. Real time PCR and Ct determination was performed using a One Step StepOne Real-Time PCR System (Thermo, Waltham). Fold change was calculated using the delta-delta Ct method. (2 ^ -(($Ct_{miRNA} – Ct_{U6})_{exp}$ - ($Ct_{miRNA} – Ct_{U6})_{control}$)) or (2 ^ -(($Ct_{mRNA} – Ct_{GAPDH})_{exp}$ -($Ct_{mRNA} – Ct_{GAPDH})_{control}$)). A minimum of three biological replicates was used for all experiments. Values are reported as the mean ± SEM. Statistical analysis was determined using Ct values or fold change where appropriate. For experiments with multiple variables statistical analysis was performed using two-way ANOVA, test statistic .05 followed by Bonferroni post hoc testing. For experiments with more than two conditions one-way ANOVA was used, test statistic .05, followed by Dunnett's Multiple comparison test. When comparing two conditions a student's T-test was used, test statistic, .05. Matching was used where appropriate when samples were obtained from the same donor or the same animal.

2.6 SDS-PAGE and Western Blot: Protein samples were loaded onto a 4-12% bis-tris gel and transferred to a nitrocellulose membrane using a semi-dry transfer. The membrane was blocked and incubated overnight at 4°C with primary antibodies (see table 2.2 for antibody sources and concentrations). After washing secondary antibodies

Table 2.2 Antibody information

Antigen	Manufacturer	Host species	Dilution
For immunostaining			
Iba1	Wako	Rb	1:500
GFAP	Dako	Rb	1:500
MAP2 (for ICC)	Sternberger	Ms	1:1000
MAP2 (for IHC)	Abcam	Ckn	1:1000
Synaptophysin	Synaptic Systems	Ms	1:1000
SMI-32	Sternberger	Ms	1:1000
SOX2	Millipore	Rb	1:1000
Nestin	Millipore	Ms	1:1000
For Western			
P-STAT3 (Y705)	Cell Signaling	Rb	1:2000
STAT3	Millipore	Rb	1:1000
PTEN	Cell Signaling	Rb	1:1000
P-Akt (Ser 473)	Cell Signaling	Rb	1:1000
Akt 1/2/3	Santa Cruz	Rb	1:1000
SOCS1	Thermo	Rb	1:1000
Caspase 3	Cell Signaling	Rb	1:1000

were incubated for 1 hour at RT. For peroxidase secondary antibodies ECL substrate was used to develop the membrane, imaging and analyses was performed using a Carestream Imaging system (Carestream, Rochester). For secondary antibodies labeled with infrared dyes, imaging and analysis was performed with an Odyssey Imaging System (LI-COR, Lincoln). Significance was calculated using a student's T-test, test statistic .05.

2.7 Histology on formalin fixed paraffin embedded tissue: Animals were sacrificed at indicated times after injury. Brains were removed and fixed in 4% paraformaldehyde. overnight, paraffin embedded, and cut into 5-μm slices using a microtome. Before staining slides were warmed to 60°C for one hour then allowed to cool. Slides were cleared with xylene then dehydrated through graded ethanol washes.

2.7.1 Luxol fast blue staining: After hydration to 95% ethanol slides were stained with filtered 0.1% Luxol fast blue in a solution of 0.5% acetic acid at 60°C overnight. The next day slides were rinsed in 95% ethanol followed by distilled water then differentiated in 0.05% lithium carbonate for one min and 70% ethanol for 1 min. Slides were counterstained with 0.5% cresyl violet for 30 min at 60°C, rinsed in distilled H_2O, and differentiated in 95% ethanol for 5 min. Coverslips were mounted using Cytoseal (Thermo, Waltham). Slide scanning was performed by the UNMC tissue sciences facility using a Ventana's Coreo Au Slide Scanner at 40x magnification.

2.7.2 Terminal deoxynucleotidyl transferase dUTP nick end labeling (TUNEL): ApopTag Peroxidase *In situ* apoptosis detection kit (Millipore, Temecula) was used for TUNEL staining according to manufacturer's directions in conjunction with TSA plus cyanine 5 kit (PerkinElmer, Waltham). Briefly, hydrated slides were treated with 20

µg/mL proteinase K, then terminal deoxynucleotidyl transferase (TdT) was used to transfer digoxigenin (DIG) labeled nucleotides onto fragmented DNA. The tail of DIG labeled nucleotides was then detected using an anti-DIG antibody conjugated to peroxidase. A TSA plus cyanine 5 kit (PerkinElmer, Waltham) was used to develop the fluorescent stain. Coverslips were mouned onto slides using prolong Gold Antifade Mountant with DAPI (Life Technologies, Carlsbad) and imaged using a Zeiss Observer.Z1 microscope.

6.7.3 Immunohistochemistry: Staining was performed as described by Yelamanchili et al. [167]. Tissue was hydrated with a graded alcohol series. Antigen retrieval was performed with citrate buffer pH 6 at 90° C for 40 min and washed. Tissue was blocked in a solution of 1% BSA and 3% NGS in PBS, and incubated with primary antibody overnight at 4°C. Primary antibodies used are described in Table 2.2. The following day tissue was washed with TBS and incubated with 3% H_20_2 in PBS for 10 min. After thorough washing tissue was incubated with anti-Rabbit secondary labeled with a peroxidase enzyme (ImmPRESS, Vector labs, Burlingame) for one hour, rinsed, and developed with DAB Plus substrate system (Thermo, Waltham) for 10 min. Tissue was then washed with TBS, stained with haematoxylin, and dehydrated. Coverslips were mounted with cytoseal (Thermo, Waltham).

2.7.4 *In situ* hybridization: *In situ* hybridization procedure was similar to that described by Chaudhuri *et al.* [168] Care was taken at all steps to avoid RNase contamination and solutions were all made with Diethylpyrocarbonate (DEPC) treated water. Tissues were first cleared with xylene and hydrated with a graded ethanol series, and then citrate antigen retrieval was performed. To crosslink miRNA and improve stability, tissue was treated with 0.16 M ethylcarbodiimide (EDC) in 0.13 M 1-methylimidazole, 300 mM NaCl

pH 8.0. After several washes, tissue was incubated in hybridization buffer (50% deionized formamide, 10 mL Tris-HCl, .25% SDS, 1 x Denhardt's solution, 600 mM NaCl, 1 mM EDTA and 200 µg/mL yeast tRNA) at 37°C. Afterwards, tissue was hybridized with 5' and 3' digoxin labeled locked nucleic aced probes (Exiqon,Vedbæk) at a concentration of 4 pM per 100 µM overnight at 37°C. Tissues were then washed with 2 x and .2 x saline sodium citrate buffer at 42°C. To quench endogenous peroxidase tissues were treated with 3% H_2O_2 in PBS for 10 min. After thorough washing tissue was blocked with 1% bovine serum albumin (BSA) and 3% goat serum in phosphate buffered saline (PBS). Tissues were incubated at 4°C overnight with anti-digoxigenin-POD, Fab fragments (Roche, Basel) at a concentration of 1:100. In experiments where dual immunohistochemistry and *in situ* hybridization were used antibodies to cell-type specific markers were included in the overnight incubation. Antibodies used were MAP2 (Abcam, Cambridge) (1:1000), GFAP (Dako, Brasschaat) (1:500) and Iba1 (Wako, Kampenhout) (1:500). Corresponding Alex Fluor secondary antibodies (Invitrogen, Carlsbad) were incubated for one hour. Afterwards the peroxidase signal was amplified using the TSA plus cyanine 5 (PerkinElmer, Waltham). Tissues were stained with DAPI and coverslips mounted with proLong Gold Antifade Mountant with DAPI (Life Technologies, Carlsbad) and imaged using a Zeiss Observer.Z1 microscope.

2.8 Cryosectioning: At indicated times after injury animals were anesthetized with isofluorane followed by transcardial perfusion. First animals were perfused with PBS with 2.5% sucrose. Then animals were perfused with 4% paraformaldehyde (PFA), 2.5% sucrose, and PBS. After perfusion brains were post-fixed in 4% PFA with 2.5% sucrose in PBS. After 24 hours brains were transferred to 30% sucrose and stored at 4°C until they sunk, ~3 days. Brains were frozen using 2 methyl butane on dry ice and stored at -80°C until they were sectioned on a cryostat. A 4 mm coronal section, including the

injury site was sectioned into 50 μM slices and every fifth section was collected in 0.1 M phosphate buffer.

2.9 Fluoro-Jade C staining: Free-floating cryosections were mounted on gelatin coated slides and air dried overnight. Slides were incubated in .06% potassium permanganate followed by .0001% Fluoro-Jade C (Histochem, Jefferson) and .0001% DAPI (Sigma, St. Louis) in 1% acetic acid. Tissue was then dried in a 60°C oven and incubated in zylene for 1 min, then coverslips were mounted with DPX (Sigma, St. Louis). A Zeiss Observer.Z1 microscope was used for imaging. Three slices between bregma -2.5 and -1.5 were imaged for quantification. For cortex three images were taken in the boundary zone for each slice. For the hippocampus each of the three slices per slide images were taken of the dentate gyrus, CA3, and CA1 regions. Fluorojade C positive cells were counted using Image J[169] by a blinded observer. The average number of fluorojade positive cells per slice is reported. Significance was calculated using a student's T-test, test statistic .05.

2.10 Immunohistochemisty: Free-floating cryosections were incubated with 3% H_2O_2 to quench endogenous peroxidase. After thorough washing sections were blocked with 10% NGS + 0.3% TX in PBS. Tissues were incubated with Iba1 (Wako, Kampenhout) (1:500) in 0.3% TX +3% NGS in PBS at 4°C overnight. ImmPRESS HRP Anti-Rabbit IgG (Vector labs, Burlingame) was used as a secondary and DAB Plus substrate system (Thermo, Waltham) was used for developing. Sections were then mounted on gelatin-coated slides, allowed to dry overnight, incubated in xylene for 1 min, and mounted with cytoseal (Thermo, Waltham). Slides were imaged using a light microscope at 100 x magnification. Images were quantified using Image J [169] to calculate the percent area covered by Iba1 staining in

the hippocampus and cortex. Student's t-test was used to calculate significance, test statistic of .05.

2.11 Behavioral testing: Mice were allowed to acclimate to the testing room for 30 min prior to any behavioral testing. All testing was performed between the hours of 10:00 and 16:00 by a single technician. Whenever possible testing was arranged so that the least stressful tests were done first to reduce confounding factors. Values are reported as the mean ± SEM. For experiments with multiple variables statistical analysis was performed using two-way ANOVA, test statistic .05 followed by Bonferroni post hoc testing. For experiments with more than two conditions one-way ANOVA was used, test statistic .05, followed by Tukey's post hoc testing. When comparing two conditions a student's T-test was used, test statistic, .05.

2.11.1. Rotarod: Testing of mice on the accelerating rotarod apparatus was performed with or without training before injury. A seven cm rotarod was used. For testing in the acute to sub-acute phase, mice were trained on the rotarod for 3 days, injury then 1, 3, 5, and 7 days post injury. For testing in the chronic phase testing was performed without training on 3 consecutive days. On the first day of training (acute phase) or testing (chronic phase) mice were allowed to habituate to the rotarod apparatus for 5 min prior to the first trial. For all studies the rotarod apparatus was set to accelerate from 0-35 rpm in 2 min, testing was stopped after 2 min. Mice were tested 3 times a day and allowed to rest for a minimum of 30 min between tests. The latency to fall was detected by weight-based sensors and recorded. The average latency to fall for three trials was averaged for each day. Procedure was similar to that performed by O'Connor *et al.*[170]

2.11.2. Elevated zero maze: The behavior of mice in an open field maze (34 cm inner diameter, 46 cm outer diameter, on 4 braced legs 40 cm off the ground) was recorded for 6 minutes. Between trials the equipment was cleaned with 70% EtOH. Testing was similar to that described in Heisler et al [171].

2.11.3. Open field: individual mice were placed into a white 50 x 50 x 38 cm arena and their behavior was recorded for either 20 min for testing in the chronic phase or for 10 min for acute phase testing. The arena was cleaned with 70% EtOH between trials.

2.11.4. Novel object: Novel object testing was performed in the same 50 x 50 x 38 cm white arena as used for open field testing. Novel object testing was always performed after open field testing so that mice would be acclimated to the arena. First the mouse was placed into the arena with two identical objects placed in different corners and recorded for 5 min. Second, the mouse was moved back to its home cage for an interval of 3 hours. Third, the mouse was placed back into the arena, but one of the two identical objects was replaced with a novel object. Again the exploratory behavior of the mouse was recorded for 5 min. Before the first round of testing and between each round, both the objects and arena were cleaned with 5% acetic acid followed by water to reduce the scent of previous test subjects.

2.11.5. Social interaction: Experimental mice were matched with a same-sex conspecific of similar size. The experimental mouse and then the test mouse were placed in opposite corners of a neutral cage with clean bedding. The interactions between the two mice were recorded for 20 min. Bedding was replaced and cage cleaned with 70% EtOH between each trial. A blinded observer recorded duration of time

spent in proximity as well as frequency of proximity, genital sniff, face sniff, chase, wrestle, and tail rattle using Stopwatch software (Georgia State University).

2.11.6. Tail suspension: Mice were suspended from the tail from a 1.2 cm diameter metal bar 30 cm off the table for 6 min and their behavior recorded. Time spent mobile versus immobile was scored by a blinded observer using Stopwatch software (Georgia State University). Procedure was similar to that reported by Heisler *et al*.[171]

2.11.7. Neurological Severity Score Testing. Mice were tested 3 days post injury as described in Flierl *et al.* [172]. Mice were scored on their ability to perform the described tasks. Inability to complete the task resulted in a score of one. These scores were added together to give the neurological severity score [87] with a maximum score of 10. For the beam walking component the mice were placed on a platform connected to another platform by a 3 cm beam and given three min to cross to the opposite platform. Failure to do so resulted in a score of 3. If the mouse successfully crossed the first beam, it was replaced with a second beam, this time of 2 cm width. If the mouse was not able to cross the 2 cm beam it was given a score of 2. If the mouse was able to cross the 2 cm beam, the beam was replaced by a 1 cm beam. Failure to cross this beam resulted in a sore of 1. Ability to cross all three beams resulted in a score of 0.

2.12 Human NPC and Neuronal culture: Cells were obtained from UNMC tissue core facility. This work is in accordance with IRB and ESGRO guidelines, approval number 546-11-ES. Culture conditions were similar to reported previously [173]. Cells were plated either in suspension with growth factor rich medium to generate human neural progenitor cell (hNPC) cultures or on poly-D-lysine coated plates with neuronal medium for human neuronal cultures (hNeu). Both culture were grown at 37°C, with 5% O_2 and

5% CO_2 in a humidified incubator Media components are listed in Table 2.3. For neuronal cultures, media was half exchanged every 3-4 days. For hNPC, media was changed every other day. NPC cultures were characterized by immunocytochemistry for NPC markers Nestin (Millipore, Billerica) and Sox2 (Millipore, Billerica). To verify multipotency neurospheres were dissociated and plated onto Matrigel (Corning, Corning) coated coverslips, then cultured in a minimal media of X-VIVO-15 (Lonza, Basel) and N2 (Life Technologies, Carlsbad) for 14 days, presence of astrocyte marker GFAP (Dako) and neuronal marker MAP2 (Sternberger) was verified by immunocytochemisty. For comparison of hNPC and hNeu, RNA was isolated from NPC after 7 div and neurons after 14 div. Neurons were treated with 10 ng/mL of IL-6 or CNTF at 13 div. and harvested 24 hours later for RNA purification. For measurement of P-STAT3 hNeu were treated with 10 ng/mL IL-6 or CNTF for 0, 15, or 30 min on div 14. For inhibitor experiments hNeu were treated with 1 μM Stattic (Sigma, St. Louis) 30 min prior to cytokine treatment, then harvested 24 hours later. Before cytokine or inhibitor treatments hNPC were dissociated from neurospheres and plated onto Matrigel (Corning, Corning) coated coverslips. To measure STAT3 activation hNPC were treated with 10 ng/mL CNTF for 30 min. For inhibitor experiments hNPC were treated with 2.5 μM Stattic or .6 nM Jak1 inhibitor for 48 hours.

2.13 Mouse NPC and neuronal culture: E14 mouse brains were digested with trypsin, mechanically dissociated and plated in suspension culture in growth media for mouse NPC culture (mNPC) or on poly-D-lysine coated plates in neuronal media for neuronal cultures. Media are listed in Table 2.3. Media was supplemented every 3rd day and after 7 days neurospheres were harvested for RNA purification. mNeu were grown *in vitro* 14 days before harvesting for RNA purification. Both culture were grown at 37°C, with 5%

O_2 and 5% CO_2 in a humidified incubator. Cells were harvested for RNA purification using Trizol (Life Technologies, Carlsbad) and stored at -80°C.

2.14 SH-SY5Y culture. SH-SY5Y cells were grown in DMEM/F12 with GlutaMAX (Thermo, Waltham) and 10% FBS at 37°C at 5% CO_2 in a humidified incubator. For differentiation, cells were treated for 4 days with 10 μM retinoic acid. Cells were harvested for RNA purification using Trizol (Life Technologies, Carlsbad) and stored at -80°C.

2.15 Preparation of hippocampal slices for electrophysiology: Hippocampal slices were prepared as reported previously [174]. Four to six-week old male miR-21 KO and WT littermates were anesthetized with isofluorane. Brains were quickly removed and placed in oxygenated artificial cerebrospinal fluid (ACSF). Components of cutting-ACSF (in mM): $C_5H_{14}ClNO$ (110.0), NaH_2PO_3 (1.25), KCl (2.5), $MgSO_4$ (7.0), $CaCl_2$ (0.2), $C_6H_7NaO_6$ (11.6), $C_3H_3NaO_3$ (3.1), $NaHCO_3$ (25.0), Dextrose (25.0), equilibrated with 95% O_2 and 5% CO_2, osmolarity 310 ± 10. Hippocampi were dissected and 400 μm-transverse slices were made using a tissue chopper. Hippocampi were placed on a mesh support and equilibriated to oxygenated recording-ACSF for at least one hour prior to recording. Components of recording-ACSF (in mM): NaCl (125.0), KCl (3.0), $CaCl_2$ (2.0), $MgCl_2$ (1.2), NaH_2PO_3 (1.25), $NaHCO_3$ (26.0) and glucose (10.0), osmolarity 300 ± 10. Before recording, individual slices were transferred to the recording chamber. The recording chamber was perfused with recording 30 ± 1°C ACSF at a rate of 2 mL/min.

2.16 Recording of long-term potentiation: Recording was performed as reported previously [174]. Constant current stimulation (0.05 Hz, 50–400 μA) was applied to the Schaffer collateral-commissural fibers using an insulated bipolar tungsten electrode to

Table 2.3 Media for primary neural cultures

Species	**Neuron**	**NPC**
Mouse	50% DMEM/F12 w/ GlutaMAX 50% DMEM 1x B27	DMEM/F12 w/ GlutaMAX 1 x N2 20 ng/mL $bFGF_2$
Human	Neurobasal 1 x B27-AO 0.5 mM L-Glutamine	X-VIVO-15 20 ng/ mL $bFGF_2$ 20 ng/ mL EGF 10 ng/ mL LIF 60 ng/ mL N-acetyl cysteine 1 x NSF1 1 x N2

elicit a field excitatory post-synaptic potential (fEPSP) in the CA1 stratum radium. fEPSPs were recorded using glass recording electrodes with a diameter of 2.5 – 5 µm and an Axopatch-1D amplifier (Molecular Devices, Sunnyvale). Intensity of stimulation was adjusted to generate 50% maximal response. Baseline response was recorded for at least 20 min prior to high frequency stimulation (HFS). HFS was 100 Hz, 500 ms delivered twice in a 20 s interval. After HFS response was recorded for 40 min to determine LTP. Three sweeps were averaged for each recording. Electrical signals were filtered at 1kHz and digitized at 3.5 kHz using a Digidata 1320 interface (Molecular Devices). Data were analyzed with pCLAMP 10 software (Molecular Devices). The initial slope of the fEPSP was determined and the average fEPSP for baseline recordings was set as 100. Data expressed as the mean ± SEM.

2.17 Excitotoxicity assays: Hippocampal neurons were isolated from miR-21 KO and WT P0 mouse pups as described by Beaudoin *et al.* [175]. Briefly, hippocampi were dissected and digested with .25% trypsin in HBSS for 20 min at 37°C, then washed and triturated. Cells were filtered with a 70 µm filter and plated in neuronal media consisting of Neurobasal media (Thermo, Waltham), 1x B27 (Thermo, Waltham), and 0.5 mM L-glutamine. A full media exchange was done 15 min after plating on poly-D-lysine coated plates to remove cell debris. 1/3 media exchange was performed every 3-4 days. On div 13 neurons were treated with NMDA at specified concentrations with 10 µM glycine in artificial CSF (1.3 mM CaCl2, 5.4 mM KCl, 140 mM NaCl2, 33 mM glucose, 25 mM HEPES acid, pH 7.35) for 30 min at 37°C. After 30 min conditioned media was returned to the wells. To determine toxicity alamarBlue (Invitrogen, Carlsbad) and lactate dehydrogenase [176] assays were used. 24 hours after treatment positive control wells were treated with 2% triton-X for 15 min at 37°C, 100 µL of neuronal medium was removed and 50 µL was used for LDH assay using the Cytotoxicity Detection Kit (Roche,

Basel) according to manufacturers directions. Percent Cytotoxicity was calculated by subtracting the no treatment control from the experimental and dividing by the triton-x positive control. For alamarBlue assay 10 µL alamarBlue (Invitrogen, Carlsbad) was added to the100 µL remaining in each well. After 2 hours at 37°C fluorescence was measured at 540 nm excitation and 590 nm emission for 5s. Percent viability was calculated by dividing the fluorescence at 590 of the experimental condition by the no treatment control. Values are reported as the mean ± SEM. Statistical analysis was performed using two-way ANOVA, test statistic .05.

2.18 Extracellular vesicle isolation: Extracellular vesicles were isolated from brains as described previously [177] using a method adapted from Perez-Gonzalez *et al.* [178]. Seven days after injury animals were anesthetized with isoflurane and decapitated. Brains were extracted, cerebellum and brain stem were removed and the two hemispheres separated. For each sample 4 ipsilateral or 4 contralateral hemispheres were pooled. In total 12 mice for each condition were utilized. This resulted in 3 pooled samples of each hemisphere from TBI mice and 3 pooled samples of each hemisphere from sham surgery controls, for a total of 12 samples altogether. After removal, tissue was snap frozen in liquid nitrogen and stored at -80°C. Samples were thawed and digested in 20 units/ml papain in Hibernate A (Life Technologies, Carlsbad), enzymatic digestion was stopped by addition of cold Hibernate A, and the solution was further homogenized by trituration. Tissue fragments were removed by centrifugation and the supernatant passed through a series of successively finer filters (40 µm, 5 µm, and 0.2 µm). Remaining cell fragments were removed by centrifugation and the EV containing supernatant was submitted to several PBS washes followed by ultra-centrifugation. A sucrose gradient was established using five concentrations of sucrose ranging from 0.25 M to 2 M. The extracellular vesicle pellet was re-suspended in the middle concentration

(0.95 M), inserted into the gradient, and centrifuged at 200,000 × *g* for 16 hours at 4°C. The extracellular vesicle containing central sections of the sucrose gradient were removed and re-suspended to a total volume of 30 ml with PBS.

2.19 EV-RNA isolation and sequencing: The suspensions from the EV isolation were subjected to ultra-centrifugation to pellet the EV. The pellets were then subjected to miRNA extraction using the mirVana miRNA Isolation Kit (Life Technologies, Carlsbad) following the manufacturer's instructions. RNA samples were then sent to LC Sciences (Houston) for miRNA sequencing. Venny (http://bioinfogp.cnb.csic.es/tools/venny/) was used to create Venn diagrams

2.20 Electron Microscopy: To validate the purity of EV isolation three hemispheres from three mice were pooled and snap frozen in liquid nitrogen and stored at -80°C. EV isolation was performed as described above and the sample was submitted to the University of Nebraska Medical Center Electron Microscopy Core Facility to undergo microscopy by a FEI Tecnai G2 Spirit transmission electron microscope.

Chapter 3: Expression of inflammation-associated miRNA in a controlled cortical impact (CCI) model of TBI

3.1 Background: Neuroinflammation contributes to neurological dysfunction after TBI [179]. However, to date clinical trials targeting neuroinflammation in TBI have been unsuccessful. Identifying new regulators of neuroinflammation in TBI would provide a better understanding of TBI pathophysiology and provide possible therapeutic targets. It has recently been discovered that in peripheral immune responses miRNAs play critical role in modulating inflammation [180, 181]. However, the expression of inflammation-associated miRNA has not been examined in TBI. Several profiling studies have examined the expression of miRNA after TBI in various models [144-149], but very little is known about the functional role of miRNAs in TBI. Well-known miRNA regulators of the immune response, miR-155 and miR-146, miR-223 and miR-21 were all elevated in at least one report describing miRNA profiling following TBI; but there is a large degree of inconsistency due to differences in models, species, and times after injury [144-149]. The aim of this work was to determine whether inflammation-associated miRNAs were elevated in our CCI mouse model, characterize their temporal expression after CCI and examine their relationship to pro-inflammatory cytokine expression.

3.2 Results:

3.2.1 Identification of appropriate anatomical region for studies of inflammation-associated miRNAs

Before examining miRNA levels a survey of CCI pathology was performed. These studies allowed us to determine the temporal profile of glial activation, cell death, neuronal degeneration, and axonal injury after TBI. The overall aim was to determine appropriate anatomical regions and time points for examination of inflammation-

associated miRNAs. Many inflammation-associated miRNAs also have roles in apoptosis, especially miR-21 [182] and miR-155 [183, 184]. Therefore we wanted to identify areas of the injured brain that: 1) lacked significant apoptotic cell death and tissue loss, 2) showed robust inflammation and 3) had evident neuronal pathology. To achieve this we examined the brains of mice 1, 3, and 7 days after CCI using various histological methods.

In the unilateral model of CCI used for these studies the injury was induced in the parietal cortex between lambda and bregma on the left side. The hippocampus is just deep to this injury site. To visualize tissue loss and white matter pathology in various neuroanatomical regions we performed luxol fast blue staining in conjunction with cresyl violet. Luxol fast blue is a myelin stain used to show demyelination and cresyl violet stains the Nissl substance, or rough endoplasmic reticulum, found at high concentrations as a granular mass in neuronal cell bodies. After both moderate (0.5 mm injury depth) and severe (1.0 mm injury depth) CCI there was significant damage to the corpus callosum, particularly at 7 days after injury (Fig. 3.1). Severe injury showed a greater amount of cortical loss and more hippocampal involvement as well as enlargement of the lateral ventricle. Even in craniotomy only controls some cortical tissue loss was observed. This is consistent with reports of other groups showing that craniotomy alone can induce mild traumatic brain injury [185, 186]. To determine sites of apoptotic cell death after CCI terminal deoxynucleotidyl transferase dUTP nick end labeling (TUNEL) was performed. The majority of TUNEL positive cells were found in the cortical boundary zone at the edge of the lesion (Fig. 3.2). Combined, the loss of cortical tissue and the concentration of TUNEL positive cells in the cortex raised serious concerns for examination of inflammation-associated miRNA in this region. Several inflammation-associated miRNAs also have roles in regulation of apoptotic signaling. Therefore, it would be difficult to differentiate these two functions in lesioned cortical tissue. In

Figure 3.1

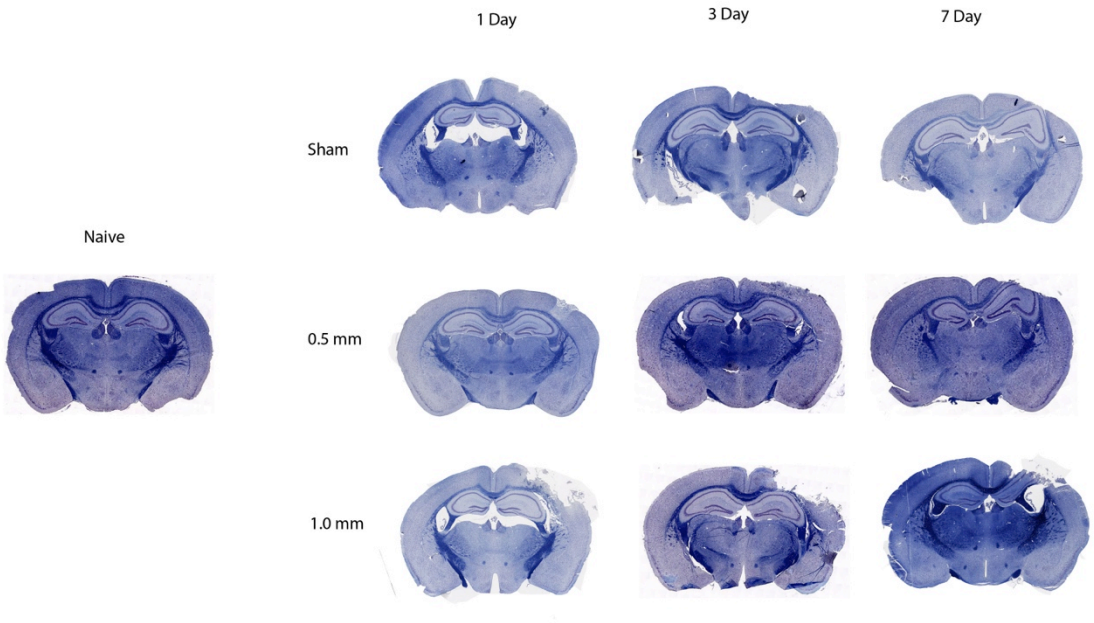

Figure 3.1 Anatomical characterization of CCI. Myelin (Blue) and Nissl (Purple) staining of mouse brains 1, 3, or 7 days after craniotomy only (Sham), Moderate CCI (0.5 mm), and Severe CCI (1.0 mm). Naïve brain is shown for comparison. Staining was performed in duplicate, representative images are shown.

Figure 3.2

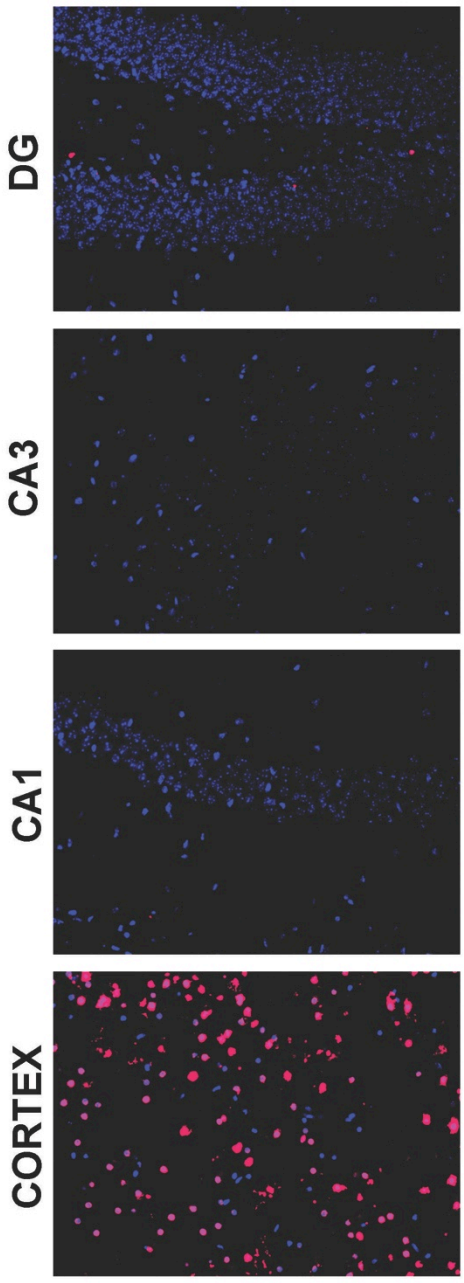

Figure 3.2 Apoptotic cell death in the hippocampus and cortex after moderate CCI. Staining for apoptotic cells using TUNEL (magenta). DAPI was used to stain the nucleus (blue). Images were from ipsilateral hemisphere 1 day after moderate CCI (0.5 mm) in the sub regions of the hippocampus (dentate gyrus (DG), CA1, and CA3) and the lesion boundary of the cortex. Original magnification 400x.

contrast, the hippocampus had barely detectable levels of TUNEL positive cells and did not show tissue loss. While lack of tissue loss and apoptotic cells satisfied the first criteria, it was also important that the anatomical region used for analyses showed evidence of a robust inflammatory response.

Next, to identify anatomical regions that met the criteria of robust glial activation we examined expression of ionized calcium binding adaptor molecule 1 (Iba1) and glial fibrillary acidic protein (GFAP) by immunohistochemistry. Reactive microglia were identified by increased Iba1 staining and bushy or ameboid morphology (Fig. 3.3). It is important to note that activated microglia cannot be differentiated from invading mononuclear cells using this method. Increased staining with Iba1 was seen in the ipsilateral cortex and hippocampus 1 and 3 days after injury. To identify activated astrocytes we used glial GFAP staining (Fig. 3.4). Both protoplasmic astrocytes in the cortex and hippocampus and fibrous astrocytes in the corpus callosum showed increased GFAP expression. The GFAP staining in the ipsilateral cortex and hippocampus was highest 3 and 7 days after injury. Interestingly, GFAP expression was also increased in the ipsilateral cortex of craniotomy only animals 1 day after injury, suggesting again that craniotomy induces a mild traumatic brain injury. Also striking was increased GFAP expression in the contralateral corpus callosum after TBI. Increased Iba1 and GFAP staining was seen in both the ipsilateral cortex and hippocampus. Contralateral hemispheres also showed some increase in glial activation, however, it was much less dramatic. While the cortex of craniotomy only controls showed increased astrocyte reactivity, the hippocampus did not. Therefore, both the cortex and hippocampus meet the criteria of robust glial response after CCI.

In addition to changes in glial activation, we wanted to determine regions of evident neuronal pathology. Staining of neurons with microtubule associated protein 2 (MAP2) and synaptophysin revealed loss of these important neuronal markers in the

Figure 3.3

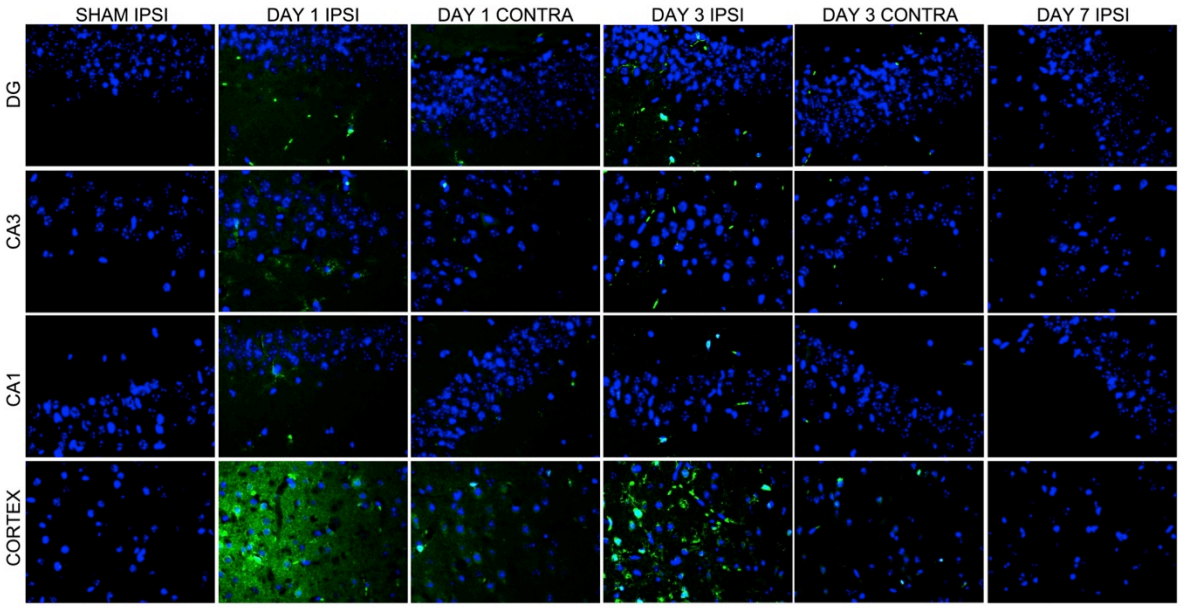
SHAM IPSI
DAY 1 IPSI
DAY 1 CONTRA
DAY 3 IPSI
DAY 3 CONTRA
DAY 7 IPSI
DG
CA3
CA1
CORTEX

Figure 3.3 Microglial and macrophage activation at various times after moderate CCI in the hippocampus and cortex. Staining for Iba1 positive microglia and macrophages (green). DAPI was used to stain the nucleus (Blue). Images were taken from ipsilateral (IPSI) and contralateral (CONTRA) hemisphere. Mice were sacrificed 1, 3, or 7 days after moderate CCI (0.5 mm) or 1 day after craniotomy (SHAM) and compared to naïve controls. Hippocampus sub regions (dentate gyrus (DG), CA1, and CA3) and the lesion boundary of the cortex are shown. Original magnification 400x. Staining was performed in duplicate, representative images are shown.

Figure 3.4

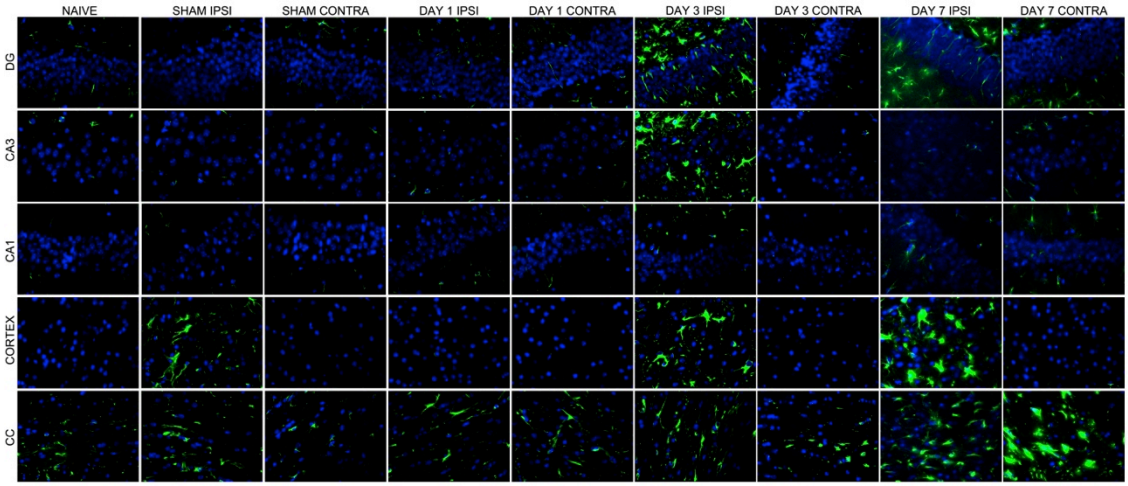
NAIVE
SHAM IPSI
SHAM CONTRA
DAY 1 IPSI
DAY 1 CONTRA
DAY 3 IPSI
DAY 3 CONTRA
DAY 7 IPSI
DAY 7 CONTRA
DG
CA3
CA1
CORTEX
CC

Figure 3.4 Astrocyte activation at various times after moderate CCI in the hippocampus and cortex. Staining for GFAP positive astrocytes (green). DAPI was used to stain the nucleus. Images were taken from ipsilateral (IPSI) and contralateral (CONTRA) hemisphere. Mice were sacrificed 1, 3, or 7 days after moderate CCI (0.5 mm) or 1 day after craniotomy (SHAM) and compared to naïve controls. Hippocampus sub regions (dentate gyrus (DG), CA1, and CA3) and the lesion boundary of the cortex are shown. Original magnification 400x. Staining was performed in duplicate, representative images are shown.

injury boundary zone after CCI but not in craniotomy only controls (Fig. 3.5). Interestingly CCI increased the expression of both MAP2 and synaptophysin in the cortex and hippocampus not directly involved in the lesion (Fig. 3.6) Interestingly, increased synaptophysin staining was also seen by Shojo and Kibayashi after fluid percussion injury [187]. They concluded that increased synaptophysin staining was due to accumulation of synaptic vesicles and corresponded with neurodegeneration. Finally, white matter damage was visualized using SMI-32, an antibody that recognizes dephosphorylated neurofilament-H and serves as a marker of white matter damage [188]. A strong increase in SMI-32 staining was observed in the corpus callosum and hippocampal alveus both white matter tracts which are deep to the injury site at all time points after CCI, while little to no staining was observed in craniotomy only controls (Fig 3.7). While not as profound, SMI-32 reactivity was also found in the contralateral hemispheres. Interestingly, SMI-32 staining increased from 3 to 7 days in the ipsilateral white matter tracts. Other groups have also reported progressive increase in SMI-32 staining from 3-7 days after CCI [189]. Together with the progressive white matter damage at seen at day 7 shown with luxol fast blue staining, increased SMI-32 staining at day 7 suggests progressive white matter damage. The combination of white matter degeneration and changes in expression of neuronal proteins is sufficient to suggest evident neuropathology in both the cortex and hippocampus. Therefore both these regions satisfy the third critera for examination of inflammation-associate miRNAs.

Overall, these data paint a portrait of CCI induced pathology and allowed us to determine an appropriate anatomical region for the study of inflammation-associated miRNAs. For the study of inflammation-associated miRNAs we proposed that an anatomical region meet three criteria: 1) lack significant apoptotic cell death and tissue loss, 2) show robust inflammation and 3) have evident neuronal pathology. While both the cortex and hippocampus showed increases in activated glia, the cortex was the site

Figure 3.5

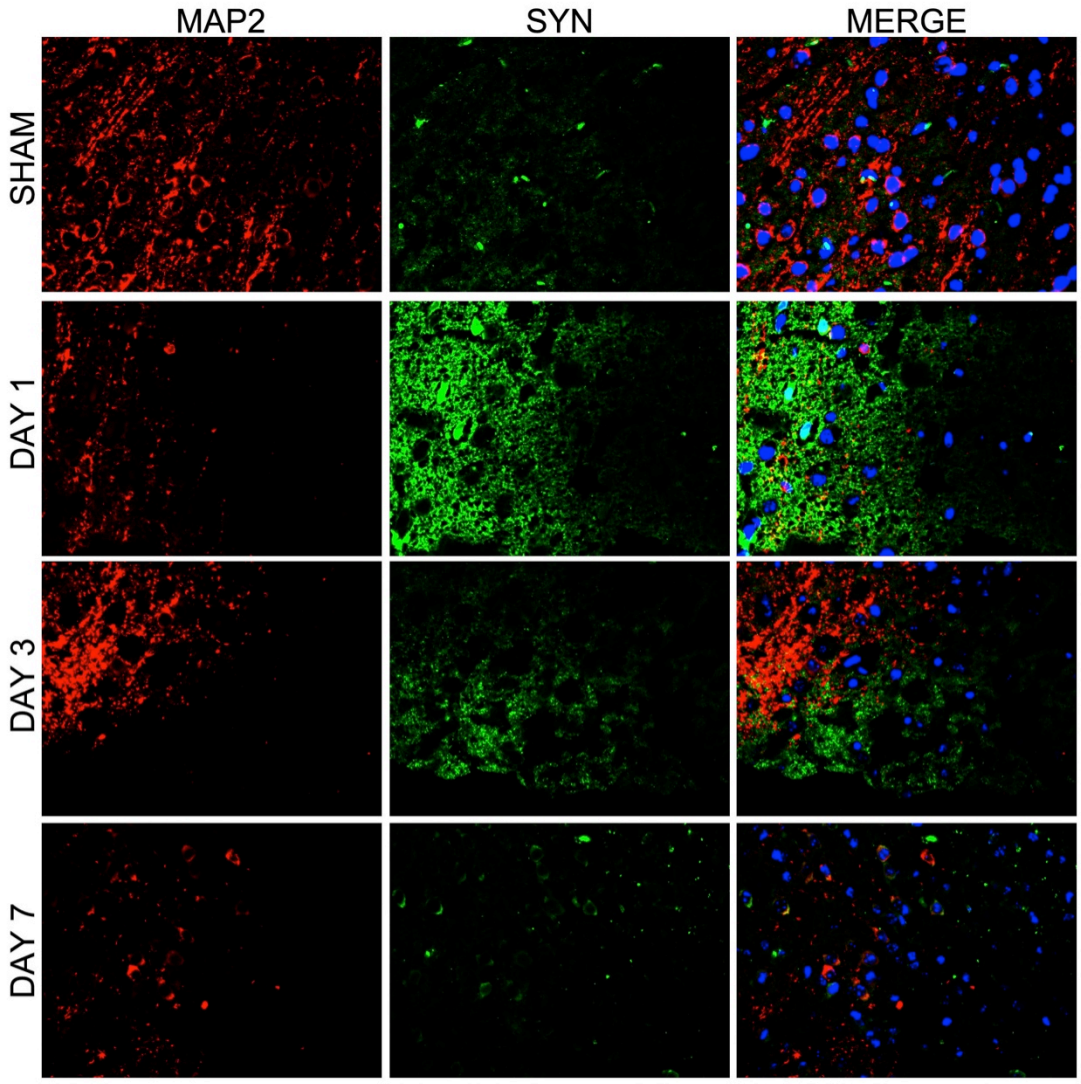

Figure 3.5 Loss of neuronal markers at the lesion site. Staining for neuronal markers MAP2 (red) and Synaptophysin (green). DAPI was used to stain the nucleus. Images were taken at the edge of the lesion and the lesion boundary in the injured hemisphere. Mice were sacrificed 1, 3, or 7 days after moderate CCI (0.5 mm) or 1 day after craniotomy (SHAM). Original magnification 400x. Staining was performed in duplicate, representative images are shown.

Figure 3.6

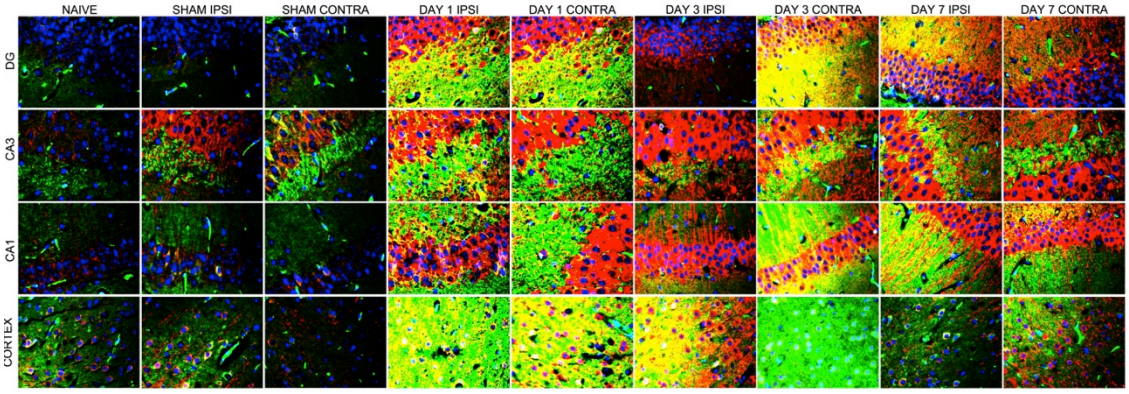
NAIVE
SHAM IPSI
SHAM CONTRA
DAY 1 IPSI
DAY 1 CONTRA
DAY 3 IPSI
DAY 3 CONTRA
DAY 7 IPSI
DAY 7 CONTRA
DG
CA3
CA1
CORTEX

Figure 3.6. Increase in neuronal markers after moderate CCI. Staining for neuronal markers MAP2 (red) and Synaptophysin (green). DAPI was used to stain the nucleus. Images were taken from ipsilateral (IPSI) and contralateral (CONTRA) hemisphere. Mice were sacrificed 1, 3, or 7 days after moderate CCI (0.5 mm) or 1 day after craniotomy (SHAM) and compared to naïve controls. Hippocampus sub regions (dentate gyrus (DG), CA1, and CA3) and the lesion boundary of the cortex are shown. Original magnification 400x. Staining was performed in duplicate, representative images are shown.

Figure 3.7

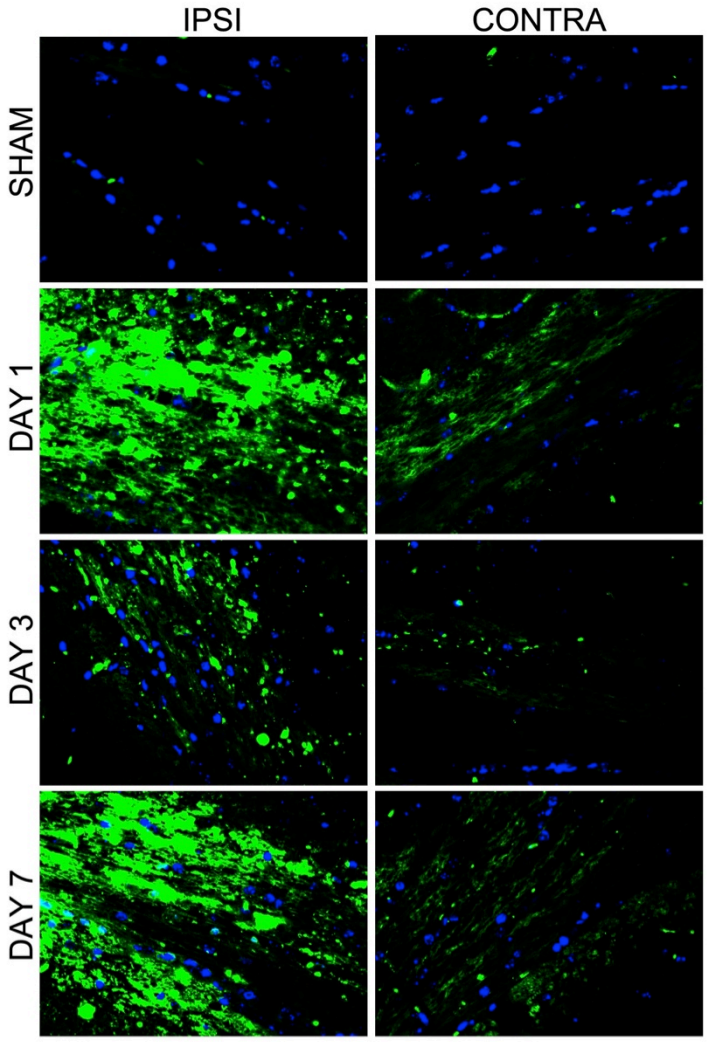

Figure 3.7. White matter damage after moderate CCI. Staining with SMI-32, a marker of axonal damage (green). DAPI was used to stain the nucleus. Images were taken from ipsilateral (IPSI) and contralateral (CONTRA) hemisphere. Mice were sacrificed 1, 3, or 7 days after moderate CCI (0.5 mm) or 1 day after craniotomy (SHAM) and compared to naïve controls. Hippocampus sub regions (dentate gyrus (DG), CA1, and CA3) and the lesion boundary of the cortex are shown. Original magnification 400x. Staining was performed in duplicate, representative images are shown.

of the majority of cell death, tissue loss and neuronal degeneration. In addition, we observed progressive white matter damage and increased levels of MAP2 and synaptophysin in both the cortex and hippocampus. Therefore, based on our three criteria we chose to focus or study of inflammation-associated miRNAs on the hippocampus.

3.2.2. Temporal expression of inflammation-associated miRNAs in the hippocampus after moderate CCI.

To determine whether inflammation-associated miRNAs were elevated after TBI and examine their temporal profile RNA was extracted from injured (ipsilateral) and uninjured (contralateral) hippocampi from the same animal at times spanning the acute and sub-acute phase after injury and in naïve and sham controls. Levels of miR-155, miR-146a, miR-21, and miR-223 were examined by qPCR. These miRNA were chosen based on their importance in regulating inflammatory responses and being positively identified in at least one profiling study of TBI. Levels of miRNAs examined did not change between hemispheres in naïve or sham controls. We found that miR-155, miR-21 and miR-223 were all elevated after TBI (Fig. 3.8A-C). No change was observed in miR-146 levels (Fig. 3.8D). The expression of miR-155 was significantly increased at 1, 3, and 7 days after injury between ipsilateral and contralateral hippocampi, and returned to baseline by 14 days (Fig. 3.8A). Expression of miR-21 showed a complementary trend, only elevated significantly at 14 days after injury relative the uninjured hemisphere, but not at 1, 3, or 7 days (Fig. 3.8B). Expression of miR-223 was significantly elevated in the ipsilateral hippocampus only at 1 day after injury relative to the contralateral hemisphere (Fig. 3.8C). Overall, changes were observed in three of the four inflammation-associated miRNA examined, but each showed a distinct temporal profile.

Figure 3.8

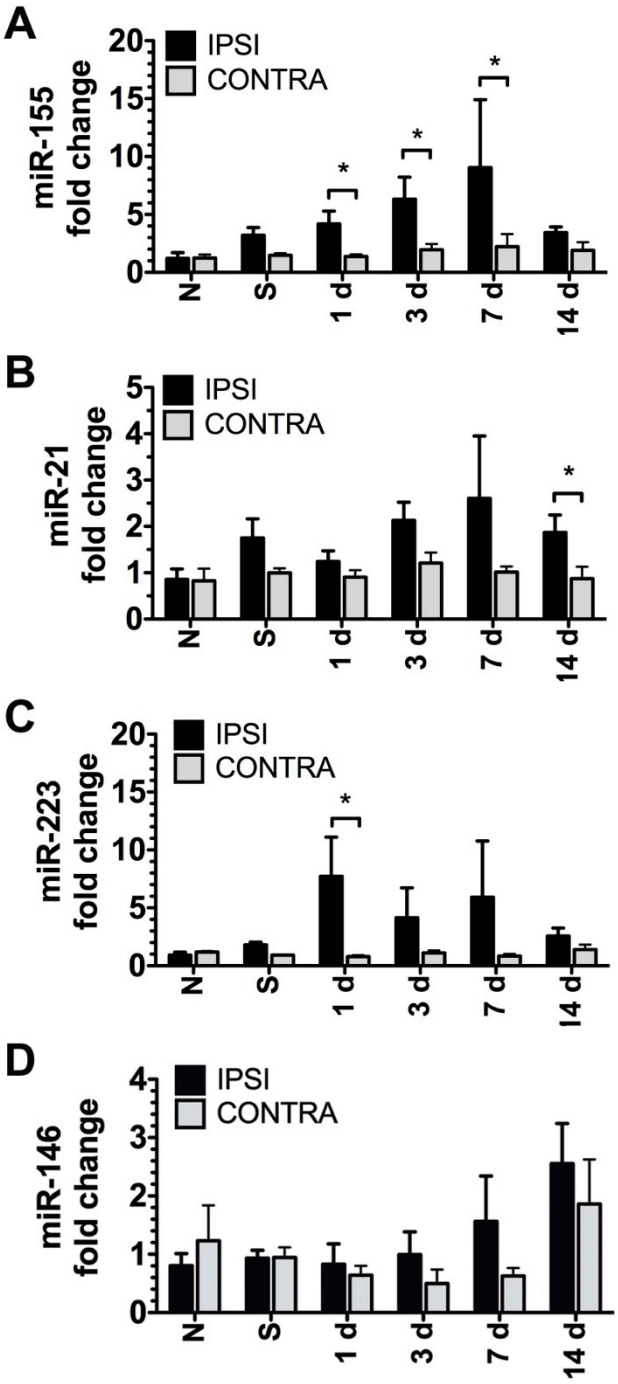
A
miR-155
fold change
IPSI
CONTRA
20
15
10
5
0
*
*
*
N
S
1 d
3 d
7 d
14 d
B
miR-21
fold change
IPSI
CONTRA
5
4
3
2
1
0
*
N
S
1 d
3 d
7 d
14 d
C
miR-223
fold change
IPSI
CONTRA
20
15
10
5
0
*
N
S
1 d
3 d
7 d
14 d
D
miR-146
fold change
IPSI
CONTRA
4
3
2
1
0
N
S
1 d
3 d
7 d
14 d

Figure 3.8 Expression of inflammation-associated miRNAs in the hippocampus after CCI. Levels of miR-155 (A), miR-21 (B), miR-223 (C), and miR-146 (D) in the ipsilateral (IPSI) and contralateral (CONTRA) hippocampus were measured 1, 3, 7, and 14 days after CCI by qPCR at 0.5-mm injury depth and in naïve animals and sham surgery controls. Data are expressed as fold change relative to naïve mice normalized to snRNA U6. The mean ± SEM from three animals are shown. Statistical analysis was performed on ΔCt values using a two-way ANOVA, difference between hemispheres was significant for miR-155 ($p < .0001$), miR-21 ($p < .001$), and miR-223 ($p < .05$). Bonferroni post-hoc tests were performed on each time point, *, $P < .05$, relative to the contralateral hemisphere.

3.2.3 Temporal expression of pro-inflammatory cytokines in the hippocampus after moderate CCI.

Increases in pro-inflammatory cytokines after TBI are found in both patients [190] and rodent models [191]. To examine the relationship between inflammation-associated miRNA and neuroinflammation, we examined the temporal expression profile of pro-inflammatory cytokines in the hippocampus after CCI. Expression of pro-inflammatory cytokines IL-1β, TNFα, and IL-6 were measured in the ipsilateral and contralateral hippocampus from the same animal 1, 3, 7, and 14 days after injury and in naïve and sham controls. The same RNA samples were used for both miRNA and mRNA analysis. Expectedly, levels of proinflammatory cytokines increased in the ipsilateral hemisphere after CCI (Fig. 3.9). All the three cytokines examined showed increased levels in the ipsilateral compared to the contralateral hippocampi, with peak expression 1 day post injury. Both IL-1β (Fig. 3.9A) and IL-6 (Fig. 3.9C) were not elevated in the sham controls and did not change 3, 7, or 14 days after injury. In contrast, increase in TNFα expression persisted at 3 days after injury (Fig. 3.9B). Additionally, TNFα expression was increased in the ipsilateral hemisphere of sham animals. Other groups have also reported increased inflammation in sham controls [185, 186]. We also note that the 8-fold increase between naïve and the ipislateral sham cortex is only a fraction of the CCI induced increase (~60 fold). These data suggest that TNFα is highly sensitive to CNS damage and that relative to other cytokines; its increased expression persists for several days after injury. The main finding here was an acute increase in gene expression of the pro-inflammatory cytokines after TBI.

3.2.4. Correlation between expression of inflammation-associated miRNAs and pro-inflammatory cytokines.

Figure 3.9

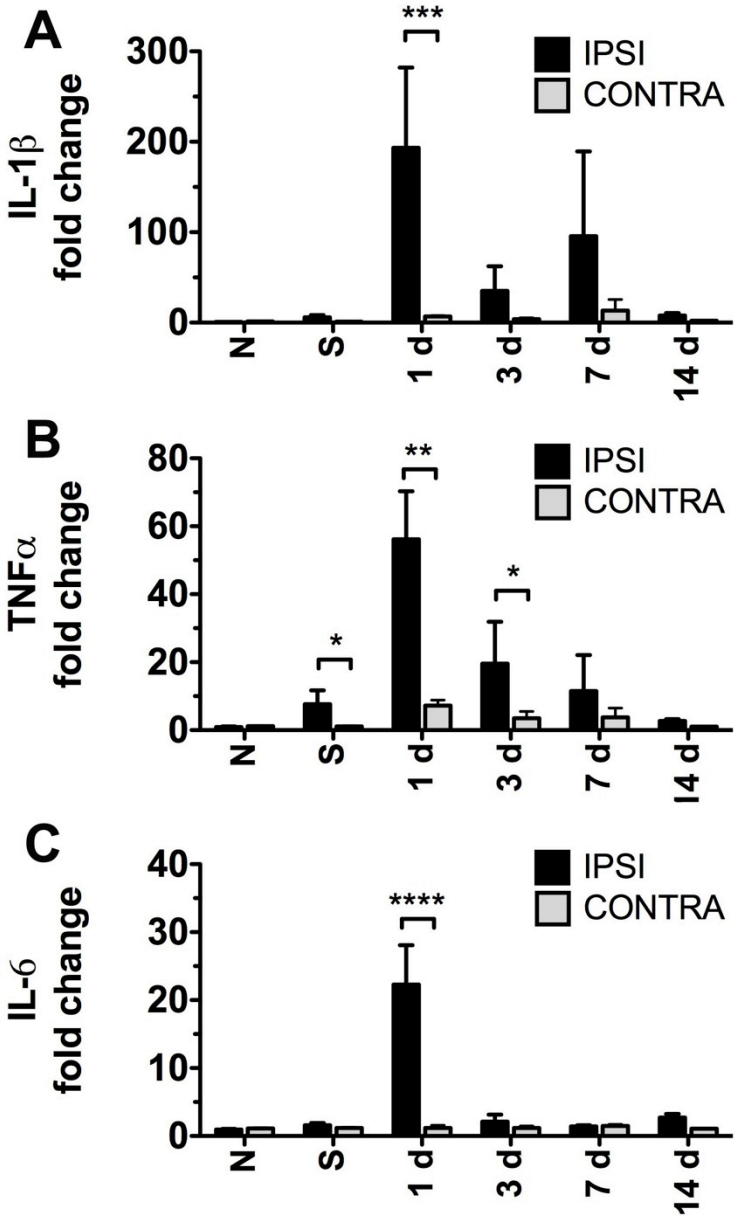
A
IL-1β
fold change
300
200
100
0
***
IPSI
CONTRA
N
S
1 d
3 d
7 d
14 d
B
TNFα
fold change
80
60
40
20
0
**
*
*
IPSI
CONTRA
N
S
1 d
3 d
7 d
I4 d
C
IL-6
fold change
40
30
20
10
0
****
IPSI
CONTRA
N
S
1 d
3 d
7 d
14 d

Figure 3.9 Expression of inflammatory cytokines in the hippocampus after CCI. Levels of IL-1β (A), TNFα (B), and IL-6 (C) in the ipsilateral (IPSI) and contralateral (CONTRA) hippocampus were measured 1, 3, 7, and 14 days after CCI by qPCR at 0.5-mm injury depth and in naïve animals and sham surgery controls. Data are expressed as fold change relative to naïve mice normalized to GAPDH. The mean ± SEM from three animals are shown. Statistical analysis was performed on ΔCt values using a two-way ANOVA, difference between hemispheres was significant for IL-1β ($p < .0001$), TNFα ($p < .0001$), and IL-6 ($p < .0001$). Bonferroni post-hoc tests were performed on each time point, *, $P < .05$; **, $P < .01$; ***, $P < .001$; ****, $P < .0001$; relative to the contralateral hemisphere.

In the peripheral immune system levels of miR-155 correlate with expression of IL-1β and TNFα suggesting a relationship between these two classes of molecules [192]. To examine the relationship between the inflammation-associated miRNA and pro-inflammatory cytokines after CCI we performed a Pearson's correlation analysis (Fig. 3.10). The strongest association was between miR-155 and IL-1β, r = .72 (Fig. 3.10A). The second strongest association was found between miR-155 and TNFα (r = .63), followed by miR-21 and IL-1β (r = .55). The only cytokine-miRNA pair that did not show any correlation was IL-6 and miR-21 (p = .38) (Fig. 3.10B). This was surprising as miR-21 is known to be induced by IL-6 in the periphery [193]. In summary, there was a clear association between inflammatory cytokines and inflammation-associated miRNAs indicating that there is a strong relationship between these two classes of molecules.

3.2.5 Localization of miR-155, miR-21, and miR-223 in the brain after CCI.

To validate qPCR findings that expression of inflammation-associated miRNAs was increased after CCI and to further describe their localization in different anatomical regions we performed *in situ* hybridization (Fig. 3.11). Brains from mice 1, 3, and 7 days after CCI as well as naïve and sham controls were analyzed. Similar to results from qPCR experiments, we found increased levels of miR-155, miR-21, and miR-223 in the hippocampus after TBI. We also found increased expression in the boundary zone of the cortex. Expression of inflammation-associated miRNAs was not observed in the brains of naïve mice. The ipsilateral hemisphere of sham mice was positive for miR-155, but not miR-21 or miR-223. The contralateral hemisphere at day 1 and 3 was also positive for miR-155 in contrast to qPCR results (Fig. 3.11A). One striking feature of miR-155 expression was its nuclear localization as evidenced by co-localization with DAPI staining of the nucleus. As was seen in qPCR experiments, miR-21 expression was more delayed. Of the timepoints examined the highest levels of miR-21 expression were

Figure 3.10

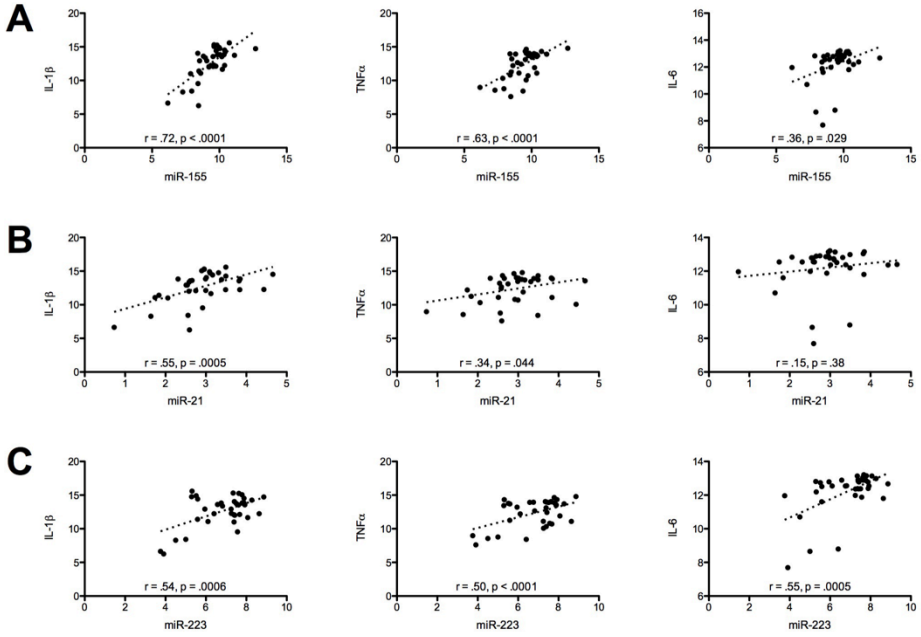
A
IL-1β
r = .72, p < .0001
miR-155
TNFα
r = .63, p < .0001
miR-155
IL-6
r = .36, p = .029
miR-155
B
IL-1β
r = .55, p = .0005
miR-21
TNFα
r = .34, p = .044
miR-21
IL-6
r = .15, p = .38
miR-21
C
IL-1β
r = .54, p = .0006
miR-223
TNFα
r = .50, p < .0001
miR-223
IL-6
r = .55, p = .0005
miR-223

Figure 3.10 Correlation of inflammation-associated miRNAs with expression of pro-inflammatory cytokines. Correlation was calculated using ΔCt values for cytokines and miRNAs measured from the same hippocampal RNA. Correlation of TNFα, IL-1β, and IL-6 with miR-155 (A), miR-21 (B), and miR-223 (C) are shown. Pearson's r and p values as indicated. Thirty-six paired values from 1, 3, 7, and 14 days after CCI at 0.5-mm injury depth, naïve animals, and sham controls were used to determine correlation. Trend line (dashed) based on linear regression.

Figure 3.11

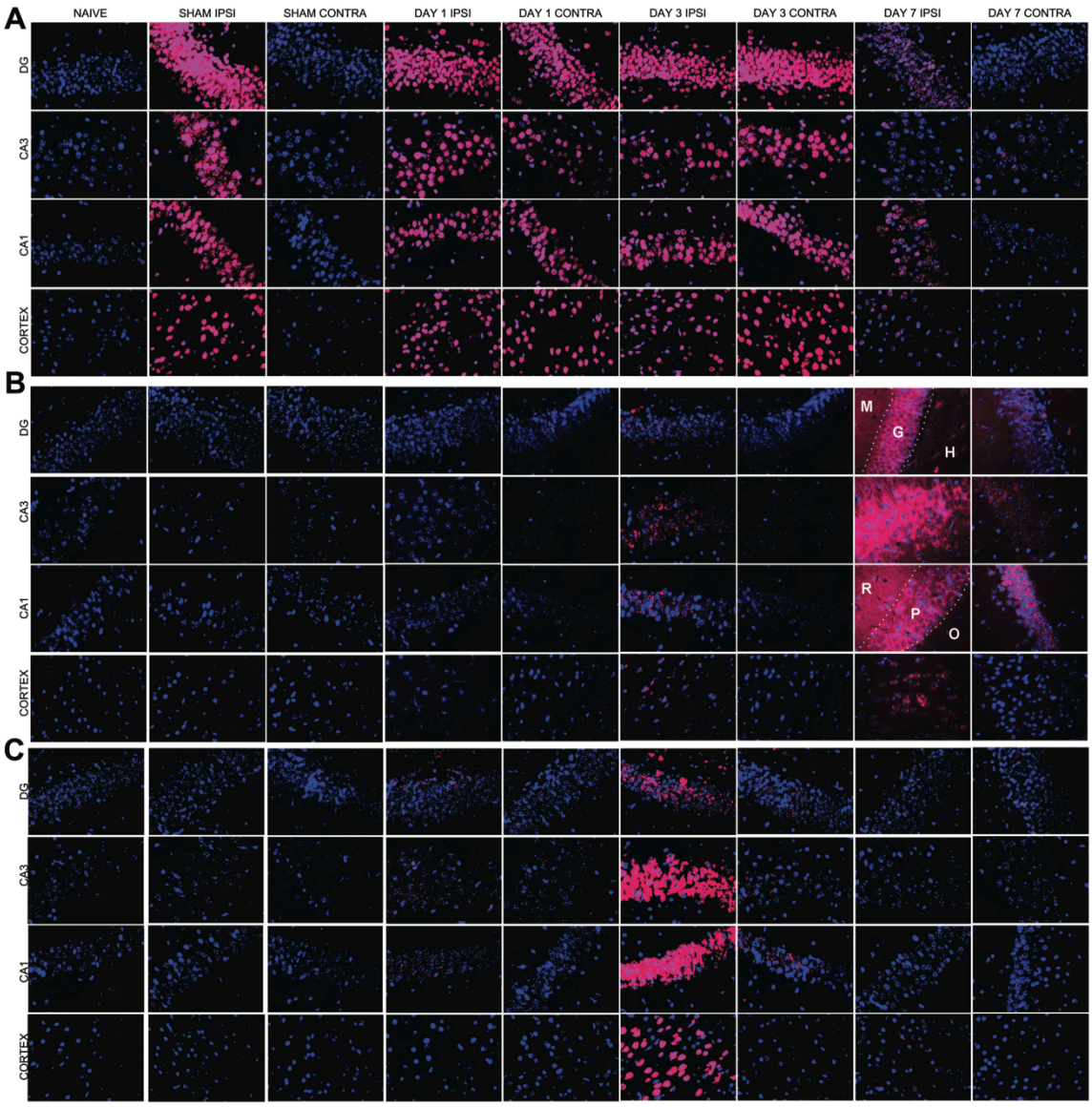
A
NAIVE
SHAM IPSI
SHAM CONTRA
DAY 1 IPSI
DAY 1 CONTRA
DAY 3 IPSI
DAY 3 CONTRA
DAY 7 IPSI
DAY 7 CONTRA
DG
CA3
CA1
CORTEX
B
M
G
H
R
P
O
C

Figure 3.11 Localization of inflammation-accociated miRNAs after CCI in the hippocampus and cortex. Expression of miR-155 (A), miR-21 (B), and miR-223 (C) after CCI. Fluorescence *in situ* hybridization was performed on tissue sections from mice 1, 3, and 7 days after .05 mm CCI or 1 day after sham surgery. The cortical boundary zone and the dentate gyrus (DG), CA1, and CA3 of the hippocampus on the ipsilateral (IPSI) and contralateral (CONTRA) hemisphere are shown. Stratum moleculare (M), stratum granulosum (G), hilus (H), stratum radiatum (R), stratum pyramidale (P), and stratum oriens (O). Nuclei are stained with DAPI are shown in blue; miRNAs are shown in magenta. Staining was performed on tissues from two animals and representative images are shown.

observed at 7 days after CCI. The localization of miR-21 was not nuclear as was seen with miR-155. Interestingly, miR-21 expression was high in the laminar layers of the hippocampus, regions densely populated with neurons. In the dentate gyrus expression of miR-21 was detected in the stratum molecular, which is composed primarily of neuronal projections and the stratum granulosum, which contains the neuronal cell bodies (Fig. 3.11B). Additionally in the CA1 region the stratum pyramidale is composed of pyramidal neurons and shows miR-21 expression as does the stratum radiatum, which contains both neuronal projections such as the Schaffer collateral as well as interneurons. The expression of miR-223 is unique from both miR-155 and miR-21 in that it was only detected at day 3 after injury and predominantly in the ipsilateral hemisphere (Fig. 3.11C).

In summary, the expression of inflammation-associated miRNAs is detectable in the hippocampus and boundary zone of the cortex after CCI. As found in qPCR experiments miR-155 was expressed at several time points after CCI, in contrast to miR-21 which showed a delayed expression pattern. As with qPCR miR-223 showed a short duration of expression in the acute period. Several differences do exist between qPCR and *in situ* results. For example, miR-155 expression was not increased in sham or contralateral hemispheres by qPCR, but was detected by *in situ*. This could be due to sampling differences between these two methods. RNA isolation from the entire hippocampus could dilute the expression of miRNA concentrated near the lesion to undetectable levels by qPCR. While differences between these two methods exist, both showed increased levels of inflammation-associated miRNAs after CCI.

3.2.6. Expression of inflammation-associated miRNAs with increasing injury severity in the hippocampus.

To gain a better understanding of the interaction between injury severity and expression of inflammation-associated miRNA and identify the ideal conditions for functional studies of miRNA, we examined the expression of miRNAs after moderate and severe TBI. In the CCI model injury severity can be altered by changing injury depth; with increased depth leading to increased lesion size and greater cognitive impairment [194]. In order to examine the effect of injury severity on the expression of inflammation-associated miRNA, levels of miR-21, miR-155, and miR-223 were measured in animals 3 days after sham surgery, moderate (0.5 mm depth) CCI, or severe (1.0 mm depth) CCI as well in naïve animals (Fig. 3.12). Injury depth was significant for miR-21 ($P < .01$) and miR-155 ($P < .01$), but not for miR-223 based on a two-way ANOVA. Consistent with Fig. 3.1, CCI at the 0.5 mm injury depth increased miR-155 at 3 days, but levels of miR-21 and miR-223 were not increased in these conditions. In contrast, CCI at 1.0 mm injury depth increased miR-21, miR-155 and miR-223 levels in the ipsilateral compared with the contralateral hippocampus. Given that the expression of all three miRNAs was present at 3 days after severe (1.0 mm) CCI, we chose to use this time point and severity for functional analysis of inflammation-associated miRNAs.

3.2.7. Targeted expression profiling of cytokines, chemokines, and growth factors at 3 days after CCI.

One area of interest for functional studies of inflammation-associated miRNAs is their ability to regulate the downstream expression of cytokines, chemokines, and growth factors after TBI. Based on the data above, 3 days after severe CCI was chosen as the ideal conditions for examining miRNA function. In moderate CCI, expression of TNFα was significantly elevated 3 days after CCI in the ipsilateral hemisphere, but IL-6 and IL-1B were not. To determine whether cytokine expression was a measurable outcome at 3 days after severe TBI we measured inflammatory cytokine expression in animals 3 days

Figure 3.12

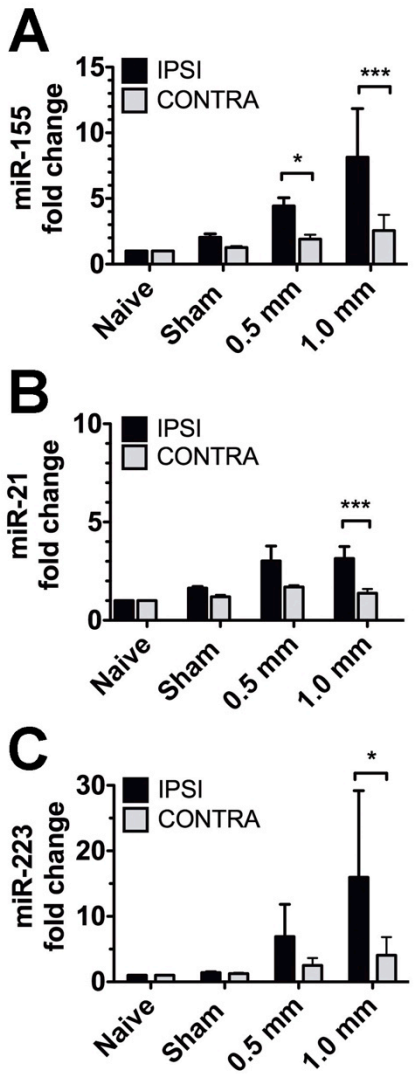
A
miR-155 fold change
IPSI
CONTRA
15
10
5
0
*
***
Naive
Sham
0.5 mm
1.0 mm
B
miR-21 fold change
IPSI
CONTRA
10
5
0
***
Naive
Sham
0.5 mm
1.0 mm
C
miR-223 fold change
IPSI
CONTRA
30
20
10
0
*
Naive
Sham
0.5 mm
1.0 mm

Figure 3.12 Expression of inflammation-associated miRNAs in the hippocampus after moderate and severe CCI. Levels of miR-155 (A), miR-21 (B), and miR-223 (C) in the ipsilateral (IPSI) and contralateral (CONTRA) hippocampus were measured 3 days after CCI by qPCR at 0.5-mm injury depth, 1.0-mm injury depth and in naïve animals and sham surgery controls. Data are expressed as fold change relative to naïve mice normalized to snRNA U6. The mean ± SEM from 3-4 animals are shown. Statistical analysis was performed on ΔCt values using a two-way ANOVA, Injury severity was significant for miR-155 ($p < .01$) and miR-21 ($p < .01$), but not miR-223. Bonferroni post-hoc tests were performed on each time point, *, $P < .05$, ***, $P < .001$ relative to the contralateral hemisphere.

after sham surgery, moderate (0.5 mm depth) CCI, or severe (1.0 mm depth) CCI as well in naïve animals. In addition we broadened the list of signaling molecules to include other cytokines, chemokines, and growth factors important in neuroinflammation. Cytokines IL-1β and TNFα, as well as chemokine CXCL10 were increased 3 days after CCI (Fig. 3.13). The expression of IL-1β was elevated in moderate injury in both the ipsilateral and contralateral hippocampi and in the severely injured ipsilateral hippocampus relative to naïve. TNFα expression was elevated in ipsilateral hippocampi of both moderate and severe injury and in the contralateral hippocampus of severe injury relative to naïve. Interestingly, we also found increased levels of CXCL10 in both the moderately and severely injured ipsilateral hippocampi relative to naive. In conclusion, the expression of IL-1β, TNFα, and CXCL10 was elevated in at least the ipsilateral hippocampi after TBI and can be used as an outcome measure for future functional studies of inflammation-associated miRNAs.

3.3 Discussion

These studies addressed 3 major questions: 1) which anatomical regions are appropriate for studying the expression and function of inflammation-associated miRNAs after CCI? 2) Are inflammation-associated miRNAs increased by CCI? 3) What is the relationship between inflammation-assoicated molecules and pro-inflammatory cytokines?

By characterizing the pathophysiology of CCI in the mouse model we identified the hippocampus as an appropriate region for studying changes in inflammation-associated miRNAs. The hippocampus showed evident neuropathology and robust glial activation without frank tissue loss or high levels apoptotic cell death. The inflammation-associated miRNAs examined here all have known roles in apoptosis [182, 184, 195,

196]. Therefore, we wanted to avoid examining tissues with high amounts of apoptotic signaling after CCI. In CCI animals we found cortical tissue loss and TUNEL positive apoptotic cells concentrated in the lesion boundary zone of the cortex. These findings are in agreement with multiple studies describing apoptosis in cortical tissue after CCI [197, 198]. Alternatively, the hippocampus showed negligible tissue loss and very few apoptotic cells. We also wanted to ensure that the anatomical region studied showed robust glial activation. Immunohistochemisty revealed increases in both Iba1 and GFAP staining in the hippocampus suggesting that either anatomical region would be appropriate to study the inflammatory response after CCI. To study the complex interaction between neuroinflammation and neuronal injury and regeneration we wanted to examine a region where neuronal pathology was evident. We found that SMI-31, a marker of phosphorylated neurofilament was present in two distinct white matter tracts, the corpus callosum and hippocampal alveus [199]. Staining with MAP2 and synaptophysin was absent in the lesioned cortex, but was upregulated in both the cortices not directly involved in the lesion and in the hippocampus. This increase in important neuronal markers suggests a regenerative response to CCI. Based on these findings we directed further experiments in inflammation-associated miRNA after CCI towards the hippocampus.

Both qPCR and *in situ* hybridization showed increases in three out of the four inflammation-associated miRNAs examined in the hippocampus after CCI. Expression of miR-155, miR-21, and miR-223 were all increased in the ipsilateral hippocampi after CCI. Sustained eleveation of miR-155 was observed in the acute period 1, 3, and 7 days after TBI. Conversely, miR-21 showed increased expression in the sub acute phase (day 7 and 14) by either pPCR or *in situ*. The expression of miR-223 showed a less sustained increase in the acute period. Somewhat surprisingly levels of miR-146 remained unchanged by CCI. In peripheral immune responses [120] and in microglia [200] miR-

Figure 3.13

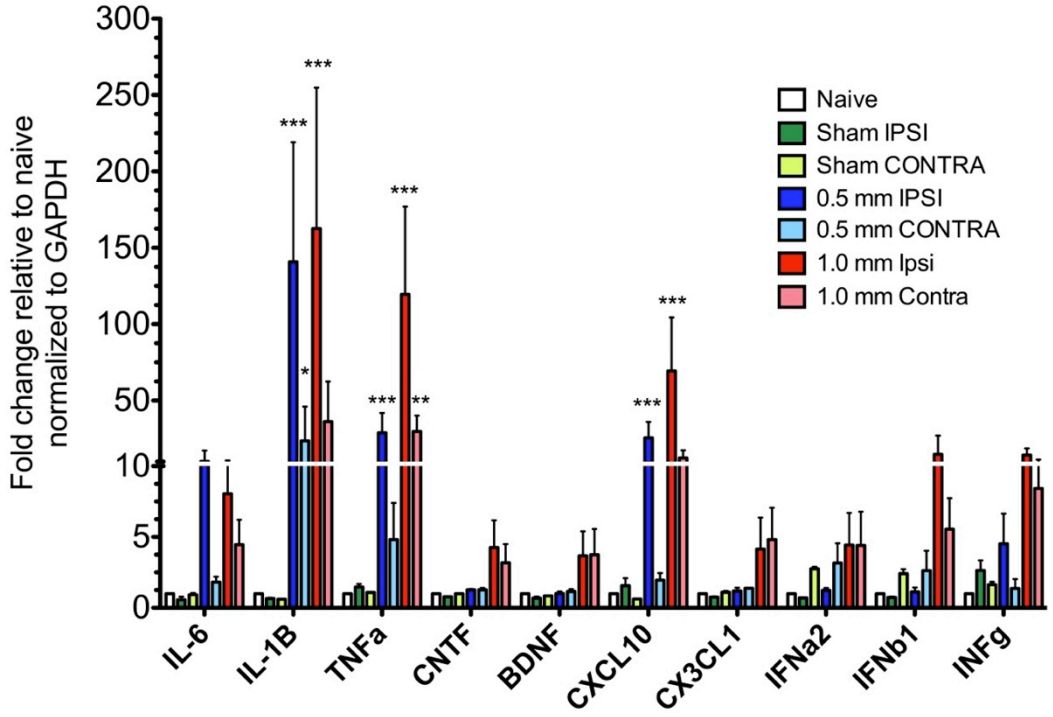
Fold change relative to naive normalized to GAPDH
300
250
200
150
100
50
10
5
0
Naive
Sham IPSI
Sham CONTRA
0.5 mm IPSI
0.5 mm CONTRA
1.0 mm Ipsi
1.0 mm Contra
IL-6
IL-1B
TNFa
CNTF
BDNF
CXCL10
CX3CL1
IFNa2
IFNb1
INFg

Figure 1. Expression of cytokines, chemokines, and growth factors in the hippocampus after moderate and severe CCI. Levels of cytokines, chemokines, and growth factors in the ipsilateral (IPSI) and contralateral (CONTRA) hippocampus were measured 1, 3, 7, and 14 days after CCI by qPCR at 0.5-mm injury depth or 1.0-mm injury depth and in naïve animals and sham surgery controls. Data are expressed as fold change relative to naïve mice normalized to snRNA U6. The mean ± SEM from 3-4 animals are shown. Statistical analysis was performed on ΔCt values using a two-way ANOVA, Bonferroni post-hoc tests were performed on each time point, *, $P < .05$; **, $P < .01$; ***, $P < .001$; relative to naïve.

146 participates in feedback inhibition, limiting the duration and magnitude of the immune response. Therefore, the lack of miR-146 could be a pathological feature of CCI.

Even though both qPCR and *in situ* hybridization identified the same general expression pattern, several differences between the regional and temporal expression of inflammation-associated miRNAs was found between these methods. One example being the detection of miR-155 in both sham and contralateral hemisphers. One possible explanation for this could be sampling differences between the two methods. The dilution of changes in miRNA levels near the injury site in RNA from the entire hippocampus might result in qPCR being a less sensitive measure of miRNA expression.

As expected, our CCI model showed striking increases in pro-inflammatory cytokines IL-1β, TNFα, and IL-6 in the injured hippocampi that peaked 1 day after injury. TNFα was elevated in craniotomy only sham controls and showed sustained elevation at 3 days after injury, indicating that it is a sensitive indicator of neuronal injury and inflammation. The expression of inflammation-associated miRNAs showed high levels of correlation with the three pro-inflammatory cytokines. These data indicated a strong relationship between these two classes of molecules, however, the nature of this relationship cannot be determined by the studies described here.

To determine the ideal conditions for future studies of the function of inflammation-associated miRNAs in CCI, we examined levels of miRNAs in both moderate and severe CCI. While in moderate CCI only miR-155 was elevated relative to the contralateral hemisphere, in severe CCI increases in miR-21 and miR-223 were detected. Additionally, increases in three inflammatory signaling molecules, IL-1β, TNFα, and CXCL10 could also be detected 3 days after severe injury. Together these studies were designed to identify the ideal circumstances for studying the functional role of

inflammation-associated miRNAs in TBI. Based on our findings we will focus our efforts on studying the function of inflammation-associated miRNAs in the hippocampus 3 days after severe injury.

Another important finding of this work was the marked elevation of miR-155 expression in the CCI model of TBI. Redell *et al*. also found that levels of miR-155 were elevated 24h after CCI [145]. However, no studies have examined the localization, association with inflammation, or function of miR-155 in TBI. Given the importance of miR-155 in other neurological conditions, further exploration of miR-155 function of TBI is warranted.

While miRNA-21 is the most studied miRNA in TBI, the late expression pattern and seemingly neuronal localization of miR-21 suggest that it may have additional roles besides regulating neuronal apoptosis, which occurs in the acute phase of injury. Several independent reports of miR-21 promoting neurite outgrowths may point to a role for miR-21 in the regenerative process after TBI [201-203].

The expression of miR-223 showed an acute increase after CCI in the ipsilateral hemisphere. Recently a report by Izumi *et al.* showed expression of miR-223 after spinal cord injury (SCI) that localized to neutrophils [204]. Given the acute increase and decrease of neutrophils in TBI lesions,[205] expression of miR-223 in neutrophils could explain the acute expression pattern seen for miR-223 in TBI.

3.4 Summary:

Several interesting inflammation-associated miRNAs were increased by TBI. Expression of miR-155, miR-21, and miR-223 were all elevated in ipsilateral hippocampi relative to contralateral hippocampi by both qPCR and *in situ* hybridization. Of the miRNA examined, miR-155 showed the largest and most consistent increase. Interestingly miR-21 had a delayed expression pattern, suggesting that it may play a role the sub-acute

phase of injury. The roles of miR-155 in inflammatory signaling in the acute phase and miR-21 in regenerative phase of CCI warrant further study. Based on our findings the ideal conditions for studying the roles of inflammation-associated miRNAs are three days after CCI in the hippocampus.

Chapter 4: Function of miR-155 in the controlled cortical impact (CCI) model of TBI

4.1 Background:

Expression of inflammation-associated miR-155 was induced by TBI. Additionally, expression of miR-155 was highly correlated with pro-inflammatory cytokines. Based on the known roles of miR-155 in the peripheral immune response [121, 122, 206, 207] we hypothesized that miR-155 could regulate neuroinflammation after TBI. *In vitro* studies of miR-155 in microglia support a pro-inflammatory role in the brain [133]. However, *in vivo* studies are still lacking. In order to examine the function of miR-155 in TBI we obtained miR-155 knockout (KO) mice and induced TBI using a controlled cortical impact (CCI) model. Using a combination of RNA and protein analysis, histological characterization, and behavioral testing we compared TBI induced changes between miR-155 KOs and WT mice.

4.2 Results:

4.2.1 Validation of miR-155 KO by *in situ* hybridization

Our previous studies showed increased miR-155 after CCI by both qPCR and *in situ* hybridization in wild-type mice. To examine it's role in TBI we obtained miR-155 knockout (KO) mice from the Jackson Laboratory. To confirm that expression of miR-155 was absent from miR-155 KO mice and to localize miR-155 after severe injury we performed *in situ* hybridization on the brains of miR-155 KO and WT control mice sacrificed 3 days after CCI (Fig. 4.1). As observed previously in moderate injury, miR-155 was detected in the hippocampus and cortex in the ipsilateral hemisphere after CCI and primarily localized to the nucleus. No staining was observed in miR-155 KOs confirming that miR-155 expression was absent in these animals.

Figure 4.1

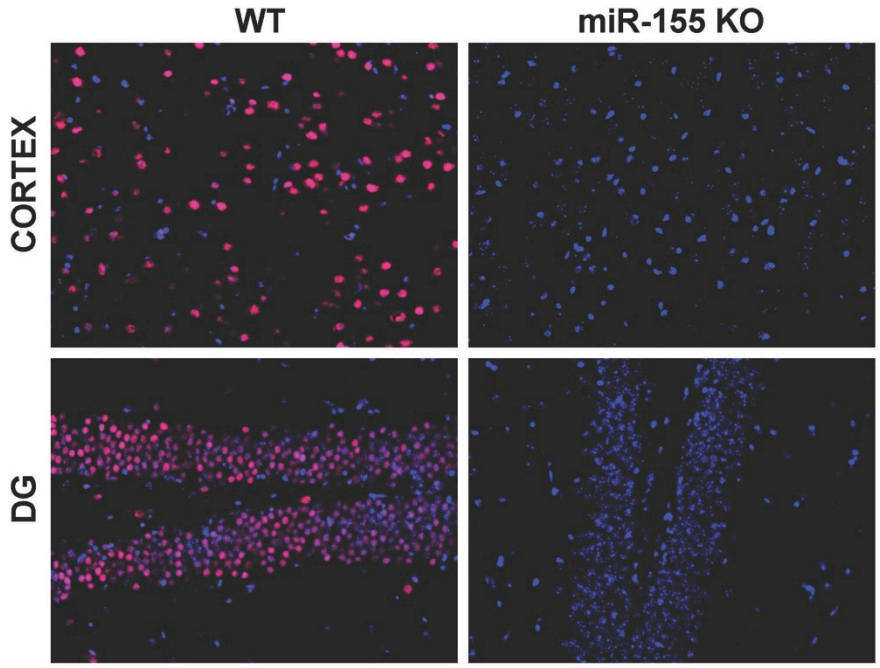

Figure 4.1 Expression of miR-155 after CCI WT and miR-155 KO. Detection of miR-155 expression (magenta) after CCI by fluorescence *in situ* hybridization performed on tissue sections from WT and miR-155 KO mice 3 days after 1.0-mm CCI. Nuclei are stained with DAPI (blue). Images are from the ipsilateral lesion boundary of the cortex and the dentate gyrus (DG) of the hippocampus. Original magnification 200x.

4.2.2 Ablation of miR-155 alters the expression of cytokines, chemokines and growth factors after CCI.

In order to understand the function of miR-155 in regulating the immune response in TBI, we subjected miR-155 KOs and wild type mice to CCI. Three days after CCI, RNA was isolated from ipsilateral and contralateral hippocampi and levels of cytokines, chemokines, and growth factors were measured by qPCR (Fig. 4.2). No changes were found in naïve miR-155 KO compared to WT mice using two-way ANOVA followed by Bonferroni post-hoc tests. Changes were found between CCI injured miR-155 KO and wild type mice. Both type I and type II interferon (IFN) expression was altered. In the ipsilateral hemisphere IFN-β was reduced in miR-155 KOs. In the contralateral hemisphere IFN-γ was reduced in miR-155 KO mice compared to wild-type. Unexpectedly, there were no differences in the expression of IL-1β or TNFα, which are regulated by miR-155 in other systems [121, 192]. In our previous profiling experiments we had seen large increases in the expression of chemokine CXCL10. We again saw a large increase in CXCL10 expression due to TBI, which was significantly reduced in the ipsilateral hippocampi of miR-155 KO mice compared to WT. Additionally, we saw a decrease of brain-derived neurotropic factor (BDNF) in the contralateral hippocampus of miR-155 KO mice. The main findings of this work were the decreased expression of IFN-β, IFN-γ, CXCL10 and BDNF in miR-155 KO hippocampi after CCI. CXCL10 is induced by both type I and type II IFN [208], and therefore the decrease in CXCL10 seen here may be secondary to the reduction in IFN.

4.2.3 Regulation of SOCS1 by miR-155 in CCI.

To further examine the changes in IFN signaling after CCI in miR-155 KO mice we examined the levels of known miR-155 target suppressor of cytokine signaling 1 (SOCS1) [206]. IFN signaling relies on signal transducer and activator of transcription 1

Figure 4.2

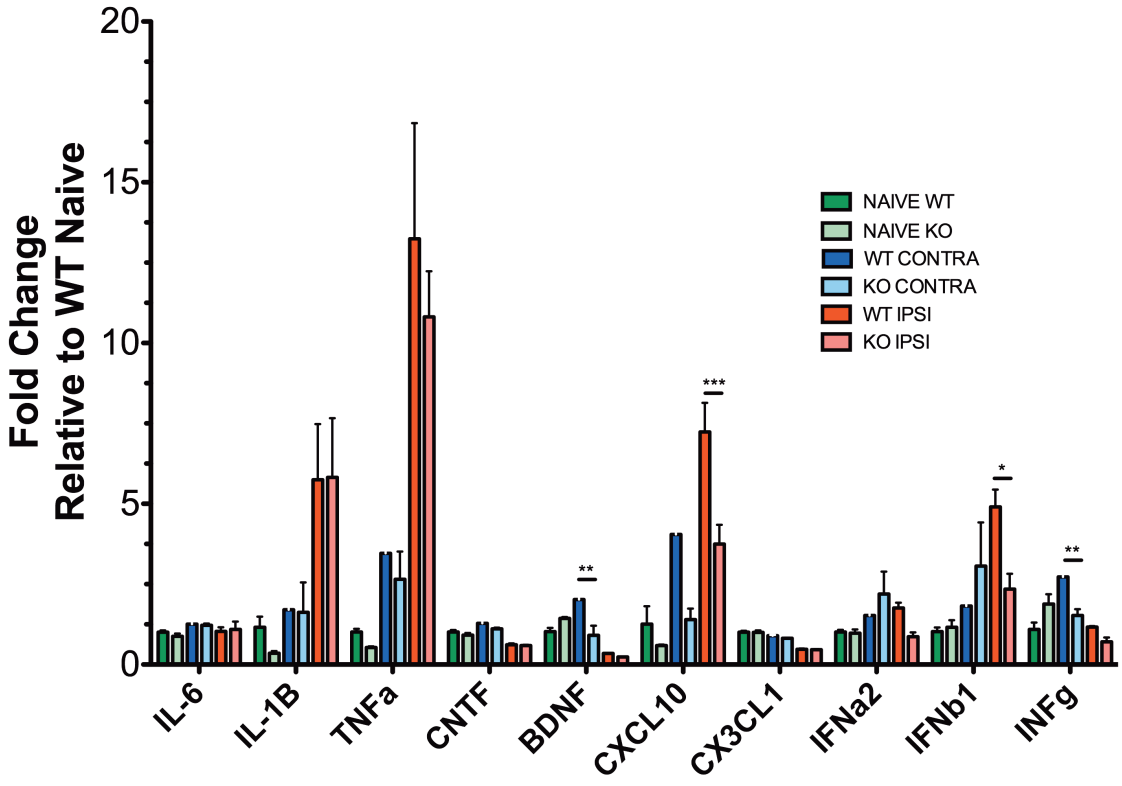
Fold Change
Relative to WT Naive
20
15
10
5
0
NAIVE WT
NAIVE KO
WT CONTRA
KO CONTRA
WT IPSI
KO IPSI
**
***
*
**
IL-6
IL-1B
TNFa
CNTF
BDNF
CXCL10
CX3CL1
IFNa2
IFNb1
INFg

Figure 4.2 Expression of cytokines, chemokines, and growth factors in the hippocampus after CCI in miR-155 KO and WT mice. Levels of cytokines, chemokines, and growth factors in the ipsilateral (IPSI) and contralateral (CONTRA) hippocampus were measured 3 days after CCI by qPCR at 1.0-mm injury depth and in naïve mice. Data are expressed as fold change relative to WT-naïve mice normalized to GAPDH. The mean ± SEM from 4 WT and 5 miR-155 KO mice are shown. Statistical analysis was performed on fold change values using a two-way ANOVA for each cytokine, Bonferroni post-hoc tests were performed on each time point, *, $P < .05$; **, $P < .01$; ***, $P < .001$.

(STAT1), which is inhibited by SOCS1 [209]. Therefore we hypothesized that removing miR-155 would increase levels of SOCS1, which in turn could decrease STAT1 activation leading to a decreased response to IFN. In order to determine whether SOCS1 was in fact increased in miR-155 KO mice we measured levels of SOCS1 protein and mRNA in miR-155 KO and WT ipsilateral hippocampi 3 days after CCI. There was no difference in SOCS1 protein level between miR-155 KO and WT hippocampi (Fig. 4.3). The lack of a change in SOCS1 protein levels could indicate that SOCS1 was not regulated by miR-155 in the brain after CCI. Alternatively the change in SOCS1 was not detectable because only a subset of cells had increased expression of miR-155 and corresponding reduction in SOCS1. If SOCS1 was decreased in a fraction of the total cells, the effect may have been diluted and immeasurable in hippocampal homogenate.

The expression of SOCS1 mRNA in the hippocampus after CCI was also measured. Surprisingly, the mRNA expression of SOCS1 was decreased in miR-155 KO mice ($P = .028$) (Fig. 4.4). Since SOCS1 is a target of miR-155; we hypothesized that its levels would increase in miR-155 KO hippocampi. The decreased mRNA levels, but unchanged protein levels could indicate compensatory effects. Alternatively, the effects could be cell type specific and unable to be detected in RNA or protein purified from tissue homogenates. There was a significant change in SOCS1 mRNA by condition ($P < .001$) with ipsilateral hippocampi showing a 2 fold increase in SOCS1 expression relative to naïve. This is the first report of increased SOCS1 expression in TBI and suggests that SOCS1 may be important for limiting the immune response after TBI.

4.2.4 Increased microglial activation in miR-155 KO after CCI.

Comparison of gene and protein expression between miR-155 KO and WT mice after CCI revealed changes in the IFN response. Several studies have shown that ectopic

Figure 4.3

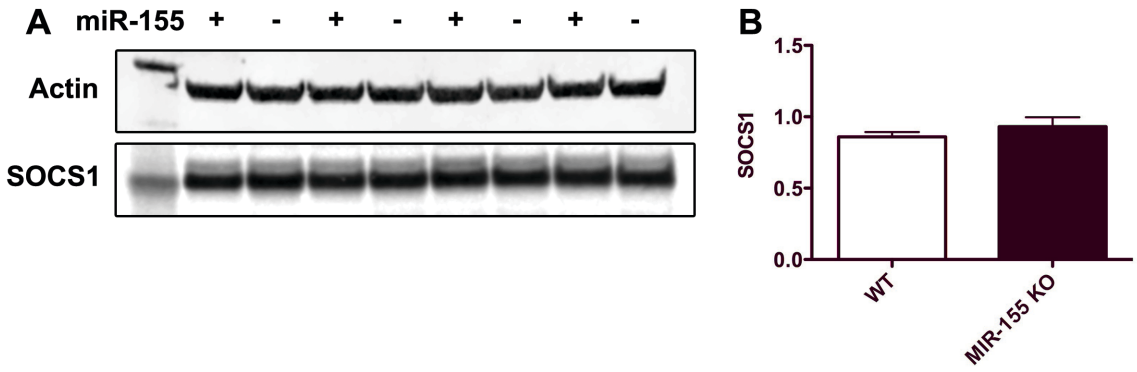

Figure 4.3. Suppressor of cytokine signaling (SOCS1) is elevated in miR-155 KO mice. (A) Levels of SOCS1 were analyzed by SDS-PAGE and Western blot in WT (+) and miR-155 KO (-) mice 3 days after 1.0 mm CCI. (B) Level of SOCS 1 was quantified by densitometry and normalized to β-actin. The mean relative density ± SEM from 4 animals are shown. Student's t-test was used to determine significance. *, P = .042.

Figure 4.4

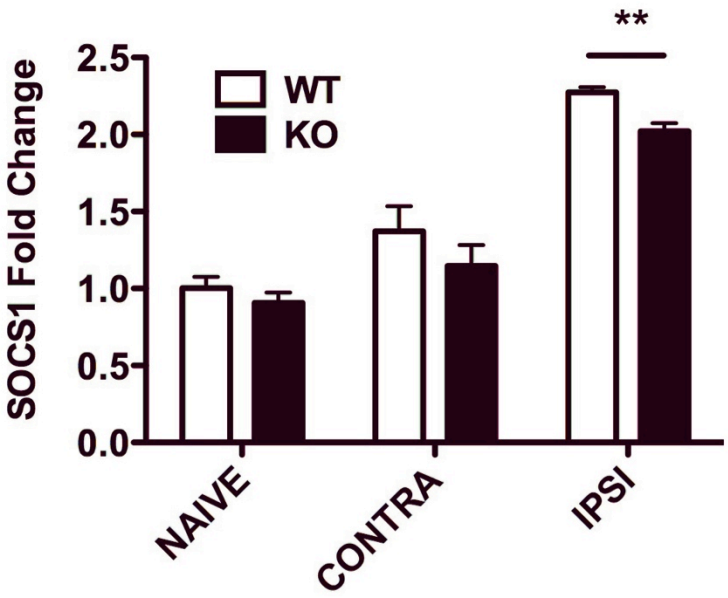

Figure 4.4 Expression of SOCS1 mRNA in the hippocampus after CCI in miR-155 KO and WT mice. Levels of SOCS1 mRNA in the ipsilateral (IPSI) and contralateral (CONTRA) hippocampus were measured 3 days after CCI by qPCR at 1.0-mm injury depth and in naïve mice. Data are expressed as fold change relative to WT-naïve mice normalized to GAPDH. The mean ± SEM from 4 WT and 4 miR-155 KO mice are shown. Statistical analysis was performed on fold change values using a two-way ANOVA (condition $P < .0001$; genotype, $P = .028$). Bonferroni post-hoc tests were performed on each time point, but no significant changes were found. Student's T-test between ipsilateral WT and miR-155 KO was significant **, $P = .0058$.

expression of miR-155 promotes microglial activation and cytokine production [210-213]. We hypothesized that microglial activation would be reduced in miR-155 KO mice. In order to characterize changes in microglial activation between miR-155 KO and WT mice we performed immunohistochemistry for microglial activation marker ionized calcium-binding adapter molecule 1 (Iba1) in the hippocampi after CCI. We hypothesized that increased SOCS1 in miR-155 KOs would reduce microglial activation. Surprisingly, we found the opposite effect (Fig. 4.5). Iba1 expression was increased in the ipsilateral hippocampus of miR-155 KOs relative to WT after CCI ($P = .046$). Increased expression of SOCS1 is discordant with an increase in microglial activation. We speculate that SOCS1 is not the only target of miR-155 involved in the inflammatory response and that increased microglial activation could be related to other miR-155 targets.

4.2.5 Neuronal localization of miR-155 after CCI. Surprisingly, microglial activation was increased after CCI in miR-155 KO mice. Additionally, we did not see changes in hippocampal SOCS1 protein after CCI. Interestingly, STAT1 can be activated in neurons after ischemic injury and contributes to cell death [214]. Also several reports have identified neuronal CXCL10 expression, which is also linked to neuronal cell death [215-217]. To determine whether miR-155 plays a role in the neuronal regulation of STAT1 and CXCL10, fluorescent *in situ* hybridization (FISH) was combined with immunohistochemistry (IHC) for neuronal marker MAP2 (Fig. 4.6) In the lesion boundary of the injured cortex we observed miR-155 staining in the nucleus of MAP2 positive cells. This indicated that neurons expressed miR-155 after CCI. We therefore proceeded to examine the role of miR-155 in neuronal cell death and degeneration.

4.2.6 Apoptosis after CCI is unaffected by miR-155 KO

Figure 4.5

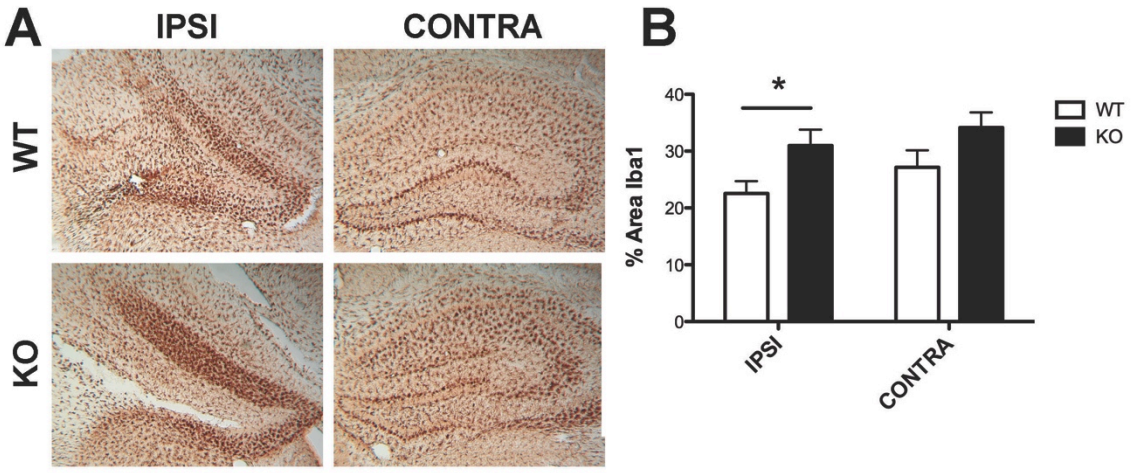

Figure 4.5 Iba1 staining is increased in the hippocampus of miR-155 KO mice after CCI. (A) Brains from WT (+) and miR-155 KO (-) mice were stained for Iba1 3 days after 1.0-mm CCI. Representative images are shown. (B) The area of the hippocampus stained with Iba1 was quantified. The mean ± SEM from 5 WT and 6 miR-155 KO animals are shown. Student's t-test was used to determine significance. *, P = .046.

Figure 4.6

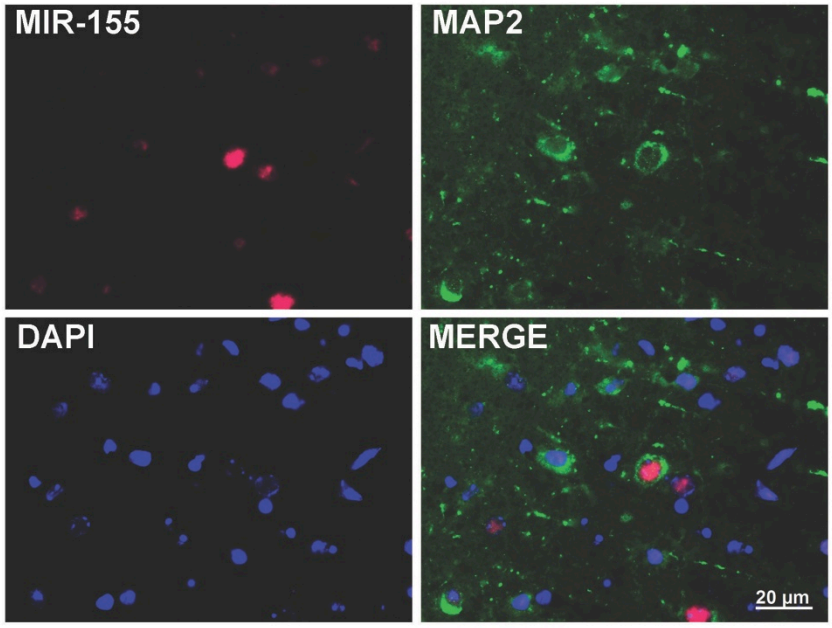

Figure 4.6 Localization of miR-155 after CCI. Detection of miR-155 expression (magenta) after CCI by fluorescence *in situ* hybridization performed on tissue sections from WT mice 3 days after 1.0-mm CCI. Co-immunohistochemisty was performed for neuroanal marker MAP2 (green). Nuclei are stained with DAPI (blue). Images are from the ipsilateral lesion boundary of the cortex. Original magnification: 630x (bar = 20 μM).

Deletion of miR-155 in the KO mice caused decreased IFN response after CCL, but increased microglial activation. Aside from its role in inflammation miR-155 can regulate apoptosis [183]. To determine whether miR-155 ablation altered levels of apoptosis in the hippocampus after CCI, we measured total and cleaved caspase 3 by Western blot (Fig. 4.7). There were no changes in cleaved caspase 3 in the injured hippocampus between WT and miR-155 KO mice (P = .20). These data indicate that miR-155 does not alter levels of apoptosis in the hippocampus after CCI. As we had shown previously with TUNEL staining, there was very little apoptotic cell death in the hippocampus after CCI. It is possible that although apoptosis and thus cleaved caspase 3 levels were low in the hippocampi, measureable differences could be found closer to the lesion site.

4.2.7 Neurodegeneration after CCI is unaffected by miR-155 deletion

To examine the effect of miR-155 KO on neuronal degeneration after CCI we used fluorojade staining. Fluorojade is specific to degenerating neurons and can be used to quantify neurodegeneraton after CCI [218]. Three days after CCI brains from miR-155 KO and WT mice were stained with fluorojade. Fluorojade positive cells in the cortex and hippocampus were counted. No changes were observed in fluorojade cell counts between genotypes in the hippocampus (P = .20) or cortex (P = .07) after CCI (Fig. 4.8). This indicates that miR-155 does not directly or indirectly influence neuronal degeneration 3 days after CCI.

4.2.8 Motor function is impaired by CCI, but not altered by miR-155 deletion

Deletion of miR-155 resulted in a reduced IFN response and increased microglial activity. To determine whether these changes have an affect on CCI outcome we performed accelerating rotarod testing. Accelerating rotarod is a common measure of motor dysfunction after CCI and in other models of TBI [95]. Animals of both genotypes

Figure 4.7

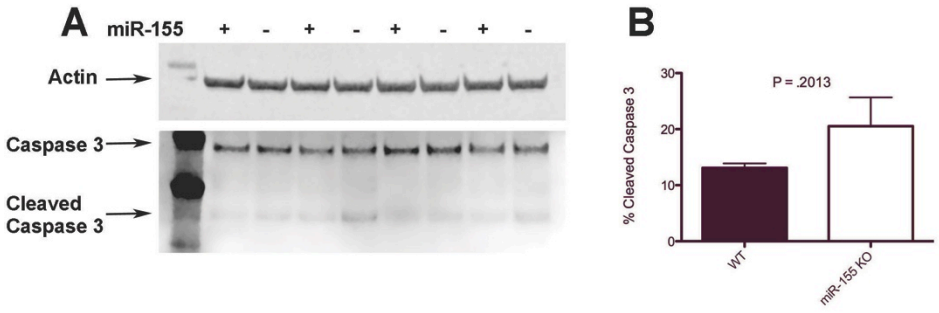
A
miR-155 + - + - + - + -
Actin
Caspase 3
Cleaved Caspase 3
B
P = .2013
% Cleaved Caspase 3
30
20
10
0
WT
miR-155 KO

Figure 4.7 Cleaved-caspase 3 levels in the hippocampus do not change in miR-155 KO after CCI. (A) Levels of caspase 3 were analyzed by SDS-PAGE and Western blot in WT (+) and miR-155 KO (-) mice 3 days after 1.0-mm CCI. (B) Cleaved-caspase 3 and full-length caspase-3 was quantified by densitometry. The ration of cleaved to full-length caspase 3 was multiplied by 100 to determine % cleaved caspase 3. The mean ± SEM from 4 animals are shown. Student's t-test was used to determine significance P = .20.

Figure 4.8

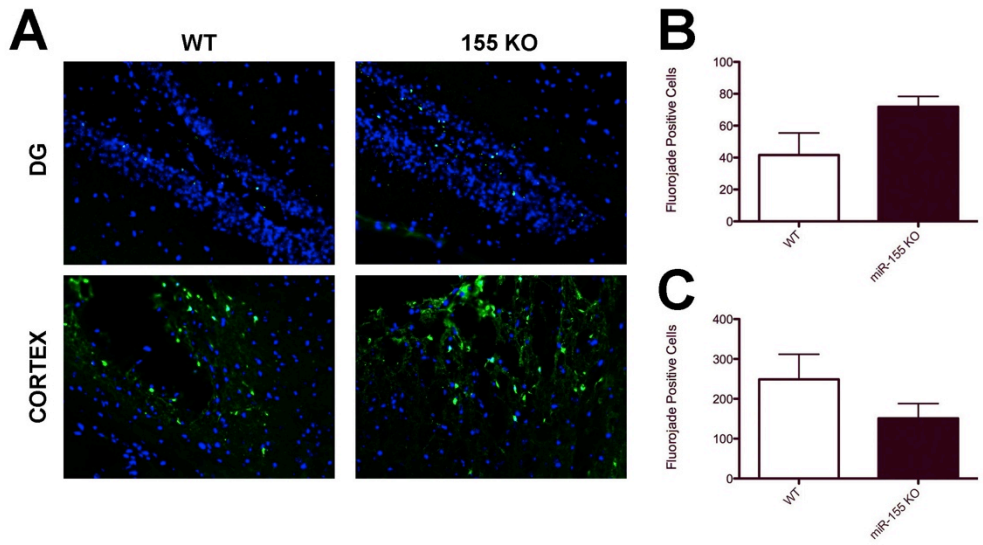
A
WT
155 KO
DG
CORTEX
B
Fluorojade Positive Cells
100
80
60
40
20
0
WT
miR-155 KO
C
Fluorojade Positive Cells
400
300
200
100
0
WT
miR-155 KO

Figure 4.8 Levels of neurodegeneration are similar between miR-155 KO and WT mice after CCI. (A) Degenerating neurons were stained with fluorojade (green) and DAPI (blue) 3 days after 1.0-mm CCI in the brains of WT and miR-155 KO mice. Images from the ipsilateral dentate gyrus (DG) and the lesion boundary of the cortex are shown. (B) Fluorojade cells were counted in three fields of the cortex, or in the DG from three slices between bregma -2.5 and -1.5. The mean ± SEM of total fluorojade cells in 5 WT and 6 miR-155 KO mice are shown. No significance was found by student's t-test, DG ($P = .20$), cortex ($P = .07$).

were trained for 3 days prior to CCI procedure. There was no difference between groups in the baseline performance on the rotarod. CCI induced changes in rotarod performance were measured at 1, 3, 5 and 7 days post injury (Fig. 4.9). The effect of injury type was significant by two-way ANOVA ($P < .0001$), but no differences between genotype were found ($P = .40$). These data show that miR-155 does not play a critical role in motor dysfunction after CCI.

4.2.9 Memory dysfunction in miR-155 KO and control mice after CCI

No changes were found in CCI induced motor dysfunction between miR-155 KO and WT mice. Given that our previous studies had focused on the expression and function of miR-155 in the hippocampus after CCI, and that the hippocampus functions in memory formation and retention, we tested memory function in miR-155 KO and WT mice after CCI. To test memory function a novel object test was used. In this test an animal is exposed to identical two objects and allowed to explore them for 5 min. After a 3 hour interval one object was replaced with a novel, unfamiliar object. Again the mouse was given 5 min to explore these two objects. The time spent exploring the novel versus familiar object was determined. If the mouse did not recognize the familiar object, then it would spend equal time with both objects. Alternatively, if the mouse recognized the familiar object it would spend more time exploring the novel object. The outcome measure of the novel object test is the recognition index, a recognition index of .5 indicates that there is no preference for the novel object. This is a standard test of mouse memory [219] and has been used to examine memory function in rodent models of TBI [220]. In this study, both genotypes showed no preference for the novel object in this test indicating memory impairment (Fig. 4.10). However, no differences were observed between the two genotypes ($P = .29$). This shows that ablation of miR-155 did not improve memory function. A floor effect was observed, since WT mice showed no

Figure 4.9

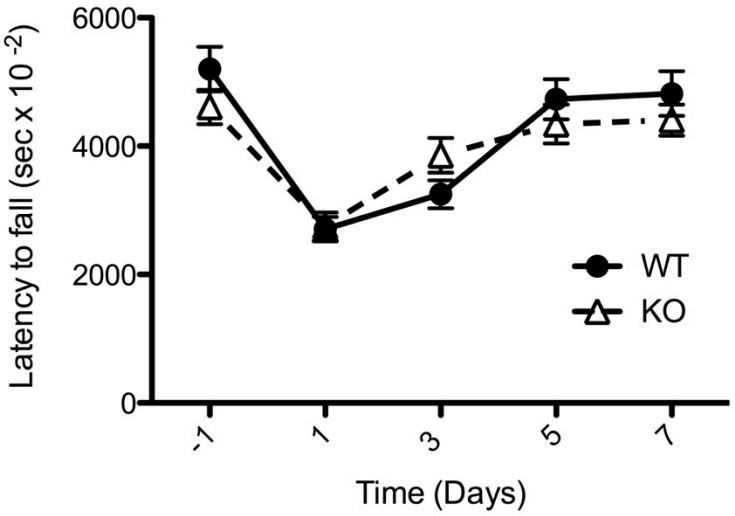
6000
4000
2000
0
Latency to fall (sec x 10 -2)
WT
KO
-7
1
3
5
7
Time (Days)

4.9 Motor function is similar in miR-155 KO and WT mice. Mice were trained on the rotarod apparatus for 3 days prior to CCI surgery the average latency to fall of 3 trials on the final day of training is shown as day -1. Rotarod testing began 1 day after 1.0 mm CCI and was repeated on days 3, 5, and 7 after surgery. The mean latency to fall ± SEM is shown. WT, n = 18, KO n = 20. Time after injury was significant by two-way ANOVA ($P < .0001$), but no effect of genotype was found ($P = .40$).

Figure 4.10

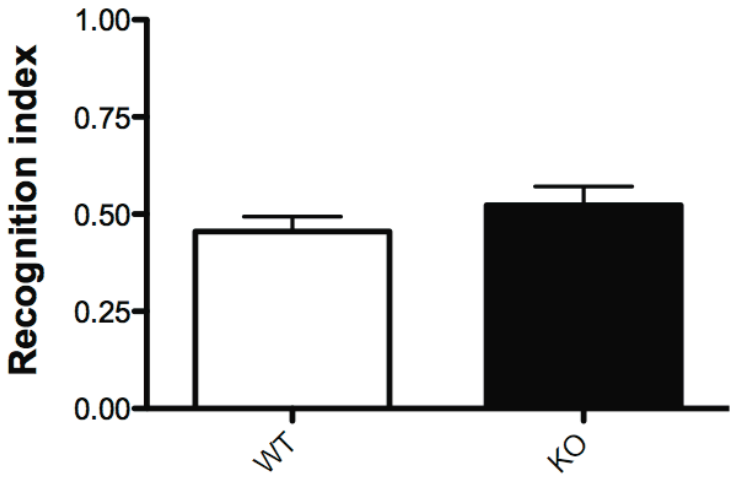

4.10 Cognitive function is similar in miR-155 KO and WT mice. Cognitive function was measured by novel object testing in miR-155 KO (KO) and wild type (WT) mice 11 days after 1.0-mm CCI. The mouse was familiarized to two identical objects, after 3 hours one of the familiar objects was replaced with a novel object. Exploration of the two objects was measured using Ethovision software (Noldus) and defined as the nose of the mouse within 2 cm of the object. The ratio time spent exploring the novel object to time spent exploring both objects is shown as the recognition index. A recognition index of .5 indicates no preference for the novel object. The mean ± SEM of WT (n = 18) and miR-155 KO (n = 20) are shown. No significance was found by student's t-test, P = .29.

measurable preference for the novel object, we could not measure negative changes in memory function in miR-155 KO mice. In summary, no evidence was found for a difference in memory function between miR-155 KO and WT mice after CCI.

4.2.9 Anxiety was decreased in miR-155 KO mice after CCI.

As an additional measure of both motor activity and as a test for anxiety, open-field testing was performed. This test has been used to evaluate both motor activity [221] and anxiety [220] in TBI models. For open field testing a mouse was placed in an unfamiliar arena and allowed to explore it for 10 min. During this time the behavior was recorded and the overall distance traveled was measured. Using this outcome measure, there were no changes in overall distance moved between miR-155 KO and WT mice ($P = .28$)(Fig. 4.11A). This finding agreed with the results of the rotarod test (Fig. 4.9), which found no changes in motor function between the two groups. Another use of the open field test is measurement of anxiety in rodents [222]. As prey animals rodents prefer to avoid open spaces. The center of the open field is relatively exposed compared to the walls. To measure anxiety, the number of times the mouse entered the center quadrant was measured. Comparing the two genotypes using this measure we found an increase in center entries in miR-155 KO mice after TBI ($P = .049$)(Fig. 4.11B). This indicated that miR-155 KO mice had decreased anxiety compared to controls after CCI, without evident motor dysfunction.

4.3 Discussion:

In previous work we had identified that miR-155 was elevated in the hippocampus after CCI in mice. Due to its known role in inflammation and cytokine signaling, we investigated its function in CCI induced neuroinflammation. Changes were found in the levels of inflammatory cytokines and in glial activation in miR-155 KO mice compared to

Figure 4.11

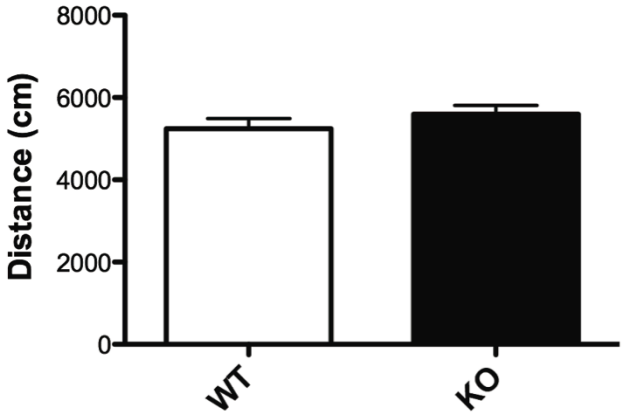
8000
6000
4000
2000
0
Distance (cm)
WT
KO

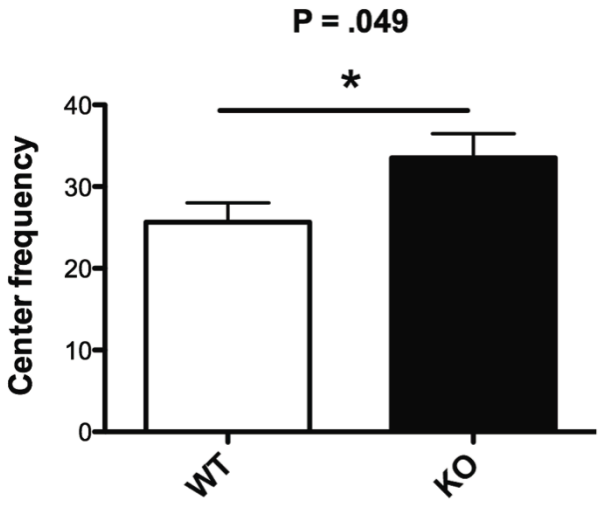
P = .049
*
40
30
20
10
0
Center frequency
WT
KO

4.11 Anxiety is reduced miR-155 KO compared to WT mice after CCI. Activity and anxiety was measured by novel object testing in miR-155 KO (KO) and wild type (WT) mice 10 days after 1.0-mm CCI. Each mouse was allowed to explore a open arena for 10 min. (A) The overall movement over the 10 min interval was measured (B) The number of times each mouse entered the center quandrant was also measured. Movement of animals within the arena was recorded and movement and center frequency were calculated using Ethovision software (noldus) The mean ± SEM of WT (n = 18) an miR-155 KO (n = 20) are shown. Center frequency (P = .049), but not overall movement (P = .28), was significant by student's t-test. *, P < .05.

controls after CCI. In miR-155 KO mice levels of IFN-β and IFN-γ were reduced. Additionally, IFN induced chemokine CXCL10 was also reduced in miR-155 KO compared to WT mice. Together these findings showed an important role for miR-155 in the promotion of the IFN response. Interestingly, we also identified decreased BDNF expression in miR-155 KO mice. BDNF was predicted to be a miR-155 target through *in silico* methods [223]. But regulation of BDNF by miR-155 has not been reported *in vitro* or *in vivo*.

We found that levels of protein SOCS1, an important negative regulator of IFN signaling, were unchanged in miR-155 KO mice. SOCS1 is a validated target of miR-155 [206] that functions to inhibit STAT1, a key transcription factor for IFN signaling [209]. We expected to see decreased levels of SOCS1 in miR-155 KO mice, but detected no change in SOCS1 protein level in the injured hippocampi of miR-155 KO mice. Furthermore, there was an increase in SOCS1 mRNA in miR-155 KO mice. SOCS1 is a critical regulator of the immune response and deletion of SOCS1 is neonatal lethal [224]. Compensatory mechanisms could be responsible for decreasing SOCS1 mRNA and maintaining SOCS1 protein levels in miR-155 KO mice. Until this report, the effect of miR-155 ablation on SOCS1 or IFN signaling had not been investigated in the brain or in TBI. A handful of studies have highlighted a role for miR-155 in neuroinflammation. In experimental autoimmune encephalitis, a model of multiple sclerosis, mice lacking miR-155 were resistant to the progression of this inflammatory disease, primarily through reducing T-cell mediated responses [126] Also, integrity of the BBB is diminished by miR-155 [225]. However, we are the first to identify changes in IFN and CXCL10 expression in brain tissues from miR-155 KO mice.

Normally expression of IFN cytokines and CXCL10 in the brain is very low. Interestingly, CXCL10 is strongly upregulated in both rodent models and human patients after TBI [176]. The expression of CXCL10 is found in clusters of cells in the brain of TBI

models that appear to be dendritic cells [226]. Interestingly, CXCL10 is strongly induced in viral infections of the brain [227]. For example CXCL10 is induced in neurons by West Nile virus infection [215] and in simian-human immunodeficiency virus encephalitis where it induces neuronal apoptosis [216]. These studies suggest a potential pathological role for CXCL10 in the brain.

We found that after CCI miR-155 KO mice had an increase in Iba1 expression. This is counterintuitive based on *in vitro* studies suggesting miR-155 has a pro-inflammatory response in microglia [210, 211]. It is unclear why we see an increased expression of Iba1 in miR-155 KO mice, but this could be due to differences in miRNA function between cell types. However by *in situ* hybridization we did not find an increase of miR-155 in microglia, rather it was in neurons. Interestingly, the induction of miR-155 expression in neurons appeared to be largely nuclear.. While this is a unique finding, both Stat1 and CXCL10 are found in neurons and contribute to neuronal cell death [215-217]. However, if these IFN induced molecules were neurotoxic, we would expect to see decreased neurotoxicity in miR-155 KO mice, where IFNs are decreased. However, our findings did not show any significant effects of miR-155 ablation on caspase 3 cleavage or degeneration measured by fluorojade, although we could be limited by group size or by the particular time points examined.

We observed a decreased IFN response to CCI and increased microglial activation in miR-155 KO mice. We also found neuronal expression of miR-155, but no difference in apoptosis or neurodegeneration. To determine what the overall balance of these effects had on TBI outcomes, we performed behavioral testing. No changes were detected between miR-155 KO and WT mice in motor or cognitive function after CCI. Interestingly miR-155 KO mice showed reduced anxiety compared WT. Recently Fonken *et al*. identified reduced anxiety in miR-155 KO mice without TBI [228]. Future work should identify whether there is an interaction between miR-155 and TBI or whether

decreased anxiety is a function of genotype alone. The mechanism by which miR-155 ablation relates to decreased anxiety is not clear. However, interferons are known to induce sickness behaviors including mood disturbances as is seen in patients being treated with high doses of IFNα for viral infections or cancers [229].

One scenario not addressed in these studies is the role of miR-155 in defense against pathogens. It has been proposed that the evolutionary advantage of stimulation of the immune response by tissue damage is to prevent infection by pathogens at the site of injury [230]. Recent reports have identified a critical role for miR-155 in the antiviral responses [129, 206]. One function of miR-155 and IFN induction could be to facilitate an appropriate immune response to potential infections in the damaged tissue. Studies of pathogen challenge in the context of TBI may be able to address this question.

4.4 Summary: We have identified a critical role for miR-155 in regulating the interferon response to TBI. As part of the IFN response miR-155 regulates levels of CXCL10, a TBI induced chemokine. In contrast to decreased IFN response, we saw an increase in Iba1 staining, suggesting increased microglial activation in miR-155 KO mice. Despite clear changes in the immune response to TBI, no changes were found in apoptosis or neurodegeneration in miR-155 KO mice. Similarly, miR-155 KO mice showed no changes in motor or cognitive function after CCI. One unexpected effect of miR-155 KO was that it reduced anxiety after CCI, which is consistent with IFN induced sickness behavior. Future studies should examine the link between TBI induced miR-155, neuroinflammation, and sickness behaviors.

Chapter 5: The role of miR-21 in neuronal function, injury, and repair

5.1 Background: Previous studies have identified increased miR-21 in the sub-acute phase of CCI. Additionally, miR-21 is elevated in many neurological disorders (Table 5.1). *In vitro* studies have proposed a role for miR-21 in neurite outgrowth [202], neuroprotection [151], and in neuronal dysfunction [231]. To characterize the role of miR-21 in the brain we obtained miR-21 KO mice. The study of miR-21 in the brain has so far focused on pathological states. However, whether or not miR-21 has a role in the function of the healthy nervous system has not been examined. The studies outlined here examine both the normal and pathological function of miR-21 in the brain.

5.2 Results:

5.2.1 Expression of miR-21 in the brain during development.

Before examining the function of miR-21 in the brain, we set out to determine its expression during development. Levels of miR-21 were detected using qPCR and *in situ* hybridization. For qPCR experiments brains were removed from mice at embryonic day 14 and 18, and at postnatal day 1, 8, and 14. Brains were homogenized and RNA extracted. There was a steady increase in miR-21 levels with increasing age (Fig 5.1). To address the function of miR-21 during development we measured miR-21 levels in differentiated and undifferentiated neuronal cells from various sources. Cultures of human neural progenitor cells (NPC) were grown in suspension creating neurospheres (Fig. 5.2A) then plated onto matrigel-coated dishes (Fig 5.2B). Neurosheres and dissociated NPCs showed the presence of SOX2 and Nestin, NPC markers [232]. Additionally, NPC could be differentiated into both astrocytes and neurons indicating that they were multipotent (Fig 5.2C).

Table 5.1. A list of neurological conditions that show increases in miR-21 expression.

Condition	Cell type/location	Downstream effect	Upstream regulation	Citation
Nerve injury	Primary sensory neurons	Neuropathic pain	IL-1B	Sakai and Suzuki, 2013 [233]
Axotomy	Dorsal root ganglion neurons	Targets Sprouty2 Increasing axon growth	Nerve transection	Strickland *et al.,* 2011 [234]
Spinal Chord injury (SCI)	Astrocytes	Reduces hypertrophy	SCI in mouse	Bhalala *et al*., 2012 [141]
Prion	Exosomes from neurons	NA	Prion infection	Bellingham *et al*., 2012 [235]
Stroke, Hypoxia, and ischemia	Neurons and astrocytes	NA	Ischemia	Ziu *et al.,* 2011 [236]
	Neurons in ischemic boundary	Suppresses cell death *in vitro* after OGD by targeting FASLG	Middle cerebral artery occlusion (MCAO)	Buller *et al*., 2010 [237]
	microglia	Represses FasL	Hypoxia	Zhang *et al.,* 2012 [238]
	Brain tissue	Negatively correlated with PDCD4 expression	Embolic stroke mouse model	Liu *et al.,* 2013 [239]
	Hippocampus	Increased MMP9, possibly by targeting RECK	Transient ischemia, MAPK/ERK signaling	Deng *et al.,* 2013 [240]
Ionizing radiation	Hippocampal neurons	Up regulation of EGFR	EGFR/Stat3 positive regulatory loop	Shi *et al.,* 2012 [231, 241]
HIV encephalitis (HIVE)	Hippocampal neurons	Targets MEF2C	NMDA	Yelamanchili *et al.,* 2010 [231]
Traumatic Brain injury (TBI)	Hippocampus and cortex	NA	Rodent TBI	Redell, Zhao, and Dash, 2011 [242]
	Cerebral cortex	NA	Fluid-percussion injury	Ping *et al.,* 2009 [144]
Epilepsy	Hippocampus	NA	Mesial temporal lobe epilepsy	Peng *et al.,* 2013 [243]
Multiple Sclerosis (MS)	Active lesions	NA	Human MS patients, experimental autoimmune encephalitis (EAE)	Lescher *et al.,* 2012 [244]

A list of neurological conditions that show increases in miR-21 expression. Some fields were not addressed (NA) in all studies

Figure 5.1

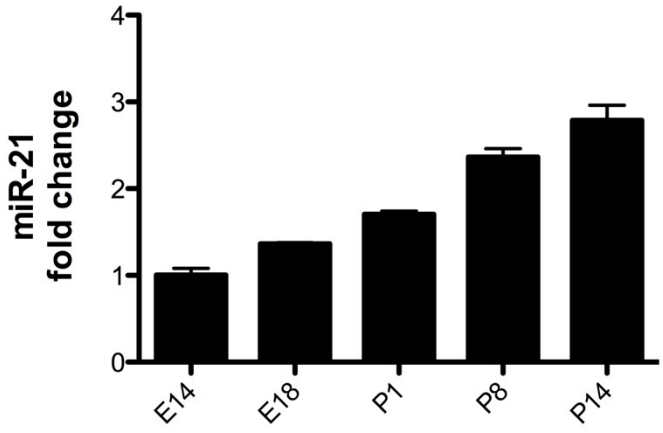

Figure 5.1 Expression of miR-21 increases during mouse development. Levels of miR-21 were measured by qPCR in mice at embryonic day 14 (E14), embryonic day 18 (E18), postnatal day 1 (P1), postnatal day 8 (P8) and postnatal day 14 (P14). Expression of miR-21 was normalized to snRNA U6 and shown as fold change relative to E14. Shown is the mean ± SEM for two replicates.

Figure 5.2

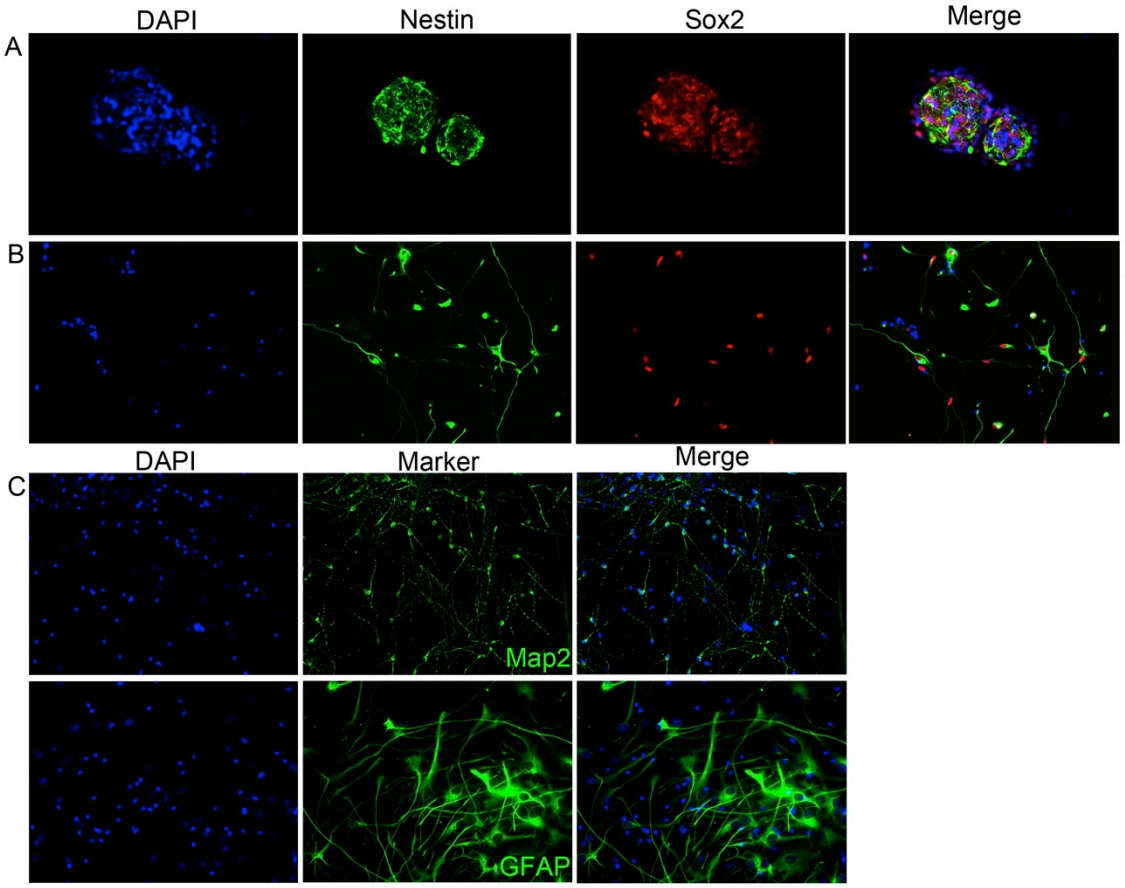

Figure 5.2 Characterization of human neural progenitor cell (NPC) cultures. (A) NPCs were grown in suspension with growth factors FGF, EGF, and LIF. (B) For treatment with cytokines or inhibitors and for differentiation experiments NPC were plated onto matrigel coated plates. NPC were stained for markers SOX2 (red) and Nestin (green). (C) NPC were differentiated by withdrawl of growth factors. Differentiated cells showed both neuronal marker MAP2 (green) and astrocyte marker GFAP (green). Nuclei in all panels were stained with DAPI.

We found that in human neural progenitor cells (NPC) miR-21 levels were higher than in neurons from the same donor (Fig 5.3A) (P = .032). Similarly cultures of mouse NPC showed a trend towards higher levels of miR-21 than mouse neurons (P = .28), but levels of miR-21 were highly variable (Fig. 5.3B) In an attempt to find a more consistent model for studying miR-21 during neuronal differentiation, we measured miR-21 expression in differentiated and undifferentiated SH-SY5Y human neuroblastoma cells (Fig. 5.3C). However, in contrast to primary neurons, miR-21 was higher in differentiated cells than in undifferentiated cells (P = .0051). This inconsistency between methods and model systems and *in vitro* and *in vivo* findings made it difficult to address any mechanistic questions related to miR-21 during development. The culture conditions of each of these differentiated and undifferentiated cell types varied greatly. Human NPC for example were grown with epidermal growth factor (EGF), fibroblast growth factor (FGF), and leukemia inhibitory factor (LIF). In contrast mouse NPC, which were grown in FGF, but not EGF of LIF. It is likely that these different culture conditions would influence the expression of miRNA-21. Due to the clear difference between human neurons and NPC, and the more translational nature of human primary cells future experiments were performed in human primary neurons and NPC.

5.2.2 Induction of miR-21 by STAT3 acting growth factors and cytokines.

Expression of miR-21 is induced in many types of neuronal injury, and some reports indicate this increased expression is in neurons [201, 233, 236]. To examine possible factors responsible for miR-21 induction in neurons after injury we treated primary human neurons with cytokines and growth factors. Rather than testing all cytokine families we focused on those that are induced by neuronal injury and signal through signal transducer and activator of transcription 3 (STAT3) STAT3 binds to miR-21 promoter through two validated binding sites [193]. This led us to focus on the

Figure 5.3

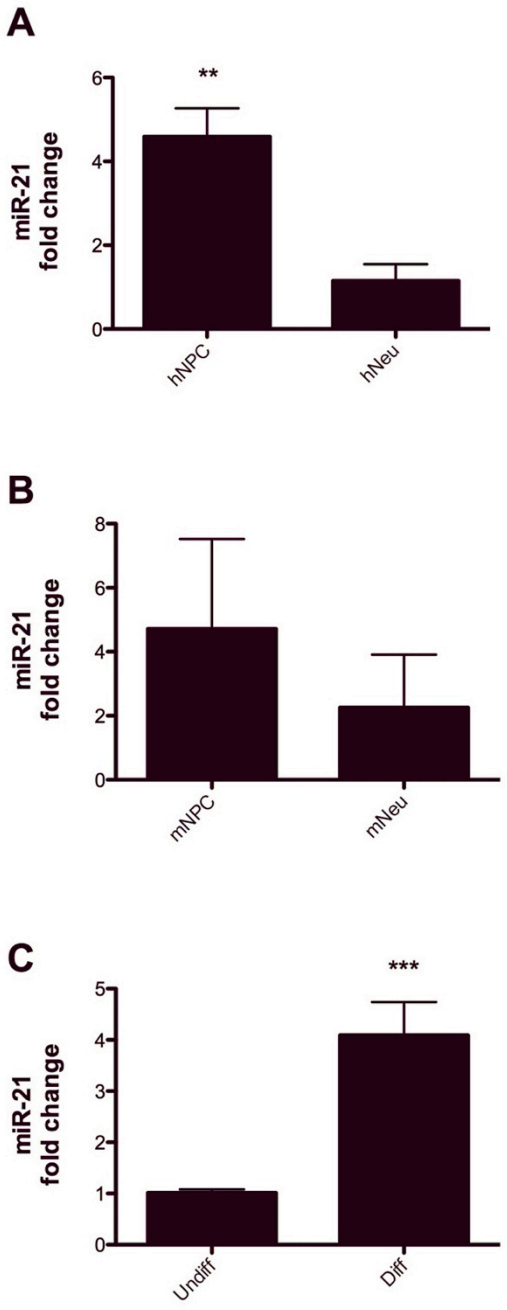
A
**
6
4
2
0
miR-21
fold change
hNPC
hNeu
B
8
6
4
2
0
miR-21
fold change
mNPC
mNeu
C
***
5
4
3
2
1
0
miR-21
fold change
Undiff
Diff

Figure 5.3 Expression of miR-21 in differentiated and undifferentiated neuronal cell types. Expression of miR-21 was measured by qPCR and normalized to snRNA U6. (A) miR-21 expression human NPC (nNPC) and human neurons (hNeu) from 4 donors shown as fold change from hNeu (P = .032). (B) miR-21 expression in mouse NPC (mNPC) and mouse neurons (mNeu) cultured from embryonic day 14 (E14) mice shown as fold change from mNeu (P = .28). (C) miR-21 expression in undifferentiated SH-SY5Y cells (Undiff) and SH-SY5Y cells differentiated (Diff) for 4 days with retinoic acid, shown as fold change from undiff (P = .0051). The mean fold change ± SEM is shown. Significance calculated by students T-test using fold change values, **, P < .01; ***, P < .001.

neurotrophic cytokines interleukin-6 (IL-6) and ciliary neurotrophic factor [245, 246]. Both IL-6 and CNTF are known to signal through STAT3 [247, 248] and have roles in neuronal injury [249, 250]. There are conflicting results regarding the expression of IL-6 receptors in neurons, some reports show that soluble IL-6 receptor is necessary for IL-6 mediated neuronal effects [251], while others report IL-6 receptor expression in neurons [252]. The expression of IL-6 receptor in cultured fetal human neurons has not been characterized, but *in vivo* fetal neurons do express at least modest amounts of IL-6 receptor. To establish induction of STAT3 activation in human neurons with IL-6, neurons were treated with 10 ng/mL IL-6 and proteins purified from the cells 0, 15, and 30, min after treatment. Sodium dodecyl sulfate poly acrylamide gel electrophoresis (SDS-PAGE) and Western blot analyses were used to measure levels of phosphorylated STAT3 (Fig 5.4). We found high levels of phosphorylated STAT3 at 30 min after IL-6 stimulation in neuronal cultures thereby suggesting that these neurons do indeed express receptors for IL-6. To determine the relative ability of IL-6 and CNTF to stimulate P-STAT3, we treated human fetal neurons with IL-6 and CNTF for 30 min and measured P-STAT3 by Western blot (Fig 5.5). We found that relative to IL-6, CNTF stimulation resulted in higher levels of P-STAT3 and that this was consistent across 4 donors. Treatment with brain derived neurotrophic factor (BDNF) is not known to signal through STAT3 [253], and no P-STAT3 was observed after treatment of neurons with 10 ng/mL BDNF. To confirm the activation of STAT3 by CNTF in neuronal cultures immunohistochemistry was performed on neurons and 30 min after treatment with 10 ng/mL CNTF. We also examined the localization of P-STAT3 in NPC post CNTF treatment. P-STAT3 by ws measured by immunocytochemistry. Interestingly, P-STAT3 levels were high in both the untreated and CNTF treated NPC, but only induced in the CNTF treated neurons (Fig. 5.6). Additionally, P-STAT3 localized to the nuclei of cells confirmed with DAPI nuclear stain. These data showed that IL-6 and CNTF could induce

Figure 5.4

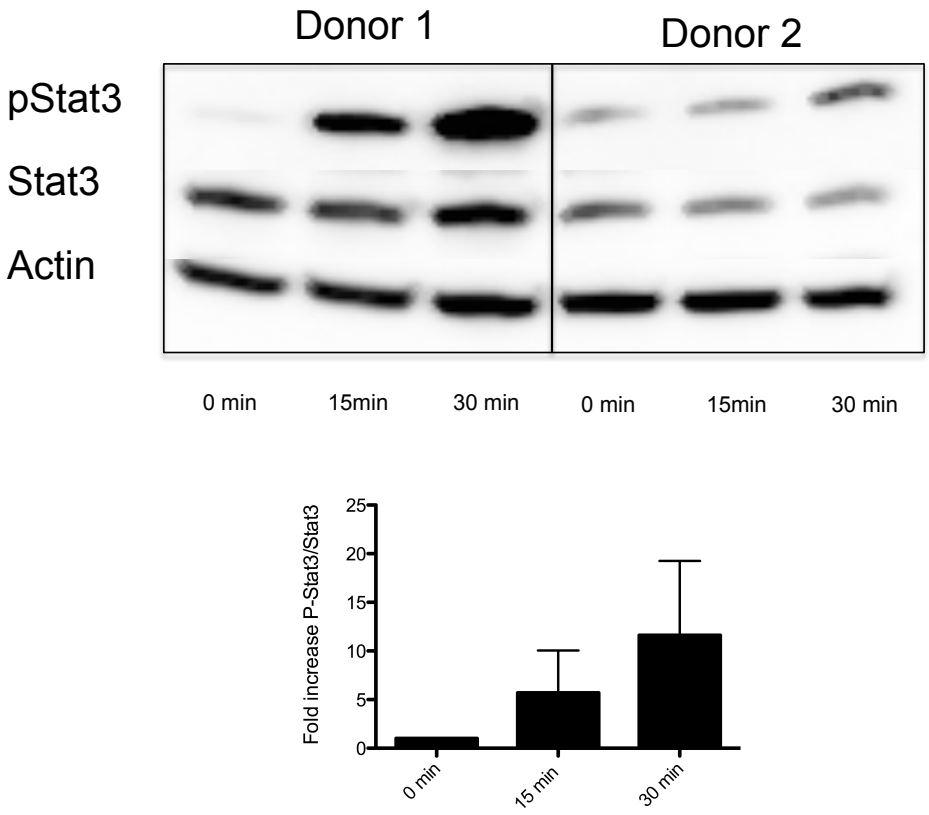
Donor 1
Donor 2
pStat3
Stat3
Actin
0 min
15min
30 min
0 min
15min
30 min
Fold increase P-Stat3/Stat3
25
20
15
10
5
0
0 min
15 min
30 min

Figure 5.4 Induction of P-Stat3 by IL-6 in human fetal neurons. (A) Neurons were grown for 14 days *in vitro* then treated with 10 ng/mL of human IL-6 for 0, 15, or 30 min. Protein was purified from the cells and SDS-PAGE and Western blot analysis was used to detect levels of P-STAT3, Total STAT3, and actin loading control. The mean P-Stat3 ± SEM for 2 donors is shown.

Figure 5.5

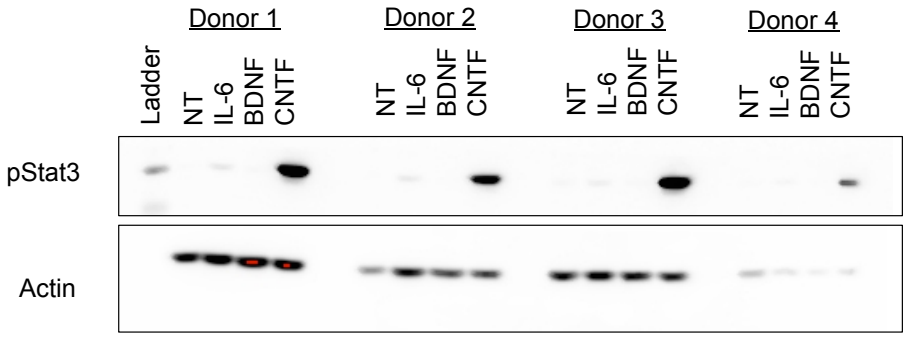
Donor 1
Donor 2
Donor 3
Donor 4
Ladder
NT
IL-6
BDNF
CNTF
NT
IL-6
BDNF
CNTF
NT
IL-6
BDNF
CNTF
NT
IL-6
BDNF
CNTF
pStat3
Actin

Figure 5.5 Induction of P-Stat3 by cytokines and neurotropic factors in human fetal neurons. (A) Neurons were grown for 14 days *in vitro* then treated with 10 ng/mL of human interleukin-6 (IL-6), brain derived neurotropic factor (BDNF), or ciliary neurotropic factor [246] for 30 min. Protein was purified from the cells and SDS-PAGE and Western blot analysis was used to detect levels of P-STAT3 and actin loading control. Samples from four individual donors are shown.

Figure 5.6

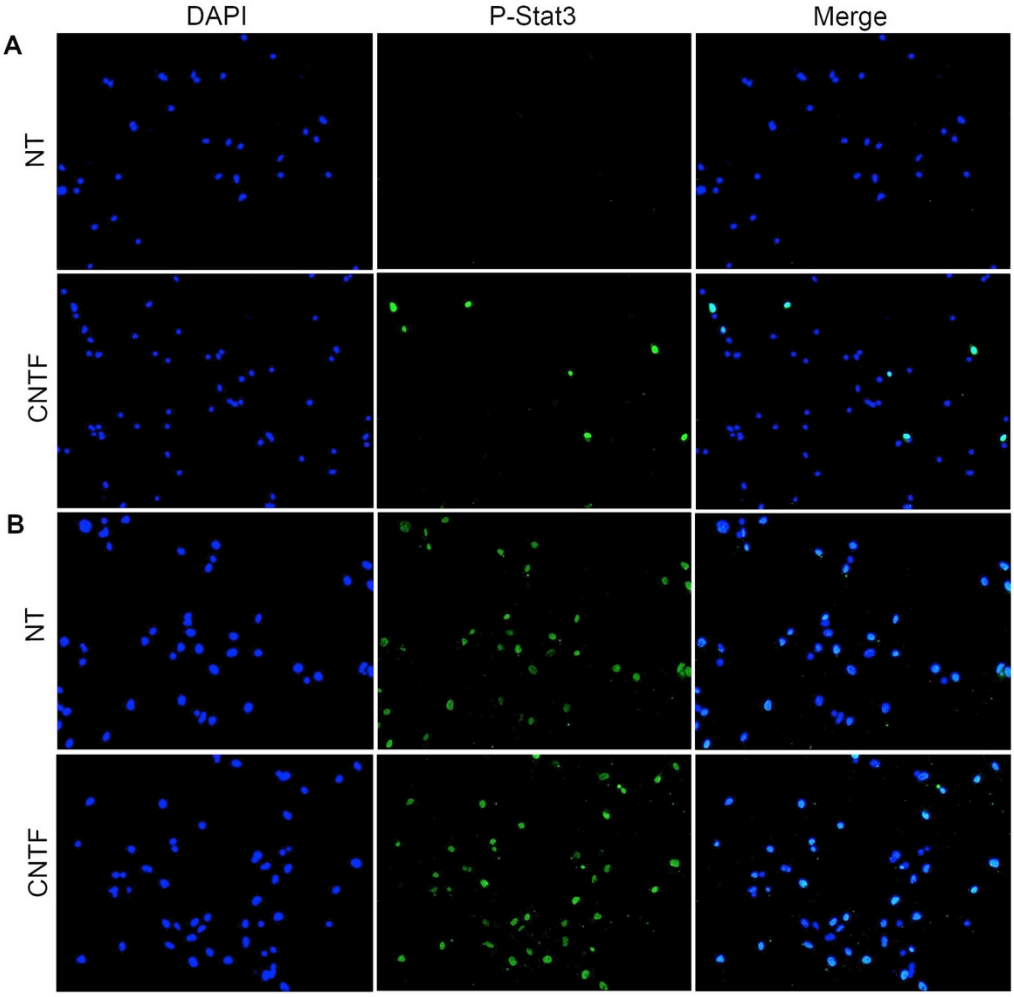

Figure 5.6 Nuclear localization of P-STAT3 after CNTF treatment in human NPC and neuronal cultures. (A) human neurons and (B) Neural progenitor cells (NPCs) were treated with 10 ng/mL cilliary neurotropic factor [246] for 30 min or no treatment (NT). Cells were fixed and stained with an antibody to P-STAT3 (green) and nuclear stain DAPI (blue). Staining was performed on cultures from 3 donors and representative images are shown.

phosphorylation of STAT3 in human fetal neuronal cultures, but that the levels of P-STAT3 were constitutively high in NPC.

Given that we saw induction of STAT3 phosphorylation in neurons after IL-6 and CNTF treatment, we then measured downstream induction of miR-21 expression. Neurons were treated with IL-6 and CNTF for 24 hours and levels of miR-21 were measured by qPCR. We found that both IL-6 and CNTF induced miR-21 expression in neurons ($P < .05$) (Fig 5.7A). Pri-miRNA is the transcriptional product of the miRNA gene, pri-miRNA is cleaved by Drosha in the nucleus into pre-miRNA-21, which is further processed by Dicer into the mature miR-21. To determine if pri-miR-21 was transcriptionally activated, levels of pri-miR-21 were measured after IL-6 and CNTF treatment in neurons. No change was found in pri-miR-21 expression after IL-6 or CNTF treatment ($P = .92$)(Fig. 5.7). These data suggest that either miR-21 is regulated at the processing level or that changes in pri-miRNA occur before the 24 h time point examined. Overall, these studies showed that both CNTF and IL-6 could induce phosphorylation of STAT3 and miR-21 expression.

STAT3 acting cytokines IL-6 and CNTF induced miR-21 expression in human neurons. Additionally miR-21 levels were higher in NPC that have constitutive STAT3 activation. These data suggest a potential link between STAT3 activation and miR-21 expression. To determine if STAT3 is essential for induction of miR-21 in neurons we used stattic, a STAT3 inhibitor that targets the SH2 domain [254]. Treatment of neurons with 1 μM stattic 30 min prior to CNTF treatment did not reduce miR-21 expression ($P = .18$) (Fig. 5.8A). Similarly, treatment of NPC with Stattic (2.5 μM) or Jak1 (0.6 nM) inhibitor did not reduce miR-21 expression ($P = .58$)(Fig. 5.8B). These findings thus suggest that miR-21 induction by CNTF is not dependent on STAT3 activation. Future studies should focus on alternative signaling pathways for miR-21 induction.

Figure 5.7

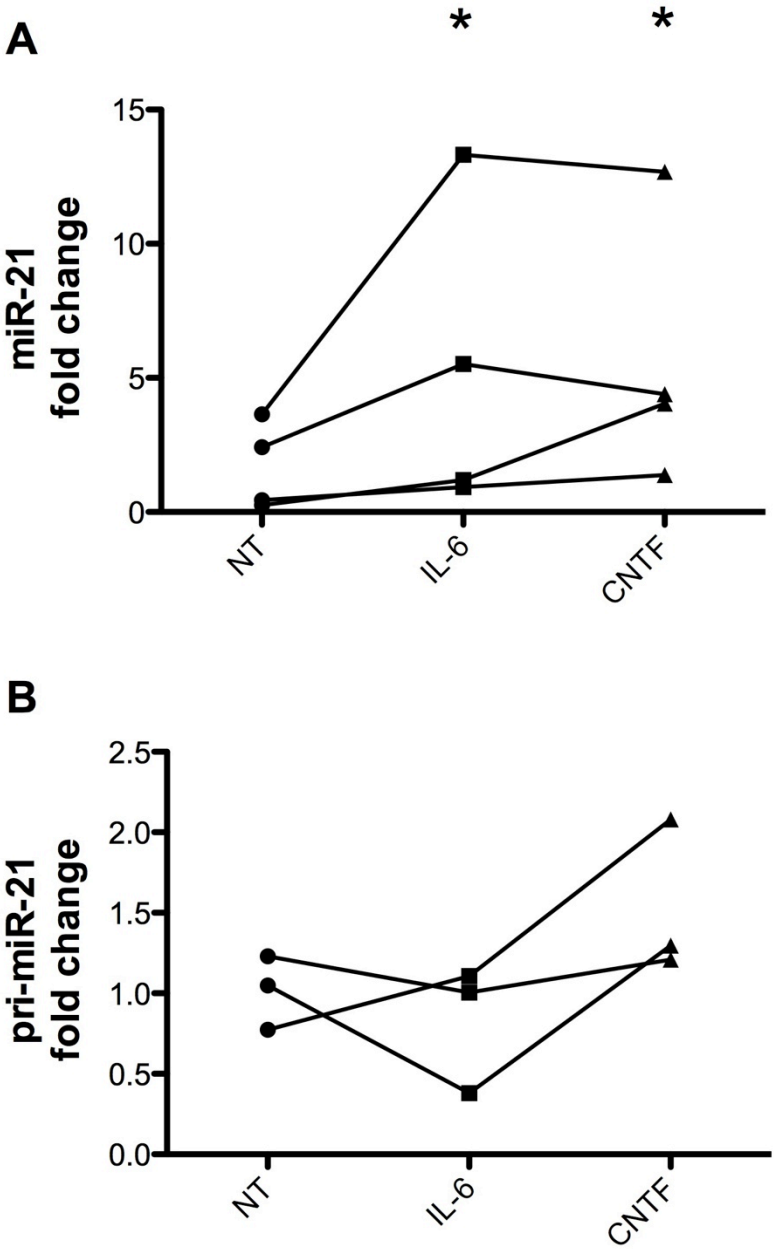
A
*
*
15
10
5
0
miR-21
fold change
NT
IL-6
CNTF
B
2.5
2.0
1.5
1.0
0.5
0.0
pri-miR-21
fold change
NT
IL-6
CNTF

5.8 IL-6 and CNTF induce miR-21, but not pri-miR-21 expression in human neurons. Human neurons were treated with 10 ng/mL CNTF or IL-6, 24 hours later cells were harvested for RNA isolation. (A) Expression of miR-21 was measured by qPCR and normalized to snRNA U6. (B) Expression of pri-miR-21 was also measured by qPCR, but normalized to GAPDH. The mean fold change relative to no treatment (NT) ± SEM is shown. One-way repeated measures ANOVA was used to calculate significance based on ΔCt values. No change in pri-miRNA expression was found ($P = .92$), *, $P < .05$ relative to NT.

Figure 5.8

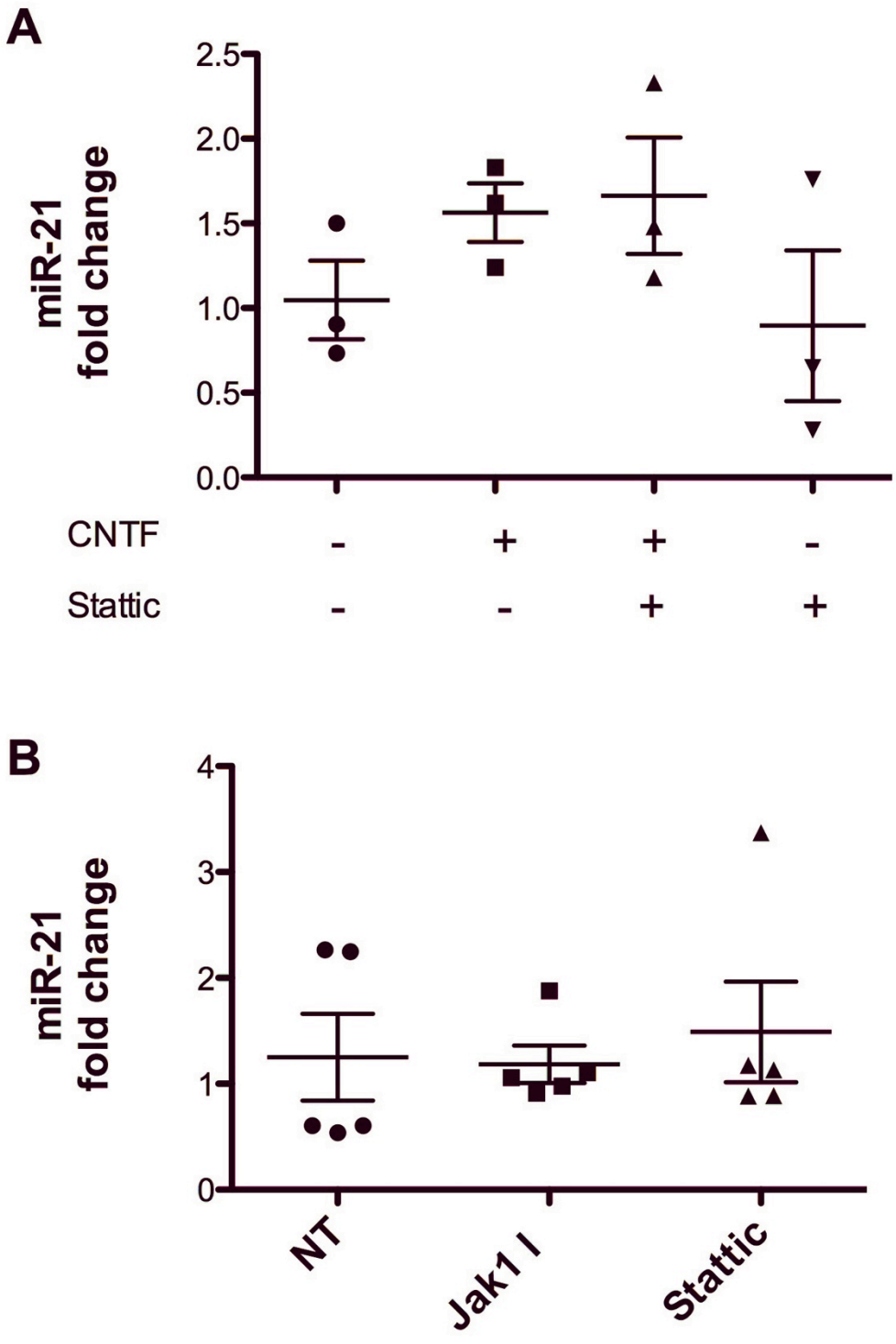
A
miR-21
fold change
2.5
2.0
1.5
1.0
0.5
0.0
CNTF
Stattic
B
miR-21
fold change
4
3
2
1
0
NT
Jak1 I
Stattic

5.8 Inhibitors of JAK1 and STAT3 do not inhibit miR-21 expression. (A) Human neurons were treated with 1 μM stattic 30 min prior to addition of 10 ng/mL CNTF, 24 hours later cells were harvested for RNA isolation. (B) Human NPC were treated with 2.5 μM stattic or 0.6 nM JAK1 inhibitor for 48 hours. Expression of miR-21 was measured by qPCR and normalized to snRNA U6, shown as fold change relative to no treatment (NT). The mean ± SEM is shown. No significance was found by 1-way repeated measures ANOVA (neurons, P = .18; NPC, P = .58).

5.2.3 Protein expression of miR-21 targets in the brains of miR-21 knockout mice

To further examine the role of miR-21 in neuronal function and injury we acquired miR-21 KO mice. These mice are viable and fertile and have changes in apoptotic cell death in cancer models [164]. Before performing function studies of miR-21 in the brain we measured levels of miR-21 targets in the hippocampi of miR-21 KO mice compared to controls. We chose to examine levels of miR-21 target Phosphatase and tensin homolog (PTEN) a negative regulator of the Akt pathway [255]. In the brain PTEN regulates plasticity [256] and deletion of PTEN causes seizures and ataxia [257]. Hippocampi were dissected from miR-21 KO, heterozygous and WT mice, and protein homogenates analyzed by Western blot analyses. No changes in PTEN levels were observed in the brains of heterozygous or homozygous knockout mice relative to WT (Fig. 5.9A). Additionally, there were no changes in phosphorylated Akt (Fig. 5.9B). These data indicate that miR-21 is not essential for PTEN regulation in 5-week old hippocampi.

5.2.4. Neuronal function measured by long-term potentiation (LTP) is normal in miR-21 KO mice

Our previous studies had shown that increased miR-21 expression in neurons can lead to dysregulation of potassium channel currents [231]. No other studies on neuronal function had been performed on miR-21 KO mice. To determine whether miR-21 KOs showed changes in neuronal function we performed long-term potentiation (LTP) recordings on miR-21 KO and WT hippocampi. LTP is a correlate for learning and memory and a measure of complex neuronal function. To record LTP a stimulating electrode is placed in the Shaffer collateral and a recording electrode is placed in the CA1 subfield of the hippocampus. A stimulus is sent through the Shaffer collateral and the excitatory post-synaptic potential is measured in the stratum radiatum of the CA1. After a baseline response is recorded a high frequency stimulus is administered to the

Figure 5.9

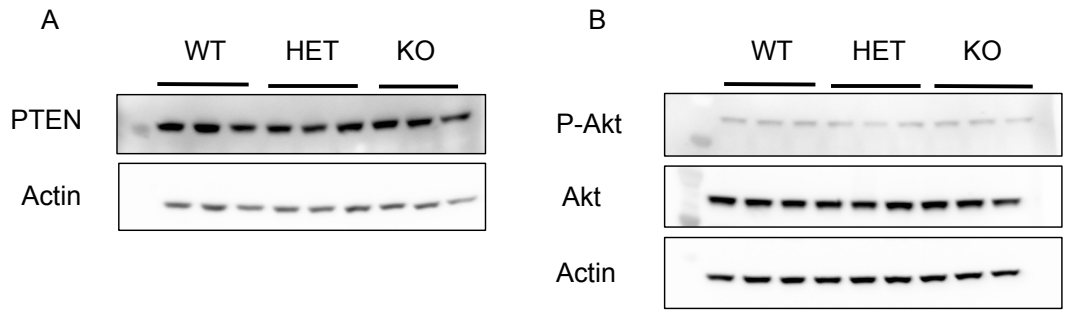

Figure 5.9 Levels of known miR-21 targets are unchanged in miR-21 KO mice. Hippocampi were dissected from 5-week old miR-21 KO (KO), Heterozygous mice (HET) and wild type (WT) mice. Protein was purified and SDS-PAGE and Western blot were used to detect levels of miR-21 targets and activation of downstream pathways. (A) Levels of miR-21 target phosphatase and tensin homolog (PTEN) and actin loading control. (B) Levels of P-Akt and total Akt, a pathway inhibited by PTEN. N = 3.

Shaffer collateral. This induces an increased responsiveness to subsequent stimuli known as the post-tetanus potentiation (PTP). After a few min the PTP is diminished, but the potentiation is still elevated above baseline. This elevation is referred to as LTP. Measurement of LTP in miR-21 KO and WT mice litter mates showed no differences (Fig 5.10). This result indicates that miR-21 KO neurons are still capable of functioning in the context of LTP.

5.2.5 Susceptibility to excitotoxicity does not change in miR-21 KO neurons

Several studies have identified a neuroprotective role for miR-21 [237, 258, 259]. To determine whether miR-21 knockout neurons showed any change in neuronal cell death we used an *in vitro* model of excitotoxicity. Excitotoxicity is related to several neurological conditions [260]. Excitotoxicity is caused by increased levels of excitatory amino acids, which bind to neurotransmitter receptors. The N-methyl D-aspartate (NMDA) receptor is thought to primarily contribute to excitotoxicity due to its calcium permeability [260]. *In vitro* models of excitotoxicity use NMDA to stimulate NMDA channels and cause delayed calcium-induced cell death. To measure differences in susceptibility to excitotoxicity in miR-21 KO neurons we cultured neurons from postnatal day 0 mouse pups and treated them with NMDA after 14 days in culture. P0 neurons were exposed to varying concentrations of NMDA for 30 min, followed by removal of NMDA and replacement of conditioned neuronal media. Cell death was then measured by increases in lactate dehydrogenase [176] release and alamar blue assay. Lactate dehydrogenase is released from dying cells and is a common measure of cell death. Alamar blue is a redox indicator of cell viability that can be used to asses neuronal viability [261]. In both the LDH and alamar blue assays we found a significant effect of NMDA concentration ($P = .013$ for alamar blue assay and $P = .0028$ for LDH assay), but no changes between miR-21 KO and WT neurons at any of the tested concentrations of

Figure 5.10

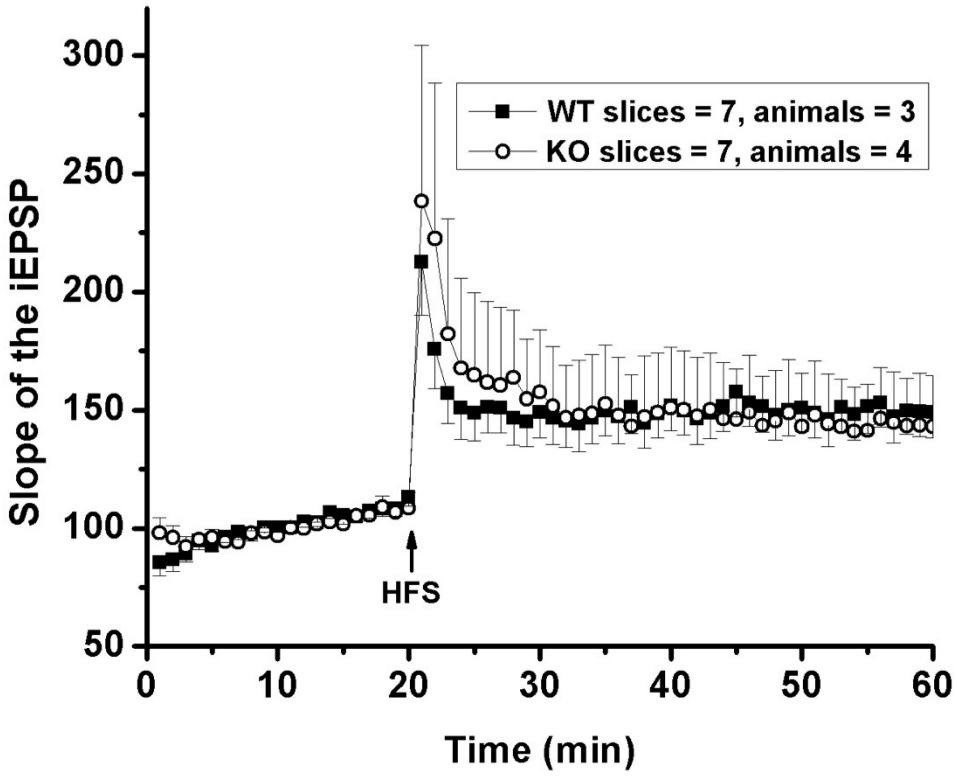
WT slices = 7, animals = 3
KO slices = 7, animals = 4
Slope of the iEPSP
300
250
200
150
100
50
HFS
0
10
20
30
40
50
60
Time (min)

Fig. 5.10 Long-term potentiation is normal in miR-21 KO mice. Hippocampal slices from 4-6 week old miR-21 KO and WT littermates were bathed in oxygenated artificial CSF for one hour before recordings were made. Stimulation of the Shaffer collateral was used to elicit field excitatory postsynaptic potentials (fEPSP) recorded from the CA1 subfield in the stratum radiatum. A 20 min baseline was recorded before high frequency stimulation (HFS, 100 Hz, 500 ms) fEPSP was recorded for an additional 40 min to measure long-term potentiation. Recordings from WT slices = 7, animals = 3, KO slices = 7, animals = 4). Shown is the mean initial slope of the EPSP ± SEM.

NMDA (P = .90 for alamar blue assay and P = .91 for LDH)(Fig. 5.11). This result was rather unexpected considering multiple reports of the neuroprotective role of miR-21. We cannot rule out a potential role for miR-21 in neuroprotection, but we were not able to measure it in this system. Compensatory mechanisms are one possible explanation for the lack of observed changes in neuroprotection. Another explanation is that miR-21 levels are too low to observe changes without induction. In previous experiments we identified CNTF as an inducer of miR-21 expression. CNTF is secreted by astrocytes after CNS damage [262]. Therefore it is possible that in a complex multicellular environment during neuronal injury miR-21 could have an effect on neuronal survival.

5.2.6 Ablation of miR-21 does not affect neurological severity score after CCI.

In order to examine the function of miR-21 in a multicellular context of neuronal injury we used a CCI model of TBI. In previous studies miR-21 was elevated at 3 days after severe (1.0 mm) CCI. To examine what effect miR-21 ablation had on neuronal survival and TBI outcome, CCI was performed on miR-21 KO and WT mice and evaluated by behavioral testing and histology. For these experiments 2 month-old miR-21 KO and WT mice were given a severe brain injury (1.0 mm depth). Neurological severity score was measured 3 days after CCI. The maximum score on the NSS is 10, a higher score indicates increased neurological impairment. A list of measures used for NSS testing is included in table 2. Using this gross measure of neurological function we found no changes between miR-21 KO mice and WT after CCI (P = .28) (Fig. 5.12) We used both male and female mice for this test and found no difference between genders (P = .60), or genotype (P = .25), or interaction between the variables (P = .44) by two-way ANOVA. Given that there was no difference between gender we examined NSS outcome of miR-21 KO vs. WT by student's T-test

Figure 5.11

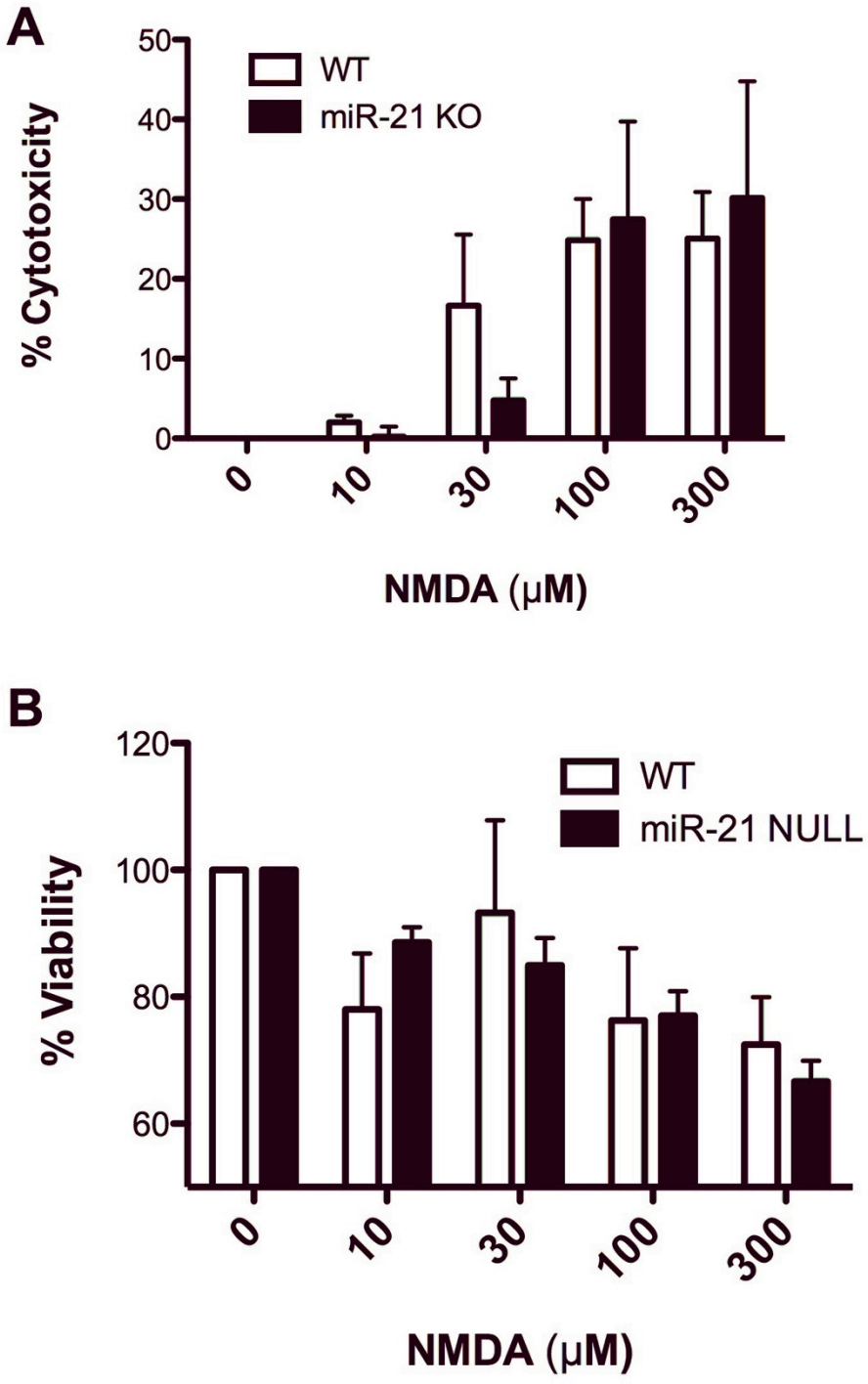
A
% Cytotoxicity
50
40
30
20
10
0
WT
miR-21 KO
0
10
30
100
300
NMDA (μM)
B
% Viability
120
100
80
60
WT
miR-21 NULL
0
10
30
100
300
NMDA (μM)

Figure 5.11 No change in neurotoxicity after NMDA treatment in miR-21 KO neurons. Neurons were cultured from postnatal day 0 mice and grown for 13 days *in vitro*. On the 13th day neuronal media was removed and cells were treated with indicated concentrations of N-Methyl-D-aspartic acid (NMDA) for 30 min in artificial CSF. After treatment conditioned media was returned and cell death was measured 24 hours later by LDH and alamar blue assays. (A) Shown is the mean % cytotoxicity ± SEM measured by LDH assay and (B) Mean % Viability ± SEM was determined using alamar blue assay. Significance was calculated using two-way ANOVA. NMDA concentration was significant (P = .013 for alamar blue assay and P = .0028 for LDH assay), but no effect of genotype was found (P = .90 for alamar blue assay and P = .91 for LDH).

Figure 5.12

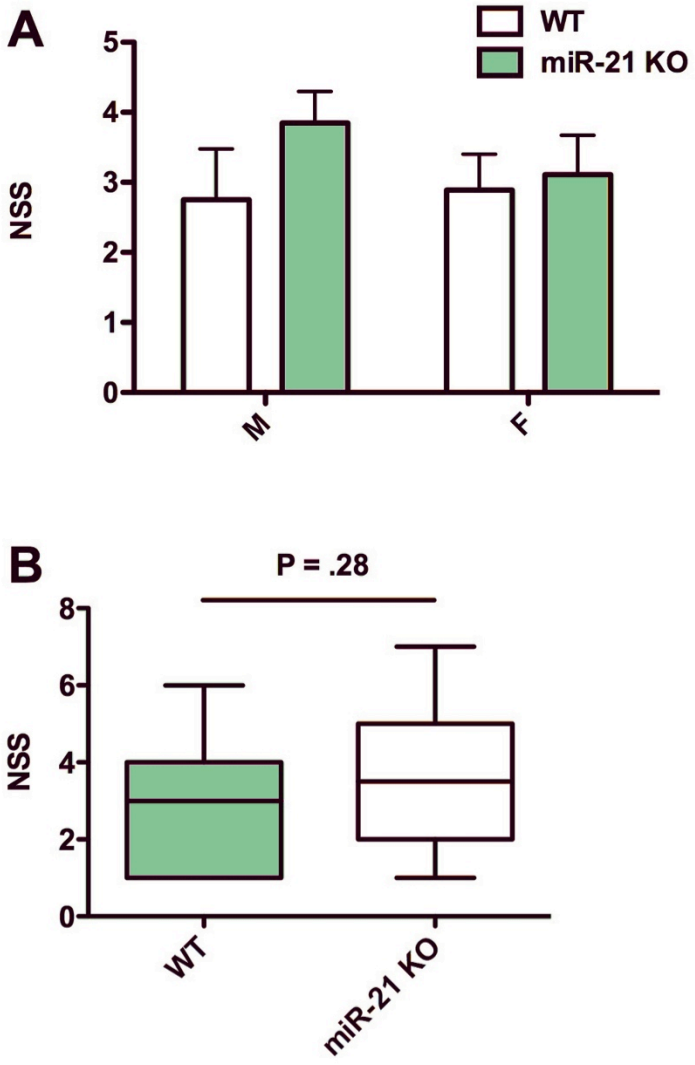

Figure 5.12. Neurological severity score [87] testing of WT and miR-21KO mice. The severity of injury 3 days after severe (1.0 mm) CCI was measured by NSS testing in miR-21 KO and WT mice. The maximum score possible is 10, with a higher score indicating higher severity. WT and miR-21KO mice were injured at 7-9 weeks old. WT, males = 8, females = 9; KO, males = 13, females = 9. (A) No significant difference was found by two-way ANOVA, (genotype, P = .25; gender, P = .60, interaction P = .44). The mean neurological severity score ± SEM is shown. (B) Combining male and female values gave no significance by student's T-test, P = .28.

and also found no significant change (P = .28) We were not able to detect a difference in NSS outcome in miR-21 KO mice. The NSS is a relatively basic outcome measure, possibly more thorough outcome assessment could detect changes between miR-21 KO and WT.

5.2.7 Neurodegeneration after CCI is unaffected by miR-21 KO

To examine to importance of miR-21 in CCI mediated neuronal degeneration we used fluorojade C (FJC) staining. FJC is specific to degenerating neurons and can be used to measure neurdegeneration after TBI in rodent models [218]. One-mm CCI was administered to miR-21 KO and WT mice, then sacrificed the mice at 3 days post injury. FJC staining was performed and FJC positive cells were counted. Again, there were no measurable change between miR-21 KO and WT mice (cortex, P = .74; hippocampus, P = .34)(Fig. 5.13). These data suggest that even in a complex multicellular model of neural injury, miR-21 KO mice do not show changes in neuronal degeneration. This finding again points to a possible compensatory mechanism in miR-21 KO mice.

5.2.8 Creation of miR-21 conditional knockout mice

In order to address the potential compensatory mechanisms found in miR-21 KO a conditional miR-21 KO was created. This mouse was designed to be inducible by a AAV-CRE system or through tissue specific expression of CRE. Functionally this means that cultured cells or tissues of live animals could be transduced with a viral vector expressing CRE recombinase, alternatively CRE can be expressed under tissue specific promoters. CRE would cause recombination at LoxP sites on either side of the miR-21 stem loop deleting the gene (Fig. 5.14). The initial steps of the mouse generation were performed by Mike McManus at the University of California San Francisco [263]. First a targeting vector was designed to insert a FRT site, lacZ gene, loxP site, Neomycin

Table 5.2 **Neurological severity score parameters.**

Task	**Score**
Exit circle within 3 min	1
Presence of seeking behavior	1
Monoparesis/hemiparesis	1
Strait walk	1
Startle reflex	1
Beam balancing for 10 sec	1
Beam walking 3 cm width in 3 min	1
Beam walking 2 cm width in 3 min	1
Beam walking 1 cm width in 3 min	1
Round stick balancing	1
Total Possible	**10**

Failure to complete each task in the allotted time was given a score of 1 for a maximum of 10 [87].

Figure 5.13

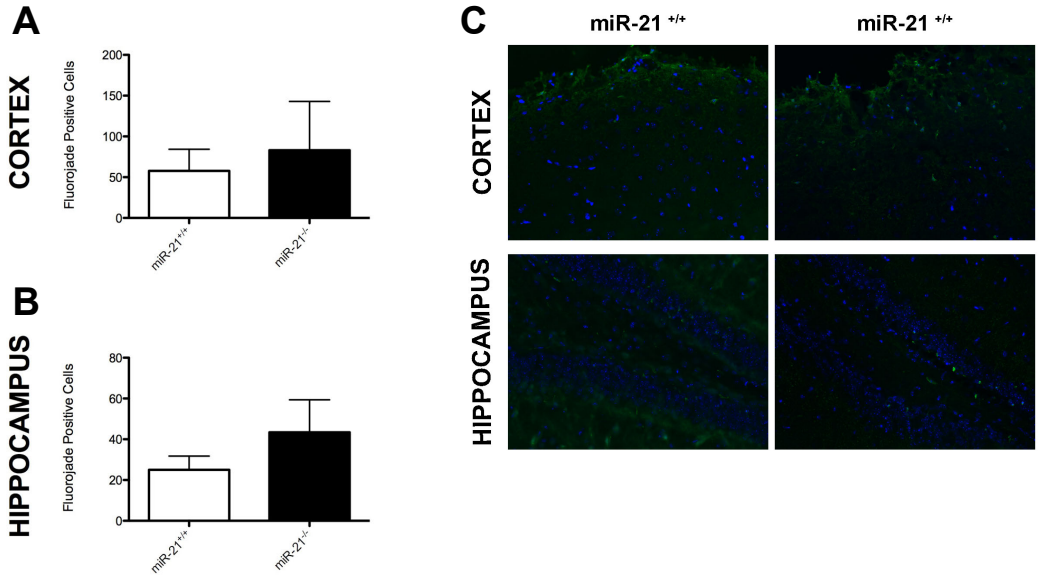
A
CORTEX
Fluorojade Positive Cells
200
150
100
50
0
miR-21+/+
miR-21-/-
B
HIPPOCAMPUS
Fluorojade Positive Cells
80
60
40
20
0
miR-21+/+
miR-21-/-
C
miR-21 +/+
miR-21 +/+
CORTEX
HIPPOCAMPUS

Figure 5.13 Levels of neurodegeneration are similar between miR-21 KO and WT mice after CCI. Degenerating neurons were stained with fluorojade (green) and DAPI (blue) 3 days after 1.0-mm CCI in the brains of WT and miR-21 KO mice. (A) Fluorojade cells were counted in three fields of the cortex, or (B) in the DG from three slices between bregma -2.5 and -1.5. The mean ± SEM of total fluorojade cells are shown, WT, n = 4 and miR-21 KO, n = 5 (C) Representative images from the ipsilateral dentate gyrus (DG) and the lesion boundary of the cortex are shown. No significance was found by student's t-test, DG (P = .74), cortex (P = .34).

cassette, FRT site, and final loxP site (FRT-lacZ-loxP-Neo-FRT-loxP) upstream of the miR-21 stem loop with an additional loxP site downstream. This construct was electroporated into embryonic stem cells to generate chimeric mice. These mice were then crossed with other strains to generate the colony. Mice containing the targeted allele were donated to Jackson laboratories. We obtained mice heterozygous for the targeted allele from Jackson laboratories. This construct is referred to as a knock out-first system as the LacZ and neomycin cassettes disrupt the expression of the gene. Once the LacZ and Neomycin cassettes are removed by Flp recombinase the target gene is expressed. Recombination with Cre recombinase removes the gene creating a true knockout. In this strain homozygosity for the targeted allele was lethal either embryonically or perinatally. The ratios of each genotype from a heterozygous cross to reach weaning age were homozygous 0/18 heterozygous 12/18 and wild type 6/18. Deletion of the miR-21 stem loop in another mouse strain (background 129S and C57Bl6) was not fatal and was used for our previous studies. However, the large neomycin/lacZ cassette likely interfered with the expression of the miR-21 host gene TMEM49 which codes for the vacuole membrane protein 1 (VMP1), which is essential for autophagy and other cellular processes [264]. Therefore heterozygous mice were bred to a Flp recombinase expressing strain to create a floxed miR-21 allele where the gene is flanked on either end by a LoxP site. The recombined allele was no longer homozygous lethal and mice homozygous for the floxed allele were generated. Floxed miR-21 mice can be used for *in vitro* or *in vivo* conditional deletion of the miR-21 gene. These mice could be breed with strains expressing Cre recombinase under tissue specific promoters to generate tissue specific strains [265, 266]. Alternatively neurotropic AAV serotypes expressing Cre recombinase could be injected to ablate miR-21 in neurons after development [267].

Figure 5.14

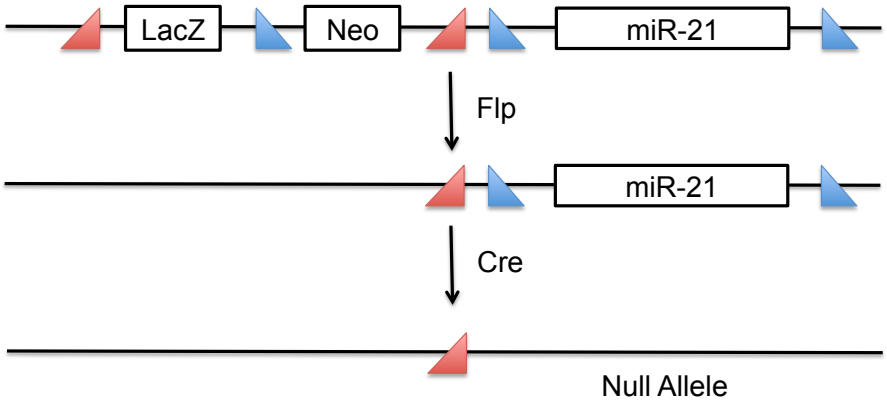

Figure 5.14 Generation of conditional miR-21 KO mice. (A) A (FRT-lacZ-loxP-Neo-FRT-loxP) cassette was inserted upstream of the miR-21 stem loop followed by an additional FRT site. Approximate location of FRT recombination sites (red triangles) and loxP recombination sites (blue triangles) are shown. (B) Crossing with a Flp recombinase expressing strain removes the LacZ and neomycin cassette leaving a floxed miR-21 stem-loop. (C) Introduction of CRE recombinase by germline or viral transduction produces a knock-out allele.

5.3 Discussion

Expression of miR-21 increases during development and can be induced by STAT3 dependent neurotrophic factors IL-6 and CNTF. Examination of the hippocampi of miR-21 KO mice revealed no changes in target PTEN or downstream phosphorylation of Akt. Additionally, miR-21 KO mice showed no changes in long-term potentiation indicating that neuronal function in these mice was intact. Despite the proposed neuroprotective properties of miR-21 [152, 237, 238, 258], we saw no changes in NMDA excitotoxicity in cultured miR-21 KO hippocampal neurons compared to WT. Additionally, we observed no changes in neurodegeneration measured by FJC in the brains of miR-21 KO mice vs. controls. There was also no difference in functional outcomes between the genotypes after CCI as measured by the NSS.

It is difficult to reconcile the evidence of a neuroprotective role for miR-21 reported by multiple independent labs with the results of these studies. One possible explanation is that compensatory mechanisms could be at play. Patrick *et al.* reported a similar finding in miR-21 KO mice in the field of cardiology [268]. Despite multiple reports by several groups that miR-21 mediated a hypertropic response in the heart [269], Patrick et al reported no change in cardiac function in miR-21 KO mice. To address these concerns we have generated a mouse carrying a floxed miR-21 allele that could be used in the future for conditional deletion of miR-21 by either tissue specific or AAV mediated CRE recombinase expression.

One significant finding of these studies was the ability CNTF to induce miR-21 in human neurons. CNTF is critical for neuronal survival and regeneration [250, 270, 271]. Clinical trials targeting CNTF have been done in ALS patients and in retinal degeneration. In the ALS trial CNTF did not produce significant improvements and in many cases dosing was limited by adverse effects such as anorexia, weight loss, and cough [246]. However, studies in retinal degenerative diseases with CNTF producing

explants have not shown toxicity [272]. As therapeutic use of CNTF poses several challenges, identifying the importance of miR-21 for the down-stream effects of CNTF could lead to a novel therapeutic target for neuroprotection and regeneration.

5.4 Summary:

CNTF induces P-Stat3 and miR-21 in human neurons. Lack of neuronal phenotype in miR-21 KO mice suggests that compensatory mechanisms could be involved. To address this issue a mouse strain with a floxed miR-21 allele was generated. This mouse can be combined with various modes of CRE delivery to make a conditional knockout for the study of miR-21 in the brain or in other systems.

Chapter 6: Traumatic brain injury increases levels of miR-21 in extracellular vesicles: implications for neuroinflammation

6.1 Background:

Traumatic brain injury (TBI) is a leading cause of death and disability worldwide and current treatment strategies are limited [4, 6, 61]. The damage caused by a TBI can be divided into the instantaneous primary mechanical injury and delayed secondary injury, which includes inflammation, neurochemical changes, and mitochondrial dysfunction [21]. A robust inflammatory response is seen post-TBI, including migration and activation of resident glia and recruitment of peripheral immune cells to the injury site [28]. As in other types of injury, cell-cell communication is critical for regulating the immune response in TBI. Although there is a wide body of research examining the roles of cell-cell mediators such as cytokines and chemokines in TBI [273], the short duration of action, along with the complex and pleiotropic nature of these molecules make them difficult drug targets [21]. In recent years several important studies have found that extracellular vesicles (EVs) can influence cell-cell communication significantly [274-276]. EVs are membrane-derived vesicles that include vesicles that originate from the plasma membrane, exosomes derived from multi-vesicular bodies, and apoptotic bodies. These EVs serve as shuttles for cellular components between cells, carrying proteins, metabolites, lipids, mRNA, and microRNA (miRNA) [277]. EV mRNA and miRNA can function within the recipient cell to alter protein expression [275, 278]. Recent studies also show that miRNA carried within extracellular vesicles can trigger inflammatory responses and neuronal damage through pattern-recognition receptors (PRRs) [276]. While several experiments have shown effects of EV associated miRNAs (EV-miRNAs) on cells in culture, less is known about how the miRNA content of EVs is altered in disease conditions and whether or not EV-miRNA has important pathophysiological

roles. No studies so far have characterized EVs in the TBI brain. The goal of this study was to investigate changes in EV microRNA after a TBI. To accomplish this we quantified levels of miRNA in EVs from mice 7 days after a TBI using next-generation sequencing. Furthermore, *in situ* hybridization was performed to analyze the expression of miRNA in the brain.

6.2 Results:

6.2.1 Characterization of CCI. While the CCI model is commonly used in TBI research, the histopathology and behavioral deficits can vary dramatically with injury depth, species, strain, and age, as well as choice of controls. We chose a 1.0 mm depth to model severe injury. While a craniotomy only (without TBI) control is used by some in the TBI field, it is associated with inflammation [185, 186]. To avoid neuroinflammation caused by craniotomy, and to better control for peripheral injury and inflammation we used a peripheral injury control where an animals were given anesthesia, analgesia, and a scalp incision.

Rotorod testing was then used to examine motor and vestibular function, as abnormalities are found after CCI [95]. Before surgery animals were trained on the accelerating rotarod apparatus for three trials a day for 3 days. On the last day of training there was no difference in latency to fall between the groups randomly selected for CCI and sham surgery (Fig 6.1A). Animals were tested daily beginning one day after surgery. CCI impaired motor function 1, 2, and 3 days after injury, by day 4 post injury motor function recovered to the level of control. Peripheral injury controls did not show a decrease in motor function after sham surgery. Since rotorod deficits were resolved at 7 days after CCI, subsequent studies were performed at this time point.

Luxol fast blue staining was then performed In order to characterize the lesion site morphology and white matter damage 7 days after CCI or sham surgery (Fig. 6.1B). Sham animals showed no evident neuropathology, however CCI induced cortical and hippocampal tissue loss on the injured side and enlargement of the lateral ventricle. Disruption of white matter tracts was clearly observable. The corpus callosum was disrupted and the fimbria was deformed.

Glial activation is a well-recognized component of TBI pathophysiology [279]. To examine the extent of glial activation at 7 days after CCI, tissues were stained for GFAP and Iba1, markers of astrocytes and microglia respectively (Fig. 6.1C). Levels of GFAP and Iba1 are both up-regulated when glial activation occurs. As expected, staining for GFAP and Iba1 increased after TBI. In addition microglial morphology shifted from ramified, resting microglia to a bushy, activated state in the injured hemisphere compared to sham controls. Activated microglia were also observed in the contralateral cortex after CCI, but to a lesser extent.

Overall, both motor impairment and neuropathology are consistent with descriptions of CCI by other groups. No changes in motor function or glial activation were seen in peripheral injury sham controls. Importantly, while motor deficits are resolved, glial activation is prominent at 7 days after injury, we chose this time point to examine the role of EV miRNA in TBI induced neuroinflammation.

6.2.2 Isolation and characterization of EV after CCI. EVs were isolated from pooled brain tissue using differential centrifugation on a sucrose gradient. Transmission electron microscopy [24] was used to characterize vesicle size (Fig. 6.2). EVs isolated from mouse brain showed a heterogeneous sized population of EVs. Intact vesicles were present indicated by the characteristic “cup shape” created by the pooling of negative

Figure 6.1

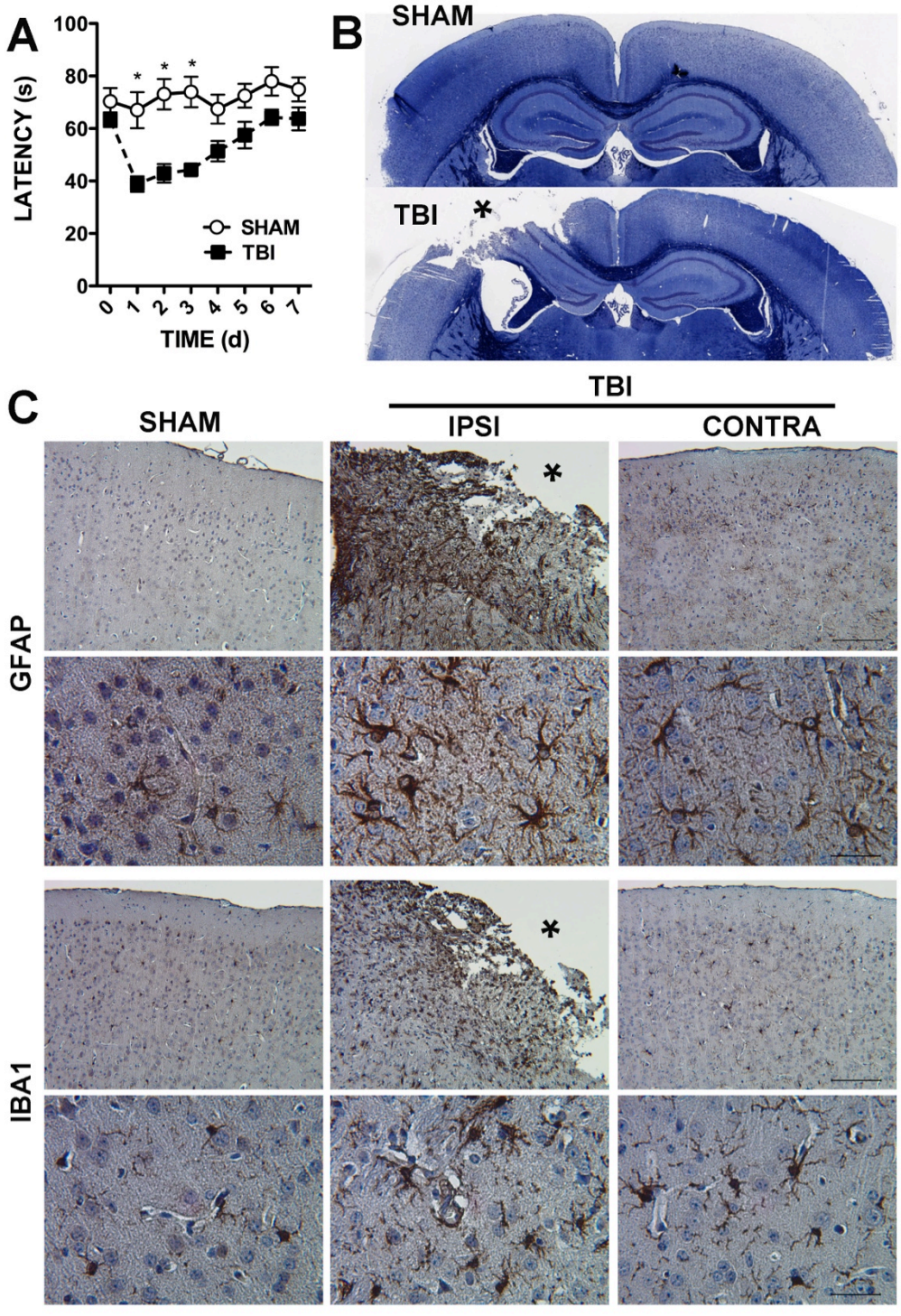
A
LATENCY (s)
100
80
60
40
20
0
SHAM
TBI
0 1 2 3 4 5 6 7
TIME (d)
B
SHAM
TBI
C
SHAM
TBI
IPSI
CONTRA
GFAP
IBA1

Figure 6.1 Characterization of CCI model. (A) Motor function in the week after CCI measured by rotarod. Sham controls and CCI mice were tested 3 times per day and trained for three days prior to injury. The average time to fall of the final training day is shown as time 0. The average time to fall of three trials for each day after injury is shown. Day 1 corresponds to 1 day after CCI. The mean ± SEM from 15 animals are shown. A two way ANOVA was used to determine statistical significance. *, $P < .001$. (B) Histology performed on mice 7 days after injury or sham surgery. Shown are representative images of three replicates. Luxol fast blue and cresyl violet staining of myelin (blue) and Nissl substance (purple) showing gross histology of the lesion, indicated by an asterisk, after CCI compared to the normal anatomy of the sham surgery control. (C) Iba-1 and GFAP immunohisochemisty (IHC) staining for microglia and astrocytes respectively in the left hemisphere of sham controls (SHAM), and the ipsilateral (IPSI) and contralateral (CONTRA) hemisphere of animals after CCI (TBI), lesion cavity indicated by an asterisk. Original magnification 10 x (bars = 100 μM), and 40 x (bars = 25 μM).

stain on top of the intact vesicle [277]. These data indicate that intact, heterogeneous EVs were isolated from mouse brain.

6.2.3 Sequencing of EV-miRNA after CCI. Recent evidence has shown that EV-miRNA can induce inflammation and neuronal damage [177, 276, 280, 281]. Therefore, understanding changes in EV-miRNAs after CCI is relevant to TBI pathology. To quantify EV-miRNAs, EVs were isolated from the left and right hemispheres of animals 7 days after CCI or sham surgery. Then miRNAs were purified from the EVs and sequenced. Brains from four conditions were used for this purpose: TBI ipsilateral (left) hemisphere, TBI contralateral (right) hemisphere, sham left hemisphere and sham right hemisphere. A heat map of all differentially expressed miRNA genes ($P < 0.05$ by ANOVA) is shown in Fig. 6.3A. Generally miRNAs clustered into those that increased or decreased in both the ipsilateral and contralateral hemispheres and those that increased only in the ipsilateral hemisphere. The largest number of differentially expressed miRNAs (59) was found in the ipsilateral hemisphere from TBI relative to the corresponding sham hemisphere, followed by the TBI ipsilateral vs. contralateral hemisphere (46). Only 7 differentially expressed genes were common between the ipsilateral and contralateral hippocampi (Fig. 6.3B). Together this indicates that the ipsilateral hemisphere shows the most distinct set of differentially expressed EV miRNAs, as would be expected considering the unilateral nature of the injury and glial activation seen by immunohistochemistry. To focus further examination, we calculated $\log_2$ values for differentially expressed miRNAs and set a threshold of $|\log_2| = 0.5$. Based on these criteria we identified 5 differentially expressed genes, 4 up-regulated and 1 down-regulated in the ipsilateral hemisphere (Fig. 6.3C). Levels of miR-212 were decreased in the ipsilateral hemisphere relative to corresponding sham and contralateral hemispheres. In contrast, miR-7b, miR-7a, and miR-21 levels were all increased in the

Figure 6.2

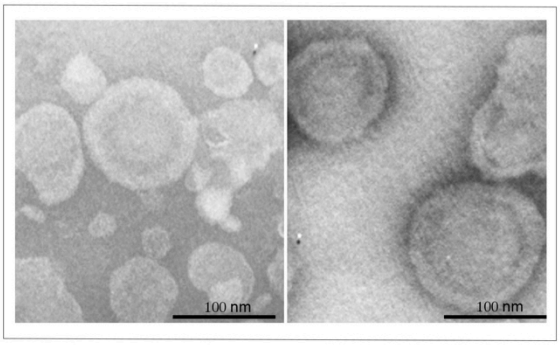

Figure 6.2 Characterization of EVs from brain tissue. Transmission electron microscopy of brain derived EVs showing a heterogeneous population of vesicles.

ipsilateral hemisphere compared to the corresponding sham hemisphere. Uniquely, miR-146 was increased bilaterally in both the ipsilateral and contralateral hemispheres compared to sham. Of all the differentially expressed EV-miRNAs, miR-21 showed the largest increase after CCI. Average counts for differentially expressed miRNAs are shown in Table 6.1.The sequences in Table 6.2 show differentially expressed miRNAs. Three of the five miRNAs have GU rich sequences that are known to mediate TLR7/8 responses [282]. In summary, CCI induced changes in miRNAs associated with EVs, particularly in the ipsilateral hemisphere.

6.2.4 Localization of miR-21 expression after CCI. Injury significantly increased EV-miR-21 in brain tissue. As homogenized brain tissue was used to isolate EVs, which cell types secrete miR-21 into EVs could not be determined. To investigate the cell-type specific expression of miR-21 after CCI we performed combined immunofluorescence and *in situ* hybridization. Images were taken in the parietal cortex adjacent to the lesion, or lesion boundary. Expression of miR-21 was higher in CCI animals than in the sham control (Fig. 6.4), which is in agreement with other reports [145, 152, 283]. Co-staining with MAP2, a cell-type specific marker for neurons, showed co-localization with miR-21, indicating that miR-21 is highly expressed in neuronal cell bodies. In contrast, miR-21 expression did not co-localize with microglial marker Iba-1, suggesting that microglia are not the primary source of EV-miR-21. However, activated microglia were found in immediately adjacent to the miR-21 positive neurons in the lesion boundary. While this staining cannot prove that the origin of EV-miR-21 is neuronal, it strongly suggests that the up-regulation in EV-miR-21 is due to an increased expression of miR-21 in neurons.

6.3 Discussion

Figure 6.3

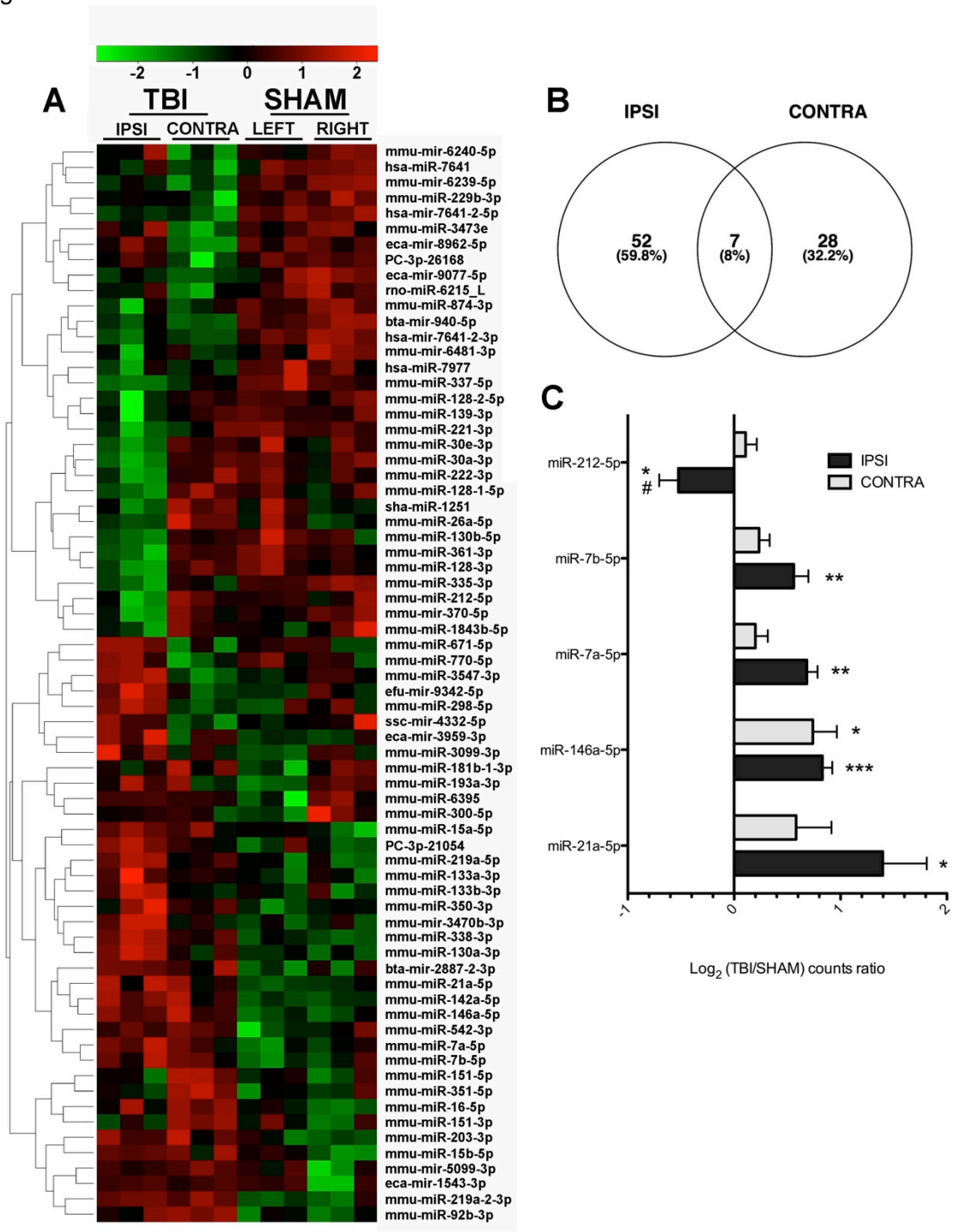
A
-2
-1
0
1
2
TBI
SHAM
IPSI
CONTRA
LEFT
RIGHT
mmu-mir-6240-5p
hsa-miR-7641
mmu-mir-6239-5p
mmu-miR-229b-3p
hsa-mir-7641-2-5p
mmu-miR-3473e
eca-mir-8962-5p
PC-3p-26168
eca-mir-9077-5p
rno-miR-6215_L
mmu-miR-874-3p
bta-mir-940-5p
hsa-mir-7641-2-3p
mmu-mir-6481-3p
hsa-miR-7977
mmu-miR-337-5p
mmu-miR-128-2-5p
mmu-miR-139-3p
mmu-miR-221-3p
mmu-miR-30e-3p
mmu-miR-30a-3p
mmu-miR-222-3p
mmu-miR-128-1-5p
sha-miR-1251
mmu-miR-26a-5p
mmu-miR-130b-5p
mmu-miR-361-3p
mmu-miR-128-3p
mmu-miR-335-3p
mmu-miR-212-5p
mmu-mir-370-5p
mmu-miR-1843b-5p
mmu-miR-671-5p
mmu-miR-770-5p
mmu-miR-3547-3p
efu-mir-9342-5p
mmu-miR-298-5p
ssc-mir-4332-5p
eca-mir-3959-3p
mmu-miR-3099-3p
mmu-miR-181b-1-3p
mmu-miR-193a-3p
mmu-miR-6395
mmu-miR-300-5p
mmu-miR-15a-5p
PC-3p-21054
mmu-miR-219a-5p
mmu-miR-133a-3p
mmu-miR-133b-3p
mmu-miR-350-3p
mmu-mir-3470b-3p
mmu-miR-338-3p
mmu-miR-130a-3p
bta-mir-2887-2-3p
mmu-miR-21a-5p
mmu-miR-142a-5p
mmu-miR-146a-5p
mmu-miR-542-3p
mmu-miR-7a-5p
mmu-miR-7b-5p
mmu-miR-151-5p
mmu-miR-351-5p
mmu-miR-16-5p
mmu-miR-151-3p
mmu-miR-203-3p
mmu-miR-15b-5p
mmu-mir-5099-3p
eca-mir-1543-3p
mmu-miR-219a-2-3p
mmu-miR-92b-3p
B
IPSI
CONTRA
52
(59.8%)
7
(8%)
28
(32.2%)
C
miR-212-5p
miR-7b-5p
miR-7a-5p
miR-146a-5p
miR-21a-5p
IPSI
CONTRA
*
#
**
**
*
***
*
-1
0
1
2
Log2 (TBI/SHAM) counts ratio

Figure 6.3 Sequencing of EV miRNAs after CCI. (A) Heat map and hierarchical clustering depicting all differentially expressed miRNAs ($P < .05$ by ANOVA). (B) Venn diagram showing differentially expressed miRNAs in ipsilateral (IPSI) vs. sham left and contralateral (CONTRA) vs. sham right. Significance was determined by T-test $P < .05$ (B). (C) MiRNAs that increase or decrease in the ipsilateral hemisphere (IPSI) relative to controls ($\log_2 > .5$) (C). Log2 values for the contralateral hemisphere (CONTRA) are also shown. The mean ± SEM from 3 replicates are shown. A one-way ANOVA was used to determine statistical significance. *, $P < .05$; **, $P < .01$; ***, $P < .001$.

The major finding of this study is that TBI induces changes in EV associated miRNAs in a rodent CCI model. Through miRNA sequencing, we found that miR-21, miR-146, miR-7a, and miR-7b all increased in the injured hemisphere relative to sham surgery control, while miR-212 expression decreased. Of these miRNAs, miR-21 showed the largest fold change. Localization of miR-21 expression through *in situ* hybridization was found overwhelmingly in MAP2 expressing neurons in the lesion boundary, suggesting that EV miR-21 could be neuronal in origin and might mediate neuron-glia signaling.

This is the first study to profile changes in brain EV-miRNA after TBI. Several previous studies have identified changes in miRNA expression in brains from TBI models [144-149]. Of these studies 3 reported a significant increase in miR-21 relative to controls [144, 145, 148]. Generally, literature on miR-21 in TBI supports a neuroprotective role for miR-21. Treatment with a miR-21 mimic improved disease outcomes in rats after CCI [152]. Also, overexpression of miR-21 reduces neurotoxicity in an *in vitro*, stretch model of TBI through miR-21 targeting of PTEN [284]. Increasingly, miR-21 is recognized as a important molecule in neuronal injury [285]. The neuroprotective and regenerative effects of miR-21 have been observed in models of stroke [237], axotomy [234], and neurodegeneration [259]. Additionally, miR-21 has roles in glial responses to injury. In spinal chord injury miR-21 reduces hypertrophy of astrocytes, reducing glial scar formation [141], whereas in experimental stroke, miR-21 targets FasL in microglia reducing microglia-mediated neuronal death [238]. Despite the potential benefits of miR-21 expression in neuronal injury, there are also drawbacks. For example, in HIV associated neurocognitive disorders elevated expression of miR-21 contributes to neuronal dysfunction by increasing potassium channel activity and targeting MEF2C, an important neuronal transcription factor [231]. Elevated miR-21 also contributes to neuropathic pain in nerve injury [233]. Nevertheless, this yin-yang role of miR-21 makes

Table 6.1.

miRNA	IPSI	CONTRA	SHAM L	SHAM R	IPSI/ SHAM L	Log2
miR-21a-5p	9,283 ± 3,860	6,610 ± 2,736	3,275 ± 295	4,179 ± 618	2.8	1.5
miR-146a-5p	3,648 ± 413	3,707 ± 1,067	2,042 ± 318	2,163 ± 444	1.8	.84
miR-7a-5p	11,393 ± 1,411	9,631 ± 1,313	7,057 ± 1,115	8,330 ± 910	1.6	.69
miR-7b-5p	8,582 ± 1,411	8,067 ± 932	5,764 ± 642	6,827 ± 1,176	1.5	.57
miR-212-5	2,988 ± 666	4,745 ± 594	4,229 ± 115	4,380 ± 931	.71	-.50

Sequencing counts of miRNAs significantly increased in the ipsilateral hemisphere ($P < .05$ with $|\log2 \text{IPSA/Sham L})| > .5$), average counts ± SD for three replicates, each pooled from 3 animals.

Table 6.2

miRNA	Sequence
miR-21a-5p	UAGCUUAUCAGACUGA**UGUUG**A
miR-146a-5p	UGAGAACUGAAUUCCAUGGGUU
miR-7a-5p	UGGAAGACUAGUGAUUU**UGUUG**U
miR-7b-5p	UGGAAGACUUGUGAUUU**UGUUG**U
miR-212-5p	ACCUUGGCUCUAGACUGCUUACU

Sequences of miRNAs significantly increased in the ipsilateral hemisphere ($P < .05$ with $|\log2| > .5$). GU rich sequences shown in bold.

Figure 6.4

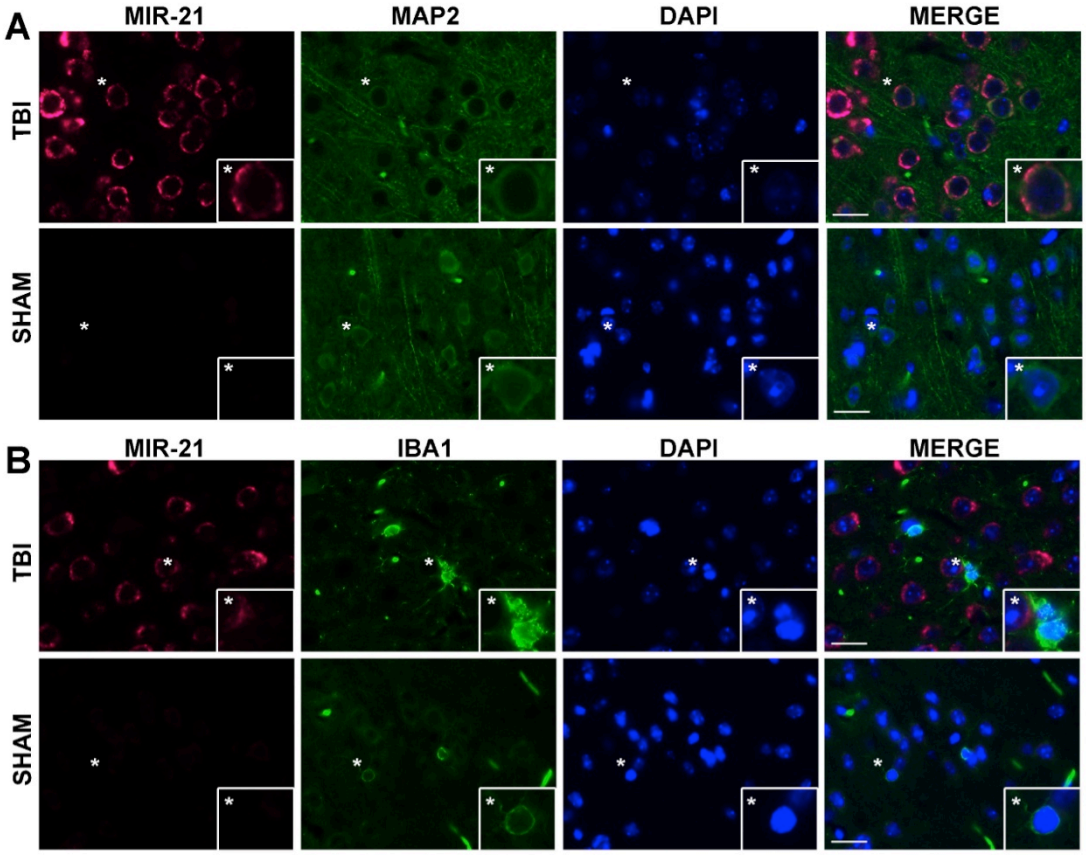
A
MIR-21
MAP2
DAPI
MERGE
TBI
SHAM
B
MIR-21
IBA1
DAPI
MERGE
TBI
SHAM

Figure 6.4 Localization of miR-21 expression after CCI. Expression of miR-21 was visualized by combined *in situ* hybridization and immunofluorescence. Staining for miR-21 (magenta) and cell-type markers (green), MAP2 and Iba1 were used to identify neurons and microglia respectively. Nuclei are stained with DAPI (blue). Original magnification 63 x (bars = 100 μm), location of insets marked with an asterisk. Staining was performed in duplicate and representative images are shown.

it an interesting target of study in neuronal injury and inflammation. Here, for the first time we have identified that miR-21 can also be associated with EVs in TBI.

In this study we profiled EV-miRNAs from the brain tissues of CCI injured mice. Previously, Patz et al also characterized EV-miRNAs after TBI, but in the cerebrospinal fluid (CSF) of patients [286]. Our miRNA sequencing did not recapitulate the miRNA profile found in this previous study. This difference could be due to several factors, such as the use of CSF vs. brain tissue, and patients versus a controlled experimental model. Outside of the TBI field, profiling of EV-miRNA from neurons and brain tissue has been performed. Interestingly, exosomes secreted by prion-infected neurons show higher levels of miR-21 than exosomes from uninfected neurons *in vitro* [235]. This supports the theory that neurons increase the release of miR-21 in EV as a response to stress. Our group and others have studied the role of miRNAs in exosomes or extracellular vesicles in HIV-associated neurocognitive disorders (HAND), conditions strongly linked with neuroinflammation [287]. One study indicated that comorbid HIV infection and opiate abuse can increase miR-29 packaging in brain EV, which in turn downregulates the important neuroprotective molecule PDGF [288]. Another study showed that in HAND, EV miR-21 is increased and mediates neurotoxicity by binding to TLR7 and causing necroptosis [177]. As more groups profile miRNA signatures of EVs, a clearer picture will form of which miRNAs are common to neuronal injury or inflammation and which are specific to disease state.

The release of miRNAs in EVs is thought to have two possible effects on target cells. The first mechanism occurs when the EV either fuses with the cell membrane or endosomal membrane to release its contents into the cytosol [278]. Mature miRNAs in the cytosol can bind to target mRNAs and decrease their translation [274]. The second mechanism of EV miRNA action is through binding of pattern recognition receptors in the endosomal compartment, primarily toll-like receptor 7/8 (TLR7/8) [276]. TLR7/8

recognizes ssRNA, and elicits an antiviral response as part of the innate response to viral pathogens[289]. Several groups have reported that miRNAs with EV can stimulate TLR7/8, but the outcome of miRNA binding to TLR7/8 is highly dependent on cell type. In immune cells, such as macrophage and microglia, TLR7/8 binding elicits a pro-inflammatory response, including secretion of TNFα [276]. Alternatively, TLR7/8 binding in neurons is toxic and can lead to cell death or synaptic loss [177, 280, 281]. The binding of miRNAs to TLR7/8 is dependent on GU rich sequences [282], as miR-21 has such a GU rich sequence it is a strong stimulator of TLR7/8 [177, 276, 280]. Recent studies have identified EV miR-21 specifically as both pro-inflammatory [276] and neurotoxic [281]. Our studies on SIV encephalitis showed that not only was miR-21 elevated in EV from encephalitic brains, but also that EV miR-21 induced necroptosis in neurons through TLR7 [177]. Therefore, the increase of EV-miR-21 reported in this study has important pathophysiological implications for TBI. Whether miR-21 in EV leads to translational regulation or TLR7/8 stimulation in recipient cells after TBI is not addressed in this study and will be an important question for future research.

Aside from miR-21, we identified 3 other miRNAs with increased levels in EVs, miR-146, miR-7a, and miR-7b. Increased expression of total brain miR-146a was reported Lei *et al.* in a CCI model of TBI [144]. Interestingly our previous studies in SIV encephalitis also found increases in EV miR-146 [177]. It is known that inflammatory stimuli such as LPS induce miR-146 [290]. Interestingly, knockout studies in mice have proven miR-146 to be an important anti-inflammatory miRNA [291]. Even more importantly miR-146 within exosomes can act functionally to reduce inflammation in recipient cells [292]. Therefore, it is possible that in TBI miR-146 within exosomes could reduce neuroinflammation. Relatively little is known about miR-7a and b compared to miR-146 and miR-21. However, some *in vitro* data suggest miR-7 can be neuroprotective [293]. The expression of miR-7 is relatively brain specific [294].

Interestingly miR-7a and b both contain a GU rich element identical to that found in miR-21 (UGUUG) indicating that they may also be ligands for TLR7/8 (6.2). We found one miRNA, miR-212, down regulated in EV after TBI. Down-regulation of miR-212 has been found in several brain diseases [295]. These include anencephaly [296], schizophrenia [297], and Alzheimer's disease [298]. Together these studies hint that deregulation of miR-212 may be pathological in the brain.

6.4 Summary: In conclusion we report here the first miRNA profile of brain exosomes in TBI. Differential expression of 5 miRNAs was found between EVs from CCI injured brain vs. uninjured controls. Of the differentially expressed miRNAs, miR-21 showed the highest increase in EVs of the injured brain. Interestingly, increased levels of miR-21 were found in neurons of the injury boundary zone near reactive microglia. This work shows that TBI induces changes in EV miRNA, which likely has important consequences for cell-cell signaling and the disease process in TBI.

Chapter 7: Behavioral phenotyping of mice in the chronic phase of TBI

7.1. Background:

Survivors of TBI experience a variety of chronic symptoms that can range from motor and cognitive disability to neuropsychiatic dysfunction. Current pre-clinical modeling of TBI in rodents generally fails to address these chronic outcomes of TBI. To improve translational efficacy, a better understanding of the chronic phenotype of rodent models of TBI is needed. Additionally, the pathophysiology that causes neuropsychiatric conditions after TBI is unknown. Animal modeling of neuropsychiatric changes after TBI could provide a mechanistic understanding of these disorders. In order to investigate changes in long-term behavioral outcomes we chose a highly utilized model of TBI, the controlled cortical impact (CCI) model. Four experimental groups naïve, craniotomy only, moderate and severe CCI, were tested using a battery of motor, cognitive, and neuropsychiatric behavioral measures.

7.2 Results:

7.2.1 Motor function 2 months after CCI is normal

To evaluate motor and vestibular function in the chronic phase of CCI we performed accelerating rotarod testing. Rotarod testing is a common measure of TBI induced deficits in rodent models [95, 170]. The accelerating rotarod utilizes a rotating cylinder as a treadmill. Mice were placed on the rod, the speed of rotation was steadily increased until the mouse fell, activating a weight based sensor below the rod. The latency to fall was then recorded. Mice were tested three times a day for three days and the trials averaged for each day. There were no differences between groups in rotarod performance indicating that motor function was not impaired 2 months after CCI (Fig 7.1).

Figure 7.1

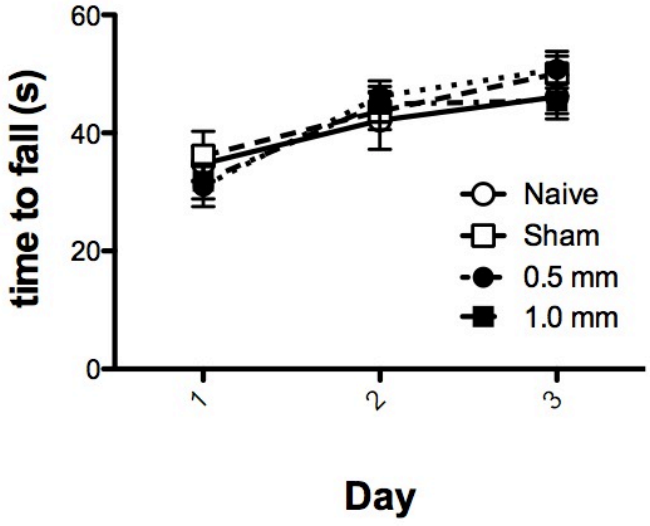

Figure 7.1 Motor testing 2 months after CCI. Motor and vestibular functions were tested by accelerating rotarod on three consecutive days in naïve, craniotomy only (Sham), moderate (0.5 mm) and severe (1.0 mm) CCI. Latency to fall was recorded by weight-based sensors. The average of three trials was reported for each day. The mean ± SEM is shown, n = 8 per group. No significance by condition was found by two way ANOVA (P .40), however the day of testing was significant (P < .0001).

7.2.2 Memory is not impaired 2 months after CCI

To evaluate memory function 2 months after CCI we performed novel object testing. Novel object testing is an ethological test of memory function [219] and has been used to evaluate animal models of TBI [299, 300]. Mice were first familiarized to two identical objects then after an interval of three hours one object was replaced with a novel, unfamiliar object. The mouse was then returned to the arena and recorded for 5 min. The time spent exploring each object was measured and a recognition index was calculated. The recognition index is a ratio of the time spent with the novel object to the time spent exploring both objects. A recognition index of .5 means that there was no preference for the novel object. Using this memory test no differences were found between the four groups (Fig. 7.2). All groups showed a recognition index greater than .6 indicating a preference for the novel object. These data indicate that 2 months after injury mice do not have deficits in memory function.

7.2.3 Evidence of hyperactivity 2 months after CCI

The open field test is both a measure of overall motor function and activity and a measure of anxiety [301]. Mice were placed in an unfamiliar 49 cm x 49 cm arena and behavior was recorded for 20 min. Both moderately (.5 mm) and severely (1.0 mm) injured mice traveled a greater distance than naïve mice and severely injured mice traveled more than craniotomy only sham controls (Fig 7.3A). Similarly both moderately and severely injured mice had increased velocity in the open field test relative to naïve controls (Fig. 7.3C). The open field test can also be used to measure anxiety, to do this the percent time spent in the center quadrant is calculated. Injured mice and controls showed no changes in anxiety by this test (Fig. 7.3B). In summary, injured mice showed increased activity and velocity in the open field test.

Figure 7.2

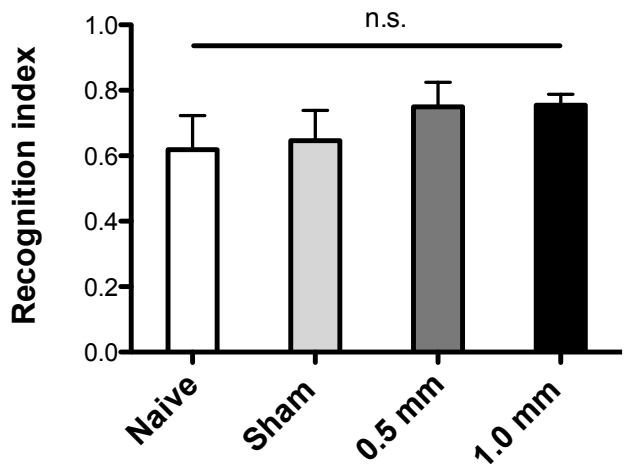

Figure 7.2 Normal memory function months after CCI. Memory was tested by novel object recognition in naïve, craniotomy only (Sham), moderate (0.5 mm) and severe (1.0 mm) CCI. The mouse was familiarized to two identical objects, after 3 hours one of the familiar objects was replaced with a novel object. Exploration of the two objects was measured using Ethovision software (Noldus) and defined as the nose of the mouse within 2 cm of the object. The ratio of time spent exploring the novel object to time spent exploring both objects is shown as the recognition index. A recognition index of .5 indicates no preference for the novel object. The mean ± SEM is shown, n = 8 per group. No significance was found by one way ANOVA (P = .53).

Figure 7.3

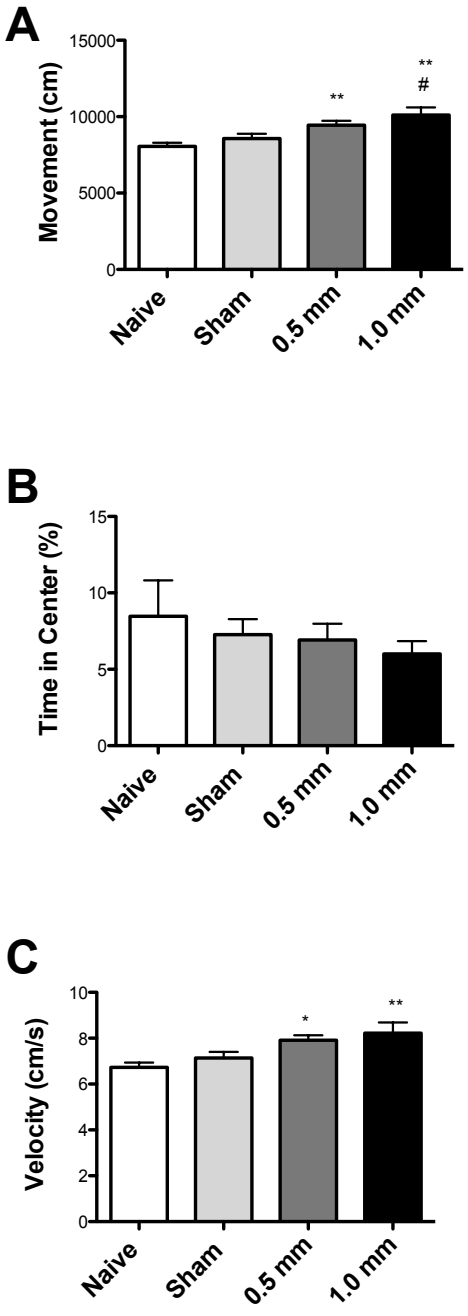
A
Movement (cm)
15000
10000
5000
0
**
**
#
Naive
Sham
0.5 mm
1.0 mm
B
Time in Center (%)
15
10
5
0
Naive
Sham
0.5 mm
1.0 mm
C
Velocity (cm/s)
10
8
6
4
2
0
*
**
Naive
Sham
0.5 mm
1.0 mm

Figure 7.3 Increased activity in injured mice 2 months after CCI. Activity and anxiety were tested by novel object recognition in naïve, craniotomy only (Sham), moderate (0.5 mm) and severe (1.0 mm) CCI two months after injury. Each mouse was allowed to explore an open arena for 20 min. (A) The overall movement over the 20 min interval (B) The % time each mouse spent in the center quandrant. (C) The velocity over the 20 min interval. Movement of animals within the arena was recorded and movement and center frequency were calculated using Ethovision software (noldus) The mean ± SEM of each group are shown, n = 8. Overall movement ($P = .0017$), but not % time in center ($P = .52$), was significant by one-way ANOVA. *, $P < .05$; **, $P < .01$ from naïve. #, $P < .05$ from sham.

7.2.4 Injured mice are disinhibited 2 months after CCI

In order to investigate the anxiety-like phenotype of injured mice, elevated zero maze testing was performed. In this modified version of an elevated plus maze mice were recorded while they explore the open, exposed arms and the closed, protected arms [302]. Over the 6 min recording period the time spent in the closed arms and the number of entries into the closed arms was determined. Interestingly severely injured mice spent significantly more time in the open arms (Fig. 7.4). No changes were observed in exits from closed arms. The increased time spent in the open arms by severely injured mice suggests decreased anxiety or disinhibition.

7.2.5 Lack of depressive phenotype 2 months after CCI

Depressive-like behavior in mice can be measured by the tail suspension test [303, 304]. Mice were suspended from a metal rod by the tail 30 cm off the counter. The time spent immobile vs. the time spent struggling was scored by a blinded observer. An increase in time spent immobile is a marker of depressive-like behavior in mice. No changes were observed between the four experimental groups in time spent immobile (Fig. 7.5). Based on this measure we did not observe depressive-like behavior in mice 2 months after CCI.

7.2.6 Sociality in mice 2 months after CCI

To measure subtle changes in social interaction between injured mice and non-injured controls we performed a social interaction test [305]. Experimental mice were placed in a clean cage with fresh bedding. Immediately after placing the experimental animal in the cage, a second non-experimental size matched con-specific was placed in the same cage. The two mice were allowed to interact for 20 min while being recorded. A blinded observer scored the time spent in proximity and scored several pro-social and aggressive behaviors performed by the experimental animal. We found no changes in

Figure 7.4

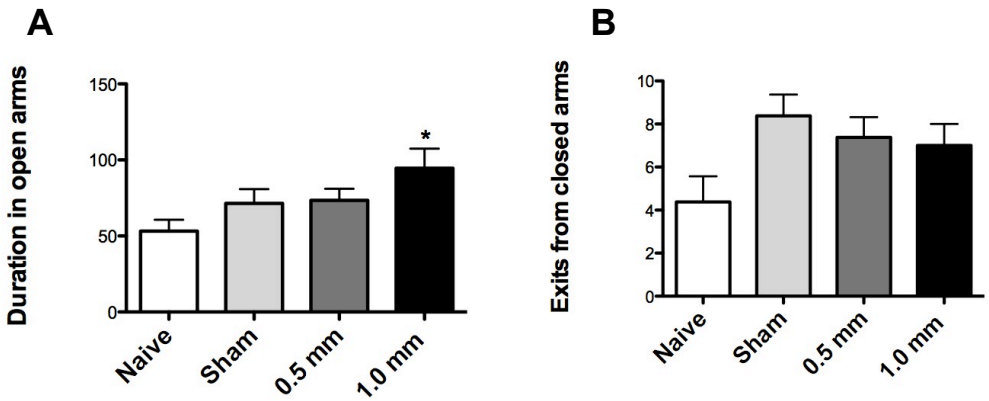
A
Duration in open arms
150
100
50
0
*
Naive
Sham
0.5 mm
1.0 mm
B
Exits from closed arms
10
8
6
4
2
0
Naive
Sham
0.5 mm
1.0 mm

Figure 7.4 Disinhibition in injured mice 2 months after CCI. Anxiety was tested in naïve, craniotomy only (Sham), moderate (0.5 mm) and severe (1.0 mm) CCI two months after injury using an elevated zero maze. (A) The duration of time spent in the open arms in seconds (B) The number of times all four paws exited the closed arms. Movement of animals within the elevated zero maze was recorded and time spent in the closed arms was calculated using Ethovision software (noldus) The mean ± SEM of each group are shown, n = 8. No differences were seen in the number of exits from closed arms by one way ANOVA ($P = .065$). *, $P < .05$ from naïve.

Figure 7.5

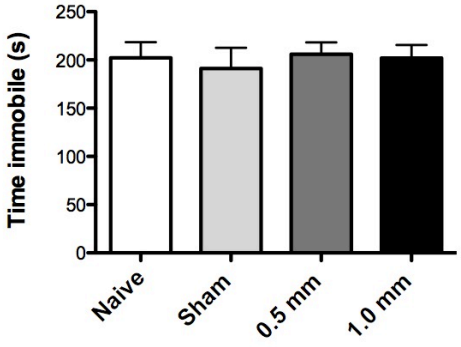

Figure 7.5 Lack of depression-like phenotype in injured mice 2 months after CCI. Depression was tested in naïve, craniotomy only (Sham), moderate (0.5 mm) and severe (1.0 mm) CCI two months after injury using a tail suspension test. Time spent immobile was scored. The mean ± SEM of each group are shown, n = 8. No significance was found by one-way ANOVA (P = .93).

any of the observed behaviors (Fig. 7.6). There was a trend towards increased aggressive behaviors in severely injured mice, but there was high variability between individual mice.

7.2.7 No difference in hyperactivity or disinhibition at 6 months after CCI

At 2 months after CCI, injured mice showed increased activity and increased time spent in the open arms of the elevated zero maze (EZM). To determine whether measured changes in hyperacitivity and disinhibition persisted these tests were repeated at 6 months after CCI. At this time point no changes were observed between groups in movement, velocity, or time spent in the center quadrant as measured by the open field test (Fig. 7.7). Similarly we found no difference between groups in the elevated zero maze (Fig. 7.8). These data suggest that the hyperactive and disinhibited phenotype of injured mice at 2 months after injury does not persist to 6 months after injury.

7.3 Discussion

The main finding of this work was disinhibition and hyperactivity in mice 2 months after CCI. Increased levels of movement and velocity were observed in both moderate and severely injured mice relative to controls indicating increased exploratory behavior. Additionally, severely injured mice spent more time in the open arms of an elevated zero maze, indicating disinhibition.

Several other groups have observed hyperactivity or increased exploratory behavior in rodent models of TBI. Increased activity was found in a CCI model [306], and diffuse axonal injury models [307, 308] as well as models of mild TBI [262, 309]. A few studies have also found decreased activity, but this was either during the acute phase when motor impairment is still a confounding factor [310] or in very severe injury [299].

Figure 7.6

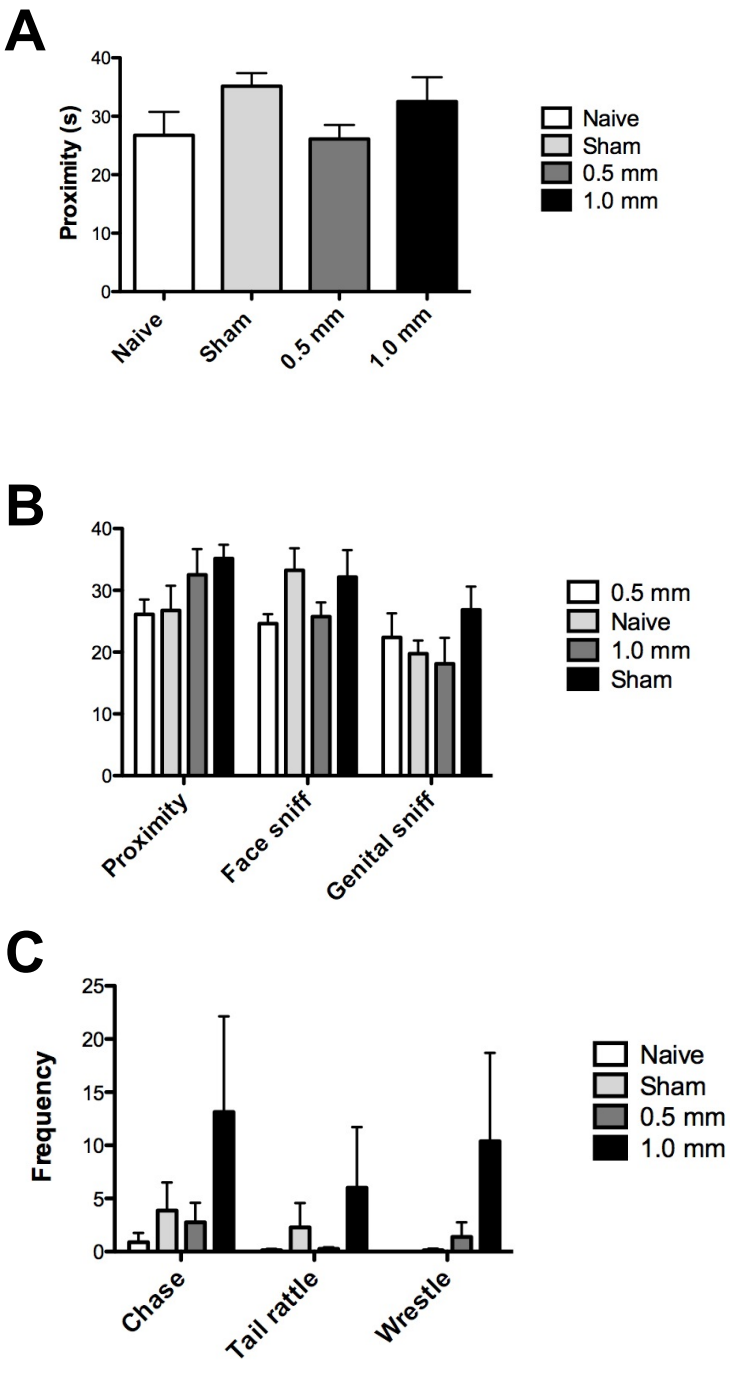
A
Proximity (s)
40
30
20
10
0
Naive
Sham
0.5 mm
1.0 mm
Naive
Sham
0.5 mm
1.0 mm
B
40
30
20
10
0
0.5 mm
Naive
1.0 mm
Sham
Proximity
Face sniff
Genital sniff
C
Frequency
25
20
15
10
5
0
Naive
Sham
0.5 mm
1.0 mm
Chase
Tail rattle
Wrestle

Figure 7.6 Sociality 2 months after TBI. Sociality was measured 2 months after TBI by a social interaction test with a weight-matched male conspecific. Naïve, craniotomy only (Sham), moderate (0.5 mm) and severe (1.0 mm) CCI were tested 2 months after injury. Time spent in proximity (A) was evaluated as well as frequency of various (B) pro-social and (C) aggressive behaviors performed by the experimental animal. The mean ± SEM of each group are shown n = 8 per group. No significance was found by one-way for any of the recorded behaviors or for proximity (P = .20).

Figure 7.7

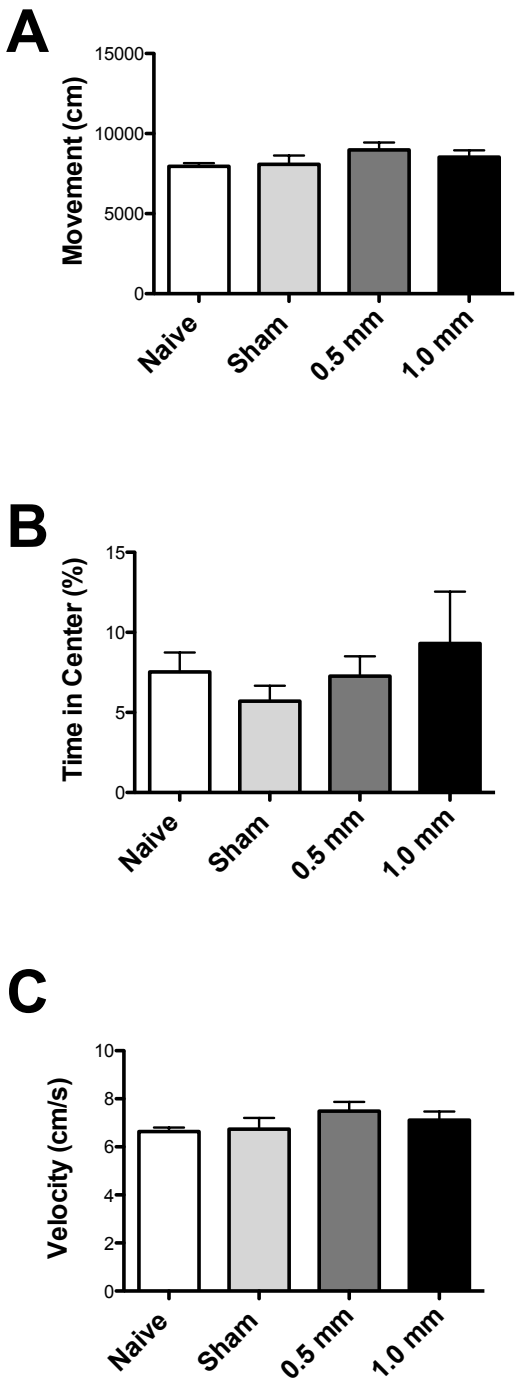
A
Movement (cm)
15000
10000
5000
0
Naive
Sham
0.5 mm
1.0 mm
B
Time in Center (%)
15
10
5
0
Naive
Sham
0.5 mm
1.0 mm
C
Velocity (cm/s)
10
8
6
4
2
0
Naive
Sham
0.5 mm
1.0 mm

Figure 7.7 No change in activity in injured mice 6 months after CCI. Activity and anxiety were tested by novel object recognition in naïve, craniotomy only (Sham), moderate (0.5 mm) and severe (1.0 mm) CCI six months after injury. Each mouse was allowed to explore an open arena for 20 min. (A) The overall movement over the 20 min interval (B) The % time each mouse spent in the center quandrant. (C) The velocity over the 20 min interval. Movement of animals within the arena was recorded and movement and center frequency were calculated using Ethovision software (noldus) The mean ± SEM of each group are shown, n = 8. None of the parameters were significantly different by one-way ANOVA (Movement, P = .331; % in center, P = .62).

Figure 7.8

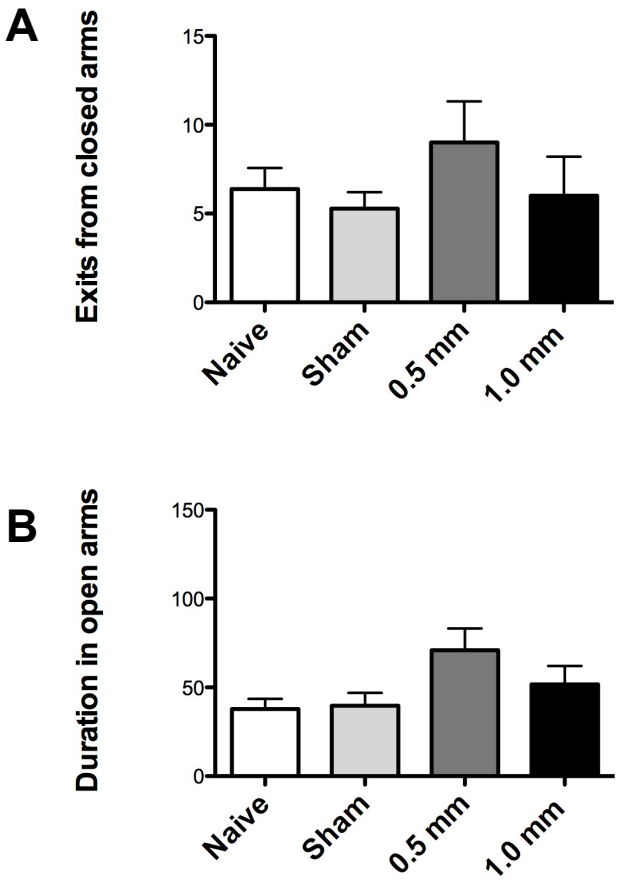
A
Exits from closed arms
15
10
5
0
Naive
Sham
0.5 mm
1.0 mm
B
Duration in open arms
150
100
50
0
Naive
Sham
0.5 mm
1.0 mm

Figure 7.8 No change in anxiety 6 months after CCI. Anxiety was tested in naïve, craniotomy only (Sham), moderate (0.5 mm) and severe (1.0 mm) CCI six months after injury using an elevated zero maze. (A) The duration of time spent in the open arms in seconds (B) The number of times all four paws exited the closed arms. Movement of animals within the elevated zero maze was recorded and time spent in the closed arms was calculated using Ethovision software (noldus) The mean ± SEM of each group are shown, n = 8. No differences were seen in the number of exits from closed arms by one-way ANOVA (Open arm duration, P = .070; exits from closed arms, P = .51).

Impulsivity and disinhibition are seen in human patients after TBI and are typically related to orbitofrontal injuries, but can also be related to injuries of the limbic system or the circuitry connecting these regions [68, 311]. To date, investigations into impulsivity or disinhibition in rodent models of TBI have been limited. Crane *et al*. showed deficits in impulse control using a stop-signal reaction time (SSRT) task after CCI injury to the medial prefrontal cortex, but this phenotype only persisted for 8 days post injury [312]. Bondi *et al*. showed changes in a CCI model using an attentional set-shifting task, which measures executive functioning 4-weeks post injury [313]. In contrast to the EZM used in this study, both of these tests require complex training and testing paradigms that would be difficult to employ as part of a standard pre-clinical battery. However, they are more accurate and sensitive tests of impulse control than the EZM.

The results of EZM testing or the closely related elevated plus maze (EPM) have rendered mixed results, some indicating disinhibition others anxiety [314]. Siopi *et al*. detected an increased number of head dippings after a closed-head, weight-drop injury model suggesting mild disinhibition 3.5 weeks after injury [315]. Washington *et al*. showed time spent in the open arms of the EPM 21 days after CCI was increased irrespective of injury severity [194]. Conversely Shultz et al. showed increased anxiety in a repeated fluid percussion injury model [316]. This diversity of findings on anxiety-like behaviors in pre-clinical models of TBI highlights the importance of injury model, species, and timing of behavioral testing on outcomes.

There is a paucity of studies of TBI associated aggression in pre-clinical models. One study gave mice a TBI during adolescence then found development of an aggressive phenotype in adulthood [317]. The social-interaction test performed here is designed to limit aggressive behavior. This is done by the use of a size matched conspecific and a clean cage. Therefore it is surprising that we detected any aggressive behaviors. The increase in aggressive behaviors shown here, though highly variable, is

intriguing. There are much more sensitive tests of aggression in rodents, such as the resident-intruder test, which uses a smaller test animal in the experimental animal's home cage. Also studies of aggression in rodents typically use strains prone to aggressive behavior. Performing testing of TBI models using both more sensitive testing and more appropriate strains and species would likely provide better modeling of TBI induced aggression. Further studies on TBI induced aggression could provide a new avenue to study the link between brain injury and aggression and develop improved treatment strategies.

7.4 Summary: Taken as a whole these findings suggest a hyperactive and disinhibited phenotype of CCI mice in the chronic phase. Disinhibition or impulsivity is a well-recognized feature of human TBI and can be associated with aggression [68]. Additionally, recent reports have linked TBI to increased risk of attention-deficit hyperactivity disorder in children [318] and adults [73]. This study shows that the CCI can model some of the long-term consequences of TBI. Future studies exploring the neuroanatomical and neurochemical correlates of these changes would further our understanding of TBI associated deficits and inform treatment strategies for TBI associated neuropsychiatric disorders.

Chapter 8: Conclusions

Traumatic brain injury (TBI) is a disorder of interest and importance. While improved trauma care has improved survival from severe TBI, no treatment has led to improved outcomes [7]. Recently, miRNAs have emerged as modulators of neuroinflammation and injury [319]. While the roles of miRNAs in peripheral inflammation and injury are increasingly well defined [109], in the context of the brain far less is known. Beginning to define the expression and function of these inflammation-associated miRNAs in TBI was the goal of this work.

To identify miRNA important to TBI induced neuroinflammation we used a mouse controlled cortical impact (CCI) model of TBI. We identified miR-155 as an inflammation-associated miRNA that increased after CCI. Studies on miR-155 KO mice after CCI revealed altered cytokine and chemokine expression as well as increased microglial activation. However, we also identified several non-canonical roles for inflammation-associated miRNA after CCI. Expression of both miR-155 and miR-21 was localized to neurons after CCI. Additionally the expression of miR-155 showed a nuclear expression pattern, suggesting it may have functions outside of traditional mRNA silencing. In other studies, we profiled miRNAs found in extracellular vesicles (EV) after CCI. We found changes in levels of EV-assoicated miRNAs, including increased levels of 3 miRNAs with GU rich sequences. GU rich sequences are important for TLR7/8 stimulation suggesting that these miRNAs could act as damage associated molecular patterns (DAMPS) in the context of CCI. Here we report that miRNA not only show altered expression, but also have functional roles in CCI. While miRNA do regulate inflammation in the context of CCI, they also have non-canonical roles both in neuronal nuclei and extracellular vesicles. Future work should focus not only on the ability of miRNA to silence target transcripts, but also consider a broader repertoire of functions for miRNAs in CNS inflammation and injury.

We began by characterizing the pathology of the CCI model to identify promising anatomical regions to study the immune response after TBI, focusing on the injured cortex and underlying hippocampus. We found frank tissue loss and apoptotic cell death in the injured cortex, but not the hippocampus. However we found increased expression of glial markers Iba1 and GFAP in both the injured cortex and the ipsilateral hippocampus. Additionally, neuropathology was evident in both the cortex and hippocampus on the injured side, shown by damage-associated markers in neurofilaments, white mater degeneration, and accumulation of neuronal markers MAP2 and synaptophysin. Therefore, we chose to study expression and function of inflammation-associated miRNAs in the hippocampus.

A panel of inflammation-associated miRNAs was chosen based on known roles in inflammation and identification by at least one miRNA profiling experiment in TBI models. The temporal expression of these miRNAs was measured over the acute and sub-acute phases of CCI using qPCR. Distinct temporal profiles were found for all the miRNAs examined. Expression of miR-155 was elevated in the acute phase up to 7 days after CCI, conversely miR-21 was only elevated in the sub-acute phase at 14 days after injury. Interestingly, miR-223 only showed a limited, acute expression. Given that miR-223 is highly linked to neutrophils, we hypothesize that the expression of miR-223 in the brain may be linked to invading neutrophils, which show a similar pattern of acute response to TBI as found in spinal cord injury. Expression of miR-223 in neutrophils could explain the acute expression pattern seen for miR-223 in TBI, but would need verification in future studies. Surprisingly, miR-146 did not show a significant increase in TBI. Expression of miR-146 is induced by NF-κB and important to for inflammation resolution in the periphery through feedback inhibition [120]. The lack of miR-146 induction could be pathological in TBI, leading to a prolonged and damaging inflammatory response.

To further characterize expression of miR-155, miR-21, and miR-223 we performed fluorescent *in situ* hybridization (FISH), which confirmed our qPCR findings. Interestingly the expression pattern of miR-155 was primarily nuclear. While at one time, nuclear expression was thought to indicate inactivity of miRNA, new studies are finding unique roles for nuclear miRNA in regulation of gene expression [105]. The expression pattern of miR-21 was also of interest. 7 days after injury miR-21 expression was found in regions of the hippocampus primarily composed of neuronal cell bodies and processes. In later experiments using combined immunofluorescence and FISH, we confirmed neuronal localization of miR-21.

To identify which miRNAs were most associated with inflammation we measured levels of pro-inflammatory miRNA after CCI and correlated their expression with inflammation-associated miRNAs. In contrast to the expression of inflammation-associated miRNAs, pro-inflammatory cytokines IL-6, TNFα, and IL-1β all peaked 1 day after injury. Although nearly all combinations of cytokines and miRNAs showed significant correlation, the association between miR-155 and IL-1β was the strongest. These studies were performed using a moderate CCI, 0.5 mm injury depth. To determine whether increasing injury severity would increase expression of inflammation-associated miRNAs and cytokines we compared naïve, sham, moderate (0.5 mm), and severe (1.0 mm) injuries three days after injury. Severely injured mice had more robust expression of inflammation-associated miRNAs and cytokines 3 days after CCI. In addition, we increased the panel of inflammatory mediators examined to include additional cytokines, chemokines, and growth factors. Using this extended panel, we found IL-1β, TNFα, and chemokine CXCL10 to be strongly induced 3 days after CCI.

To examine the role of miR-155 in TBI we acquired miR-155 KO mice. After CCI miR-155 KO mice showed no measurable motor or cognitive deficits in the acute and sub-acute time frames after CCI. Additionally, no changes in hippocampal apoptosis or

neurodegeneration were found between miR-155 KO and WT mice. However, we did find decreased interferon (IFN) expression in miR-155 KO mice after TBI, including decreased levels of IFN regulated chemokine CXCL10. We also found a decrease in anxiety after CCI in miR-155 KO mice relative to WT mice. The link between IFNs and mood disorders is well established, and patients administered IFNs show sickness behavior and mood disorders [229]. Together these data suggest that miR-155 affects the IFN response, and we speculate that this may alter mood disruptions after TBI. The mechanisms by which regulates IFN and CXCL10 expression is unknown. While we find miR-155 in neurons, the source of IFN and CXCL10 are unknown. Others have found that small populations of invading peripheral immune cells express CXCL10 in TBI, in clusters that appear to be dendritic cells [226].

Suppressor of cytokine signaling 1 (SOCS1) is a known target of miR-155 [206] and a negative regulator of the IFN response [209]. Therefore, in miR-155 KO mice we hypothesized that SOCS1 levels would be increased, leading to the observed decrease in IFN signaling. However the levels of SOCS1 in hippocampal homogenate were unchanged at the protein level. Still we note that while there were no changes in the hippocampus as a whole, levels in individual cells may still be altered. Expression of SOCS1 mRNA was decreased slightly but significantly in miR-155 KO mice, the opposite of what would be expected if miR-155 targeted SOCS1 mRNA in a cell type expressing both molecules. Thus it is unlikely that alterations in SOCS1 play a role, at least on the level of the whole hippocampus

We also found in the miR-155 KO mice subjected to TBI there was an increase in Iba1 expression indicating increased microglial activation. Other groups have shown that miR-155 is pro-inflammatory in microglia and that reducing miR-155 leads to decreased levels of microglial marker CD11b, interpreted as decreased microglia activation [210]. Our findings suggest an opposite role for miR-155 in microglial activation after TBI, since

in fact, increased microglial activation was observed in miR-155 KO mice. Therefore it is possible that miR-155 does play a role in the microglial response, but in a different manner depending on the biological and pathological setting..

To further explore the role of miR-155 in TBI we examined the cell-type specific localization of miR-155 in the brain after CCI. We found that miR-155 was highly expressed in neuronal nuclei. Whether this expression is linked to the observed changes in IFN and CXCL10 expression or anxiety remains to be determined. In viral infections of the brain CXCL10 is expressed in neurons [215, 216]. This suggests the possibility that miR-155 regulates expression of CXCL10 in neurons after CCI. However, nuclear expression is often associated with non-cannonical functions of miRNAs [320]. Future studies should address the role of nuclear miR-155 expression in neurons.

We have discovered that miR-155 regulates the IFN response after TBI including TBI induced chemokine CXCL10. We have also shown that miR-155 contributes to anxiety after TBI, likely through the IFN response. Further studies are needed to determine the exact mechanism of miR-155 regulation of the IFN response and which cell types are responsible.

Another miRNA of interest is miR-21. Increased expression of miR-21 has been seen in many types of neuronal injury [321], and we detected miR-21 in the sub-acute phase of CCI. Due to the various roles of miR-21 in neurons we characterized its expression in development, induction by neurotrophic cytokines, and role in neuronal function. The expression of miR-21 in the brain increases during development in mice from embryonic day 14 to postnatal day 14. However, different neuronal model systems had divergent expression patterns during differentiation. Expression in was higher in cultured human NPC than human neurons, but no change was found in mouse NPC and neurons, and conversely differentiated SH-SY5Y neuroblastoma cells showed higher expression of miR-21 than undifferentiated cells. To study the induction of miR-21 we

used cultured human neurons. We found that neurotrophic cytokines IL-6 and CNTF could induce miR-21. Additionally, we showed that IL-6 could stimulate STAT3 activation in human neurons, though not with the same magnitude as CNTF. The expression of IL-6 receptor in neurons depends highly on neuronal type and species. Novel findings include the discovery that IL-6 treatment of fetal human neurons can induce STAT3 signaling. Another novel finding is the induction of miR-21 in human neurons and to that miR-21 is induced by IL-6 and CNTF. Inhibitors of the Jak-Stat pathway did not inhibit miR-21 expression and levels of primary miR-21 were not elevated after treatment with IL-6 and CNTF. Future studies should examine alternative mechanisms of miR-21 induction by neurotrophic cytokines. Even though the mechanism is not understood, the induction of miR-21 by these neurotrophic cytokines may explain why so many types of neuronal injury increase miR-21 expression.

The function of miR-21 in the healthy brain is unknown. Previous data from our lab indicated that pathologically increased miR-21 could alter potassium currents in neurons [231]. However, we found that long-term potentiation, a correlate of learning and memory was not altered in miR-21 KO mice. Additionally, miR-21 targets PTEN and downstream phosphorylation of Akt were not changed in miR-21 KO mice. Together we could not identify a role for miR-21 in normal neuronal function. To determine whether miR-21 was neuroprotective in the context of injury, we utilized an *in vitro* model of excitotoxicity. Again, we did not detect any differences between miR-21 KO and WT neurons. Finally, we tested the importance of miR-21 in TBI by administering CCI to miR-21 KO mice and controls. We found no differences in function or in neuronal degeneration in miR-21 KO and WT mice. It is possible that miR-21 may play a role in neuronal development and neuroprotection, but that miR-21 KO during development induces compensatory mechanisms. To address this issue in the future we developed a mouse strain with a floxed miR-21 allele. In this stain two LoxP sites surround the miR-

21 stem loop. Cre recombinase can cause recombination at these LoxP sites resulting in gene deletion. Therefore to induce conditional deletion of the miR-21 gene, Cre can be introduced virally or through a tissue specific promoter. These mice can be used to further study the role of miR-21 in neuronal development and injury.

While miRNA are known to regulate gene expression in the cell, new evidence shows that miRNA may also be transferred between cells in extracellular vesicles (EVs). EVs containing miRNA can affect the recipient cell by decreasing mRNA expression in the cytosol [278] or binding to PRRs in the endocytic compartment [276]. In immune cells TLR7/8 recognizes viral RNA and miRNA and produces an inflammatory response [289]. Neurons also express TLR7/8 and activation of this receptor can be neurotoxic [177]. We isolated EVs from brains 7 days after CCI to examine the changes in EV-associated miRNA (EV-miRNA). Small RNA sequencing showed changes in the EV-miRNA profile after CCI. We found that miR-21, miR-146, miR-7a and miR-7b were elevated in EVs after CCI. One miRNA, miR-212 was down regulated. Three of the differentially expressed miRNA contain GU rich sequences that mediate TLR7/8 binding [282]. Of the differentially expressed miRNAs miR-21 showed the largest change. *In situ* hybridization combined with immunofluorescence, localized miR-21 to neurons near the lesion boundary. We also found reactive microglia adjacent to miR-21 expressing neurons suggesting that EV-associated miR-21 may be important for neuron-glia communication in TBI. While EV-miRNA can elicit immune responses [276] and neurotoxicity [177] *in vitro* and several studies have shown that EV-miRNA are altered in neurological disease [177, 288], the overall effect of this mechanism on disease pathology is still unclear. TBI may serve as a useful model to study the importance of EV-miRNA signaling through TLR7/8 on neuroinflammation.

Neuropsychiatric dysfunction is a common consequence of TBI [66, 322, 323]. However, mechanisms of long-term dysfunction in TBI patients are unclear. One

difficulty in performing these types of mechanistic studies is the lack of a defined neuropsychiatric phenotype of mice in the chronic phase of TBI. Here we used a battery of neuropsychological tests to determine the phenotype of mice in the chronic phase of TBI. We found no evidence of motor or cognitive dysfunction, but did detect hyperactivity and disinhibition at 2 months after CCI, primarily in severely injured mice. Disinhibition is classically found in frontal lobe injuries [68]. Given that the lesion in our model primarily involves the parietal cortex and underlying hippocampus, how this injury induces disinhibition is unclear. A recent report identified a high degree of long-range inputs to the prefrontal cortex in mouse [324]. It is possible that diffuse axonal injury may disrupt these inputs. We currently have studies in progress to elucidate the pathological correlates to these behavioral changes. These studies will examine the presence of neuroinflammation in the prefrontal cortex after CCI using immunohistochemistry and determine CCI changes in connectivity using diffusion tensor (DT) magnetic resonance imaging (MRI) and tractography.

In conclusion, this work has furthered the understanding of miRNA expression and function in TBI. While study of miRNAs in peripheral inflammation and injury has focused on regulation of cytokine signaling and immune cell function, we have found multi-faceted roles for miRNAs in brain injury. Changes in cytokine, chemokine, and glial activation were observed in miR-155 KO mice indicating that miRNAs are involved in neuroinflammation after TBI. Additionally, neuronal, nuclear, and EV-associated miRNAs were identified highlighting non-canonical roles for inflammation-associated miRNAs in TBI. Finally, we have identified disinhibition and hyperactivity in the chronic phase of CCI. Together these studies suggest an important role for miRNA in TBI and neuroinflammation. Based on this work we have identified several topics of interest for future studies of TBI: 1) The roles of inflammation-associated miRNAs in neurons, including the function of miR-155 in neuronal nuclei 2) The mechanistic link between

miR-155 expression, IFN expression, and anxiety after TBI 3) The effect of changes in EV-miRNA expression after TBI, especially in TLR7/8 activation and 4) The pathological correlates of disinhibition and hyperactivity in the chronic phase of the CCI mouse model.

References

1. Warden, D., *Military TBI during the Iraq and Afghanistan wars.* J Head Trauma Rehabil, 2006. **21**(5): p. 398-402.
2. Schneiderman, A.I., E.R. Braver, and H.K. Kang, *Understanding sequelae of injury mechanisms and mild traumatic brain injury incurred during the conflicts in Iraq and Afghanistan: persistent postconcussive symptoms and posttraumatic stress disorder.* Am J Epidemiol, 2008. **167**(12): p. 1446-52.
3. Dai, R. and S.A. Ahmed, *MicroRNA, a new paradigm for understanding immunoregulation, inflammation, and autoimmune diseases.* Transl Res, 2011. **157**(4): p. 163-79.
4. Kuo, C.Y., et al., *Functioning and disability analysis of patients with traumatic brain injury and spinal cord injury by using the world health organization disability assessment schedule 2.0.* Int J Environ Res Public Health, 2015. **12**(4): p. 4116-27.
5. Coronado, V.G., et al., *Trends in Traumatic Brain Injury in the U.S. and the public health response: 1995-2009.* J Safety Res, 2012. **43**(4): p. 299-307.
6. *CDC grand rounds: reducing severe traumatic brain injury in the United States.* MMWR Morb Mortal Wkly Rep, 2013. **62**(27): p. 549-52.
7. Gerber, L.M., et al., *Marked reduction in mortality in patients with severe traumatic brain injury.* J Neurosurg, 2013. **119**(6): p. 1583-90.
8. Selassie, A.W., et al., *Incidence of long-term disability following traumatic brain injury hospitalization, United States, 2003.* J Head Trauma Rehabil, 2008. **23**(2): p. 123-31.
9. Teasdale, G. and B. Jennett, *Assessment of coma and impaired consciousness. A practical scale.* Lancet, 1974. **2**(7872): p. 81-4.
10. Balestreri, M., et al., *Predictive value of Glasgow Coma Scale after brain trauma: change in trend over the past ten years.* J Neurol Neurosurg Psychiatry, 2004. **75**(1): p. 161-2.
11. Fearnside, M.R., et al., *The Westmead Head Injury Project outcome in severe head injury. A comparative analysis of pre-hospital, clinical and CT variables.* Br J Neurosurg, 1993. **7**(3): p. 267-79.
12. Linacre, J.M., et al., *The structure and stability of the Functional Independence Measure.* Arch Phys Med Rehabil, 1994. **75**(2): p. 127-32.
13. Whiteneck, G.G., et al., *Quantifying handicap: a new measure of long-term rehabilitation outcomes.* Arch Phys Med Rehabil, 1992. **73**(6): p. 519-26.
14. Bullock, M.R., et al., *Outcome measures for clinical trials in neurotrauma.* Neurosurg Focus, 2002. **13**(1): p. ECP1.
15. Goranson, T.E., et al., *Community integration following multidisciplinary rehabilitation for traumatic brain injury.* Brain Injury, 2003. **17**(9): p. 759-774.
16. Gouvier, W.D., et al., *Reliability and validity of the Disability Rating Scale and the Levels of Cognitive Functioning Scale in monitoring recovery from severe head injury.* Arch Phys Med Rehabil, 1987. **68**(2): p. 94-7.
17. Shukla, D., B.I. Devi, and A. Agrawal, *Outcome measures for traumatic brain injury.* Clin Neurol Neurosurg, 2011. **113**(6): p. 435-41.

18. McIntosh, T.K., et al., *Neuropathological sequelae of traumatic brain injury: relationship to neurochemical and biomechanical mechanisms.* Lab Invest, 1996. **74**(2): p. 315-42.
19. Werner, C. and K. Engelhard, *Pathophysiology of traumatic brain injury.* British journal of anaesthesia, 2007. **99**(1): p. 4-9.
20. Greve, M.W. and B.J. Zink, *Pathophysiology of traumatic brain injury.* Mount Sinai Journal of Medicine: A Journal of Translational and Personalized Medicine, 2009. **76**(2): p. 97-104.
21. Finnie, J.W., *Neuroinflammation: beneficial and detrimental effects after traumatic brain injury.* Inflammopharmacology, 2013. **21**(4): p. 309-20.
22. Hailer, N.P., *Immunosuppression after traumatic or ischemic CNS damage: it is neuroprotective and illuminates the role of microglial cells.* Prog Neurobiol, 2008. **84**(3): p. 211-33.
23. Walz, W., et al., *Extracellular ATP activates a cation conductance and a K+ conductance in cultured microglial cells from mouse brain.* J Neurosci, 1993. **13**(10): p. 4403-11.
24. Whittemore, E.R., et al., *Carbachol increases intracellular free calcium in cultured rat microglia.* Brain Res, 1993. **621**(1): p. 59-64.
25. Gehrmann, J., et al., *Microglial reaction in the rat cerebral cortex induced by cortical spreading depression.* Brain Pathol, 1993. **3**(1): p. 11-7.
26. Nimmerjahn, A., F. Kirchhoff, and F. Helmchen, *Resting microglial cells are highly dynamic surveillants of brain parenchyma in vivo.* Science, 2005. **308**(5726): p. 1314-8.
27. *CYtology and cellular pathology of the nervous system.* Archives of Internal Medicine, 1932. **50**(3): p. 508-509.
28. Gyoneva, S. and R.M. Ransohoff, *Inflammatory reaction after traumatic brain injury: therapeutic potential of targeting cell-cell communication by chemokines.* Trends Pharmacol Sci, 2015. **36**(7): p. 471-80.
29. Lee, S.C., et al., *Cytokine production by human fetal microglia and astrocytes. Differential induction by lipopolysaccharide and IL-1 beta.* J Immunol, 1993. **150**(7): p. 2659-67.
30. Shibata, M. and C.M. Blatteis, *Human recombinant tumor necrosis factor and interferon affect the activity of neurons in the organum vasculosum laminae terminalis.* Brain Res, 1991. **562**(2): p. 323-6.
31. Grassi, F., et al., *TNF-alpha increases the frequency of spontaneous miniature synaptic currents in cultured rat hippocampal neurons.* Brain Res, 1994. **659**(1-2): p. 226-30.
32. Jeohn, G.-H., et al., *Synergistic neurotoxic effects of combined treatments with cytokines in murine primary mixed neuron/glia cultures.* Journal of neuroimmunology, 1998. **85**(1): p. 1-10.
33. Stoll, G., S. Jander, and M. Schroeter, *Cytokines in CNS disorders: neurotoxicity versus neuroprotection*. 2000: Springer.
34. Iadecola, C., *Bright and dark sides of nitric oxide in ischemic brain injury.* Trends in neurosciences, 1997. **20**(3): p. 132-139.

35. Elkabes, S., E.M. DiCicco-Bloom, and I.B. Black, *Brain microglia/macrophages express neurotrophins that selectively regulate microglial proliferation and function.* The journal of neuroscience, 1996. **16**(8): p. 2508-2521.
36. Batchelor, P.E., et al., *Activated macrophages and microglia induce dopaminergic sprouting in the injured striatum and express brain-derived neurotrophic factor and glial cell line-derived neurotrophic factor.* The Journal of neuroscience, 1999. **19**(5): p. 1708-1716.
37. Dougherty, K.D., C.F. Dreyfus, and I.B. Black, *Brain-derived neurotrophic factor in astrocytes, oligodendrocytes, and microglia/macrophages after spinal cord injury.* Neurobiology of disease, 2000. **7**(6): p. 574-585.
38. del Zoppo, G.J., et al., *Microglial activation and matrix protease generation during focal cerebral ischemia.* Stroke, 2007. **38**(2): p. 646-651.
39. Bessis, A., et al., *Microglial control of neuronal death and synaptic properties.* Glia, 2007. **55**(3): p. 233-8.
40. Heppner, F.L., et al., *Experimental autoimmune encephalomyelitis repressed by microglial paralysis.* Nat Med, 2005. **11**(2): p. 146-52.
41. Bushong, E.A., et al., *Protoplasmic astrocytes in CA1 stratum radiatum occupy separate anatomical domains.* J Neurosci, 2002. **22**(1): p. 183-92.
42. Lundgaard, I., et al., *White matter astrocytes in health and disease.* Neuroscience, 2014. **276**: p. 161-73.
43. Verkhratsky, A. and A.M. Butt, *Glial physiology and pathophysiology*. 2013: John Wiley & Sons.
44. Eugenin, E.A., et al., *The role of gap junction channels during physiologic and pathologic conditions of the human central nervous system.* Journal of Neuroimmune Pharmacology, 2012. **7**(3): p. 499-518.
45. Pekny, M. and M. Pekna, *Astrocyte reactivity and reactive astrogliosis: costs and benefits.* Physiol Rev, 2014. **94**(4): p. 1077-98.
46. Burda, J.E., A.M. Bernstein, and M.V. Sofroniew, *Astrocyte roles in traumatic brain injury.* Exp Neurol, 2016. **275 Pt 3**: p. 305-15.
47. Huang, C., et al., *Critical role of connexin 43 in secondary expansion of traumatic spinal cord injury.* J Neurosci, 2012. **32**(10): p. 3333-8.
48. Wanner, I.B., et al., *Glial scar borders are formed by newly proliferated, elongated astrocytes that interact to corral inflammatory and fibrotic cells via STAT3-dependent mechanisms after spinal cord injury.* J Neurosci, 2013. **33**(31): p. 12870-86.
49. Myer, D., et al., *Essential protective roles of reactive astrocytes in traumatic brain injury.* Brain, 2006. **129**(10): p. 2761-2772.
50. Bradbury, M.W., *The blood-brain barrier.* Exp Physiol, 1993. **78**(4): p. 453-72.
51. Thal, S.C. and W. Neuhaus, *The blood-brain barrier as a target in traumatic brain injury treatment.* Arch Med Res, 2014. **45**(8): p. 698-710.
52. McKeating, E. and P. Andrews, *Cytokines and adhesion molecules in acute brain injury.* British journal of anaesthesia, 1998. **80**(1): p. 77-84.
53. Biagas, K.V., et al., *Assessment of posttraumatic polymorphonuclear leukocyte accumulation in rat brain using tissue myeloperoxidase assay and vinblastine treatment.* J Neurotrauma, 1992. **9**(4): p. 363-71.

54. Holmin, S., et al., *Intracerebral inflammatory response to experimental brain contusion.* Acta neurochirurgica, 1995. **132**(1-3): p. 110-119.
55. Dahlgren, C. and A. Karlsson, *Respiratory burst in human neutrophils.* Journal of immunological methods, 1999. **232**(1): p. 3-14.
56. Weaver, K.D., et al., *Effect of leukocyte-endothelial adhesion antagonism on neutrophil migration and neurologic outcome after cortical trauma.* J Trauma, 2000. **48**(6): p. 1081-90.
57. Whalen, M.J., et al., *Reduced brain edema after traumatic brain injury in mice deficient in P-selectin and intercellular adhesion molecule-1.* Journal of Leukocyte Biology, 2000. **67**(2): p. 160-168.
58. Isaksson, J., L. Hillered, and Y. Olsson, *Cognitive and histopathological outcome after weight-drop brain injury in the rat: influence of systemic administration of monoclonal antibodies to ICAM-1.* Acta neuropathologica, 2001. **102**(3): p. 246-256.
59. Morganti, J.M., et al., *CCR2 antagonism alters brain macrophage polarization and ameliorates cognitive dysfunction induced by traumatic brain injury.* The Journal of Neuroscience, 2015. **35**(2): p. 748-760.
60. Morganti, J.M., et al., *CCR2 antagonism alters brain macrophage polarization and ameliorates cognitive dysfunction induced by traumatic brain injury.* J Neurosci, 2015. **35**(2): p. 748-60.
61. Zaloshnja, E., et al., *Prevalence of long-term disability from traumatic brain injury in the civilian population of the United States, 2005.* J Head Trauma Rehabil, 2008. **23**(6): p. 394-400.
62. in *Gulf War and Health: Volume 7: Long-Term Consequences of Traumatic Brain Injury*. 2008: Washington (DC).
63. Annegers, J.F., et al., *A population-based study of seizures after traumatic brain injuries.* New England Journal of Medicine, 1998. **338**(1): p. 20-24.
64. Fann, J.R., et al., *Psychiatric illness following traumatic brain injury in an adult healthMaintenance organization population.* Archives of General Psychiatry, 2004. **61**(1): p. 53-61.
65. Jorge, R.E., et al., *Major depression following traumatic brain injury.* Arch Gen Psychiatry, 2004. **61**(1): p. 42-50.
66. Gomez-Hernandez, R., et al., *Social impairment and depression after traumatic brain injury.* Arch Phys Med Rehabil, 1997. **78**(12): p. 1321-6.
67. Dyer, K.F., et al., *Aggression after traumatic brain injury: analysing socially desirable responses and the nature of aggressive traits.* Brain Inj, 2006. **20**(11): p. 1163-73.
68. Greve, K.W., et al., *Personality and neurocognitive correlates of impulsive aggression in long-term survivors of severe traumatic brain injury.* Brain Inj, 2001. **15**(3): p. 255-62.
69. Gavett, B.E., R.A. Stern, and A.C. McKee, *Chronic traumatic encephalopathy: a potential late effect of sport-related concussive and subconcussive head trauma.* Clinics in sports medicine, 2011. **30**(1): p. 179-188.
70. McKee, A.C., et al., *The spectrum of disease in chronic traumatic encephalopathy.* Brain, 2013. **136**(1): p. 43-64.

71. McKee, A.C., et al., *Chronic traumatic encephalopathy in athletes: progressive tauopathy after repetitive head injury.* Journal of Neuropathology & Experimental Neurology, 2009. **68**(7): p. 709-735.
72. Konigs, M., et al., *Pediatric Traumatic Brain Injury and Attention Deficit.* Pediatrics, 2015. **136**(3): p. 534-41.
73. Ilie, G., et al., *The association between traumatic brain injury and ADHD in a Canadian adult sample.* Journal of Psychiatric Research.
74. Lee, V.M., M. Goedert, and J.Q. Trojanowski, *Neurodegenerative tauopathies.* Annual review of neuroscience, 2001. **24**(1): p. 1121-1159.
75. Johnson, V.E., W. Stewart, and D.H. Smith, *Widespread tau and amyloid‐beta pathology many years after a single traumatic brain injury in humans.* Brain pathology, 2012. **22**(2): p. 142-149.
76. Johnson, V.E., et al., *Inflammation and white matter degeneration persist for years after a single traumatic brain injury.* Brain, 2013. **136**(Pt 1): p. 28-42.
77. Leonard, B.E., *Inflammation, depression and dementia: are they connected?* Neurochemical research, 2007. **32**(10): p. 1749-1756.
78. Miller, A.H., V. Maletic, and C.L. Raison, *Inflammation and its discontents: the role of cytokines in the pathophysiology of major depression.* Biological psychiatry, 2009. **65**(9): p. 732-741.
79. Raison, C.L., L. Capuron, and A.H. Miller, *Cytokines sing the blues: inflammation and the pathogenesis of depression.* Trends in immunology, 2006. **27**(1): p. 24-31.
80. Dantzer, R., et al., *From inflammation to sickness and depression: when the immune system subjugates the brain.* Nature reviews neuroscience, 2008. **9**(1): p. 46-56.
81. Miller, A.H. and C.L. Raison, *The role of inflammation in depression: from evolutionary imperative to modern treatment target.* Nat Rev Immunol, 2015. **16**(1): p. 22-34.
82. Juengst, S.B., et al., *Acute inflammatory biomarker profiles predict depression risk following moderate to severe traumatic brain injury.* The Journal of head trauma rehabilitation, 2015. **30**(3): p. 207-218.
83. Fenn, A.M., et al., *Immune activation promotes depression 1 month after diffuse brain injury: a role for primed microglia.* Biological psychiatry, 2014. **76**(7): p. 575-584.
84. Xiong, Y., A. Mahmood, and M. Chopp, *Animal models of traumatic brain injury.* Nature Reviews Neuroscience, 2013. **14**(2): p. 128-142.
85. Thompson, H.J., et al., *Lateral fluid percussion brain injury: a 15-year review and evaluation.* J Neurotrauma, 2005. **22**(1): p. 42-75.
86. Dixon, C.E., et al., *A controlled cortical impact model of traumatic brain injury in the rat.* Journal of neuroscience methods, 1991. **39**(3): p. 253-262.
87. Saljo, A., et al., *Low-level blasts raise intracranial pressure and impair cognitive function in rats.* Journal of neurotrauma, 2009. **26**(8): p. 1345-1353.
88. Garman, R.H., et al., *Blast exposure in rats with body shielding is characterized primarily by diffuse axonal injury.* Journal of neurotrauma, 2011. **28**(6): p. 947-959.

89. Williams, A.J., et al., *Characterization of a new rat model of penetrating ballistic brain injury.* Journal of neurotrauma, 2005. **22**(2): p. 313-331.
90. Kane, M.J., et al., *A mouse model of human repetitive mild traumatic brain injury.* Journal of neuroscience methods, 2012. **203**(1): p. 41-49.
91. Crawley, J.N., *Behavioral phenotyping of transgenic and knockout mice: experimental design and evaluation of general health, sensory functions, motor abilities, and specific behavioral tests.* Brain research, 1999. **835**(1): p. 18-26.
92. Kochanek, P.M., et al., *Operation Brain Trauma Therapy: Approach to Modeling, Therapy Evaluation, Drug Selection, and Biomarker Assessments for a Multicenter Pre-Clinical Drug Screening Consortium for Acute Therapies in Severe Traumatic Brain Injury.* Journal of neurotrauma, 2015.
93. Washington, P.M., et al., *The effect of injury severity on behavior: a phenotypic study of cognitive and emotional deficits after mild, moderate, and severe controlled cortical impact injury in mice.* Journal of neurotrauma, 2012. **29**(13): p. 2283-2296.
94. FOX, G.B., et al., *Sustained sensory/motor and cognitive deficits with neuronal apoptosis following controlled cortical impact brain injury in the mouse.* Journal of neurotrauma, 1998. **15**(8): p. 599-614.
95. Fujimoto, S.T., et al., *Motor and cognitive function evaluation following experimental traumatic brain injury.* Neurosci Biobehav Rev, 2004. **28**(4): p. 365-78.
96. Fujimoto, S.T., et al., *Motor and cognitive function evaluation following experimental traumatic brain injury.* Neuroscience & biobehavioral reviews, 2004. **28**(4): p. 365-378.
97. Clemson, C.M., et al., *XIST RNA paints the inactive X chromosome at interphase: evidence for a novel RNA involved in nuclear/chromosome structure.* The Journal of cell biology, 1996. **132**(3): p. 259-275.
98. Brannan, C.I., et al., *The product of the H19 gene may function as an RNA.* Molecular and cellular biology, 1990. **10**(1): p. 28-36.
99. Bernstein, E., et al., *Dicer is essential for mouse development.* Nature genetics, 2003. **35**(3): p. 215-217.
100. Krol, J., I. Loedige, and W. Filipowicz, *The widespread regulation of microRNA biogenesis, function and decay.* Nature Reviews Genetics, 2010. **11**(9): p. 597-610.
101. Winter, J., et al., *Many roads to maturity: microRNA biogenesis pathways and their regulation.* Nature cell biology, 2009. **11**(3): p. 228-234.
102. Filipowicz, W., S.N. Bhattacharyya, and N. Sonenberg, *Mechanisms of post-transcriptional regulation by microRNAs: are the answers in sight?* Nature Reviews Genetics, 2008. **9**(2): p. 102-114.
103. Bartel, D.P. and C.-Z. Chen, *Micromanagers of gene expression: the potentially widespread influence of metazoan microRNAs.* Nature Reviews Genetics, 2004. **5**(5): p. 396-400.
104. Vasudevan, S., Y. Tong, and J.A. Steitz, *Switching from repression to activation: microRNAs can up-regulate translation.* Science, 2007. **318**(5858): p. 1931-1934.

105. Roberts, T.C., *The MicroRNA Biology of the Mammalian Nucleus.* Mol Ther Nucleic Acids, 2014. **3**: p. e188.
106. Marson, A., et al., *Connecting microRNA genes to the core transcriptional regulatory circuitry of embryonic stem cells.* Cell, 2008. **134**(3): p. 521-533.
107. Lu, J., et al., *MicroRNA expression profiles classify human cancers.* nature, 2005. **435**(7043): p. 834-838.
108. Baltimore, D., et al., *MicroRNAs: new regulators of immune cell development and function.* Nature immunology, 2008. **9**(8): p. 839-845.
109. Sonkoly, E., M. Ståhle, and A. Pivarcsi. *MicroRNAs and immunity: novel players in the regulation of normal immune function and inflammation*. in *Seminars in cancer biology*. 2008. Elsevier.
110. Mogensen, T.H., *Pathogen recognition and inflammatory signaling in innate immune defenses.* Clinical microbiology reviews, 2009. **22**(2): p. 240-273.
111. Srikrishna, G. and H.H. Freeze, *Endogenous damage-associated molecular pattern molecules at the crossroads of inflammation and cancer.* Neoplasia, 2009. **11**(7): p. 615-628.
112. Taniguchi, N., et al., *High mobility group box chromosomal protein 1 plays a role in the pathogenesis of rheumatoid arthritis as a novel cytokine.* Arthritis & Rheumatism, 2003. **48**(4): p. 971-981.
113. Porto, A., et al., *Smooth muscle cells in human atherosclerotic plaques secrete and proliferate in response to high mobility group box 1 protein.* The FASEB Journal, 2006. **20**(14): p. 2565-2566.
114. Popovic, K., et al., *Increased expression of the novel proinflammatory cytokine high mobility group box chromosomal protein 1 in skin lesions of patients with lupus erythematosus.* Arthritis & Rheumatism, 2005. **52**(11): p. 3639-3645.
115. Hanke, M.L. and T. Kielian, *Toll-like receptors in health and disease in the brain: mechanisms and therapeutic potential.* Clinical Science, 2011. **121**(9): p. 367-387.
116. Zhang, Z., et al., *Immunolocalization of Toll-like receptors 2 and 4 as well as their endogenous ligand, heat shock protein 70, in rat traumatic brain injury.* Neuroimmunomodulation, 2011. **19**(1): p. 10-19.
117. Laird, M.D., et al., *High mobility group box protein‐1 promotes cerebral edema after traumatic brain injury via activation of toll‐like receptor 4.* Glia, 2014. **62**(1): p. 26-38.
118. O'Neill, L.A., F.J. Sheedy, and C.E. McCoy, *MicroRNAs: the fine-tuners of Toll-like receptor signalling.* Nature Reviews Immunology, 2011. **11**(3): p. 163-175.
119. Ruggiero, T., et al., *LPS induces KH-type splicing regulatory protein-dependent processing of microRNA-155 precursors in macrophages.* The FASEB Journal, 2009. **23**(9): p. 2898-2908.
120. Taganov, K.D., et al., *NF-κB-dependent induction of microRNA miR-146, an inhibitor targeted to signaling proteins of innate immune responses.* Proceedings of the National Academy of Sciences, 2006. **103**(33): p. 12481-12486.

121. Ceppi, M., et al., *MicroRNA-155 modulates the interleukin-1 signaling pathway in activated human monocyte-derived dendritic cells.* Proceedings of the National Academy of Sciences, 2009. **106**(8): p. 2735-2740.
122. Worm, J., et al., *Silencing of microRNA-155 in mice during acute inflammatory response leads to derepression of c/ebp Beta and down-regulation of G-CSF.* Nucleic acids research, 2009. **37**(17): p. 5784-5792.
123. Costinean, S., et al., *Src homology 2 domain–containing inositol-5-phosphatase and CCAAT enhancer-binding protein β are targeted by miR-155 in B cells of Eμ-MiR-155 transgenic mice.* Blood, 2009. **114**(7): p. 1374-1382.
124. Jennewein, C., et al., *MicroRNA-27b contributes to lipopolysaccharide-mediated peroxisome proliferator-activated receptor γ (PPARγ) mRNA destabilization.* Journal of Biological Chemistry, 2010. **285**(16): p. 11846-11853.
125. Lagos, D., et al., *miR-132 regulates antiviral innate immunity through suppression of the p300 transcriptional co-activator.* Nature cell biology, 2010. **12**(5): p. 513-519.
126. O'Connell, R.M., et al., *Inositol phosphatase SHIP1 is a primary target of miR-155.* Proceedings of the National Academy of Sciences, 2009. **106**(17): p. 7113-7118.
127. An, H., et al., *Src homology 2 domain-containing inositol-5-phosphatase 1 (SHIP1) negatively regulates TLR4-mediated LPS response primarily through a phosphatase activity-and PI-3K-independent mechanism.* Blood, 2005. **105**(12): p. 4685-4692.
128. Boldin, M.P., et al., *miR-146a is a significant brake on autoimmunity, myeloproliferation, and cancer in mice.* The Journal of experimental medicine, 2011. **208**(6): p. 1189-1201.
129. Bhela, S., et al., *Critical role of microRNA-155 in herpes simplex encephalitis.* J Immunol, 2014. **192**(6): p. 2734-43.
130. Iwai, H., et al., *MicroRNA-155 knockout mice are susceptible to Mycobacterium tuberculosis infection.* Tuberculosis (Edinb), 2015. **95**(3): p. 246-50.
131. Eisenhardt, S.U., et al., *MicroRNA-155 aggravates ischemia-reperfusion injury by modulation of inflammatory cell recruitment and the respiratory oxidative burst.* Basic Res Cardiol, 2015. **110**(3): p. 32.
132. Du, F., et al., *MicroRNA-155 Deficiency Results in Decreased Macrophage Inflammation and Attenuated Atherogenesis in Apolipoprotein E–Deficient Mice.* Arteriosclerosis, thrombosis, and vascular biology, 2014. **34**(4): p. 759-767.
133. Cardoso, A.L., et al., *miR‐155 modulates microglia‐mediated immune response by down‐regulating SOCS‐1 and promoting cytokine and nitric oxide production.* Immunology, 2012. **135**(1): p. 73-88.
134. O'Connell, R.M., et al., *MicroRNA-155 is induced during the macrophage inflammatory response.* Proceedings of the National Academy of Sciences, 2007. **104**(5): p. 1604-1609.
135. Butovsky, O., et al., *Targeting miR‐155 restores abnormal microglia and attenuates disease in SOD1 mice.* Annals of neurology, 2015. **77**(1): p. 75-99.

136. Guedes, J.R., et al., *Early miR-155 upregulation contributes to neuroinflammation in Alzheimer's disease triple transgenic mouse model.* Human molecular genetics, 2014. **23**(23): p. 6286-6301.
137. Thome, A.D., et al., *microRNA-155 Regulates Alpha-Synuclein-Induced Inflammatory Responses in Models of Parkinson Disease.* J Neurosci, 2016. **36**(8): p. 2383-90.
138. Ponomarev, E.D., et al., *MicroRNA-124 promotes microglia quiescence and suppresses EAE by deactivating macrophages via the C/EBP-[alpha]-PU. 1 pathway.* Nature medicine, 2011. **17**(1): p. 64-70.
139. Iyer, A., et al., *MicroRNA-146a: a key regulator of astrocyte-mediated inflammatory response.* PloS one, 2012. **7**(9): p. e44789.
140. Tarassishin, L., et al., *Interferon regulatory factor 3 inhibits astrocyte inflammatory gene expression through suppression of the proinflammatory miR‐155 and miR‐155*.* Glia, 2011. **59**(12): p. 1911-1922.
141. Bhalala, O.G., et al., *microRNA-21 regulates astrocytic response following spinal cord injury.* J Neurosci, 2012. **32**(50): p. 17935-47.
142. Suarez, Y., et al., *Cutting edge: TNF-induced microRNAs regulate TNF-induced expression of E-selectin and intercellular adhesion molecule-1 on human endothelial cells: feedback control of inflammation.* J Immunol, 2010. **184**(1): p. 21-5.
143. Arner, E., et al., *Adipose tissue microRNAs as regulators of CCL2 production in human obesity.* Diabetes, 2012. **61**(8): p. 1986-93.
144. Lei, P., et al., *Microarray based analysis of microRNA expression in rat cerebral cortex after traumatic brain injury.* Brain Res, 2009. **1284**: p. 191-201.
145. Redell, J.B., Y. Liu, and P.K. Dash, *Traumatic brain injury alters expression of hippocampal microRNAs: potential regulators of multiple pathophysiological processes.* J Neurosci Res, 2009. **87**(6): p. 1435-48.
146. Liu, L., et al., *Traumatic brain injury dysregulates microRNAs to modulate cell signaling in rat hippocampus.* PLoS One, 2014. **9**(8): p. e103948.
147. Sun, T.Y., et al., *Expression profiling of microRNAs in hippocampus of rats following traumatic brain injury.* J Huazhong Univ Sci Technolog Med Sci, 2014. **34**(4): p. 548-53.
148. Meissner, L., et al., *Temporal Profile of MicroRNA Expression in Contused Cortex after Traumatic Brain Injury in Mice.* J Neurotrauma, 2015.
149. Hu, Z., et al., *Expression of miRNAs and their cooperative regulation of the pathophysiology in traumatic brain injury.* PLoS One, 2012. **7**(6): p. e39357.
150. Redell, J.B., J. Zhao, and P.K. Dash, *Altered expression of miRNA‐21 and its targets in the hippocampus after traumatic brain injury.* Journal of neuroscience research, 2011. **89**(2): p. 212-221.
151. Han, Z., et al., *miR-21 alleviated apoptosis of cortical neurons through promoting PTEN-Akt signaling pathway in vitro after experimental traumatic brain injury.* Brain research, 2014. **1582**: p. 12-20.
152. Ge, X.T., et al., *miR-21 improves the neurological outcome after traumatic brain injury in rats.* Sci Rep, 2014. **4**: p. 6718.

153. Ge, X., et al., *MiR-21 alleviates secondary blood-brain barrier damage after traumatic brain injury in rats.* Brain Res, 2015. **1603**: p. 150-7.
154. Sandhir, R., E. Gregory, and N.E. Berman, *Differential response of miRNA-21 and its targets after traumatic brain injury in aging mice.* Neurochemistry international, 2014. **78**: p. 117-121.
155. Truettner, J.S., et al., *Therapeutic hypothermia alters microRNA responses to traumatic brain injury in rats.* Journal of Cerebral Blood Flow & Metabolism, 2011. **31**(9): p. 1897-1907.
156. Peterson, K., S. Carson, and N. Carney, *Hypothermia treatment for traumatic brain injury: a systematic review and meta-analysis.* Journal of neurotrauma, 2008. **25**(1): p. 62-71.
157. Marion, D.W., et al., *Treatment of traumatic brain injury with moderate hypothermia.* New England Journal of Medicine, 1997. **336**(8): p. 540-546.
158. Wang, W.X., et al., *Mitochondria-associated microRNAs in rat hippocampus following traumatic brain injury.* Exp Neurol, 2015. **265**: p. 84-93.
159. Yokobori, S., et al., *Biomarkers for the clinical differential diagnosis in traumatic brain injury—a systematic review.* CNS neuroscience & therapeutics, 2013. **19**(8): p. 556-565.
160. Redell, J.B., et al., *Human traumatic brain injury alters plasma microRNA levels.* Journal of neurotrauma, 2010. **27**(12): p. 2147-2156.
161. Mattson, M.P. and S.W. Scheff, *Endogenous neuroprotection factors and traumatic brain injury: mechanisms of action and implications for therapy.* J Neurotrauma, 1994. **11**(1): p. 3-33.
162. Smith, D.H., et al., *A model of parasagittal controlled cortical impact in the mouse: cognitive and histopathologic effects.* J Neurotrauma, 1995. **12**(2): p. 169-78.
163. Dagan, L.N., et al., *miR-155 regulates HGAL expression and increases lymphoma cell motility.* Blood, 2012. **119**(2): p. 513-520.
164. Ma, X., et al., *Loss of the miR-21 allele elevates the expression of its target genes and reduces tumorigenesis.* Proc Natl Acad Sci U S A, 2011. **108**(25): p. 10144-9.
165. Pan, Y.W., et al., *Inducible and conditional deletion of extracellular signal-regulated kinase 5 disrupts adult hippocampal neurogenesis.* J Biol Chem, 2012. **287**(28): p. 23306-17.
166. Farley, F.W., et al., *Widespread recombinase expression using FLPeR (flipper) mice.* Genesis, 2000. **28**(3-4): p. 106-10.
167. Yelamanchili, S.V., et al., *Upregulation of cathepsin D in the caudate nucleus of primates with experimental parkinsonism.* Mol Neurodegener, 2011. **6**: p. 52.
168. Chaudhuri, A.D., S.V. Yelamanchili, and H.S. Fox, *Combined fluorescent in situ hybridization for detection of microRNAs and immunofluorescent labeling for cell-type markers.* Front Cell Neurosci, 2013. **7**: p. 160.
169. Schneider, C.A., W.S. Rasband, and K.W. Eliceiri, *NIH Image to ImageJ: 25 years of image analysis.* Nat methods, 2012. **9**(7): p. 671-675.
170. O'Connor, C., et al., *Effects of daily versus weekly testing and pre-training on the assessment of neurologic impairment following diffuse traumatic brain injury in rats.* J Neurotrauma, 2003. **20**(10): p. 985-93.

171. Heisler, L.K., et al., *Elevated anxiety and antidepressant-like responses in serotonin 5-HT1A receptor mutant mice.* Proc Natl Acad Sci U S A, 1998. **95**(25): p. 15049-54.
172. Flierl, M.A., et al., *Mouse closed head injury model induced by a weight-drop device.* Nat Protoc, 2009. **4**(9): p. 1328-37.
173. Yelamanchili, S.V., et al., *The evolutionary young miR-1290 favors mitotic exit and differentiation of human neural progenitors through altering the cell cycle proteins.* Cell Death Dis, 2014. **5**: p. e982.
174. Reiner, B., et al., *Platelet-activating factor attenuation of long-term potentiation in rat hippocampal slices via protein tyrosine kinase signaling.* Neurosci Lett, 2016. **615**: p. 83-7.
175. Beaudoin, G.M., 3rd, et al., *Culturing pyramidal neurons from the early postnatal mouse hippocampus and cortex.* Nat Protoc, 2012. **7**(9): p. 1741-54.
176. Crescitelli, R., et al., *Distinct RNA profiles in subpopulations of extracellular vesicles: apoptotic bodies, microvesicles and exosomes.* J Extracell Vesicles, 2013. **2**.
177. Yelamanchili, S.V., et al., *MiR-21 in Extracellular Vesicles Leads to Neurotoxicity via TLR7 Signaling in SIV Neurological Disease.* PLoS Pathog, 2015. **11**(7): p. e1005032.
178. Perez-Gonzalez, R., et al., *The exosome secretory pathway transports amyloid precursor protein carboxyl-terminal fragments from the cell into the brain extracellular space.* J Biol Chem, 2012. **287**(51): p. 43108-15.
179. Helmy, A., et al., *Cytokines and innate inflammation in the pathogenesis of human traumatic brain injury.* Prog Neurobiol, 2011. **95**(3): p. 352-72.
180. O'Connell, R.M., D.S. Rao, and D. Baltimore, *microRNA regulation of inflammatory responses.* Annu Rev Immunol, 2012. **30**: p. 295-312.
181. Singh, R.P., et al., *The role of miRNA in inflammation and autoimmunity.* Autoimmun Rev, 2013. **12**(12): p. 1160-5.
182. Buscaglia, L.E.B. and Y. Li, *Apoptosis and the target genes of miR-21.* Chinese journal of cancer, 2011. **30**(6): p. 371.
183. Gironella, M., et al., *Tumor protein 53-induced nuclear protein 1 expression is repressed by miR-155, and its restoration inhibits pancreatic tumor development.* Proc Natl Acad Sci U S A, 2007. **104**(41): p. 16170-5.
184. Ovcharenko, D., et al., *Genome-scale microRNA and small interfering RNA screens identify small RNA modulators of TRAIL-induced apoptosis pathway.* Cancer Res, 2007. **67**(22): p. 10782-8.
185. Cole, J.T., et al., *Craniotomy: true sham for traumatic brain injury, or a sham of a sham?* J Neurotrauma, 2011. **28**(3): p. 359-69.
186. Lagraoui, M., et al., *Controlled cortical impact and craniotomy induce strikingly similar profiles of inflammatory gene expression, but with distinct kinetics.* Front Neurol, 2012. **3**: p. 155.
187. Shojo, H. and K. Kibayashi, *Changes in localization of synaptophysin following fluid percussion injury in the rat brain.* Brain Res, 2006. **1078**(1): p. 198-211.
188. Lovas, G., et al., *Axonal changes in chronic demyelinated cervical spinal cord plaques.* Brain, 2000. **123**(2): p. 308-317.

189. Wang, G., et al., *Microglia/macrophage polarization dynamics in white matter after traumatic brain injury.* J Cereb Blood Flow Metab, 2013. **33**(12): p. 1864-74.
190. Helmy, A., et al., *The cytokine response to human traumatic brain injury: temporal profiles and evidence for cerebral parenchymal production.* J Cereb Blood Flow Metab, 2011. **31**(2): p. 658-70.
191. Kelso, M.L., et al., *Granulocyte-macrophage colony stimulating factor exerts protective and immunomodulatory effects in cortical trauma.* J Neuroimmunol, 2015. **278**: p. 162-73.
192. Li, X., F. Tian, and F. Wang, *Rheumatoid arthritis-associated microRNA-155 targets SOCS1 and upregulates TNF-alpha and IL-1beta in PBMCs.* Int J Mol Sci, 2013. **14**(12): p. 23910-21.
193. Loffler, D., et al., *Interleukin-6 dependent survival of multiple myeloma cells involves the Stat3-mediated induction of microRNA-21 through a highly conserved enhancer.* Blood, 2007. **110**(4): p. 1330-3.
194. Washington, P.M., et al., *The effect of injury severity on behavior: a phenotypic study of cognitive and emotional deficits after mild, moderate, and severe controlled cortical impact injury in mice.* J Neurotrauma, 2012. **29**(13): p. 2283-96.
195. Chen, G., et al., *miR-146a inhibits cell growth, cell migration and induces apoptosis in non-small cell lung cancer cells.* PLoS One, 2013. **8**(3): p. e60317.
196. Pan, Y., et al., *Platelet-secreted microRNA-223 promotes endothelial cell apoptosis induced by advanced glycation end products via targeting the insulin-like growth factor 1 receptor.* The Journal of Immunology, 2014. **192**(1): p. 437-446.
197. Clark, R.S., et al., *Caspase‐3 mediated neuronal death after traumatic brain injury in rats.* Journal of neurochemistry, 2000. **74**(2): p. 740-753.
198. Knoblach, S.M., et al., *Multiple caspases are activated after traumatic brain injury: evidence for involvement in functional outcome.* Journal of neurotrauma, 2002. **19**(10): p. 1155-1170.
199. Yorke, C.H., Jr. and V.S. Caviness, Jr., *Interhemispheric neocortical connections of the corpus callosum in the normal mouse: a study based on anterograde and retrograde methods.* J Comp Neurol, 1975. **164**(2): p. 233-45.
200. Saba, R., et al., *MicroRNA 146a (miR-146a) is over-expressed during prion disease and modulates the innate immune response and the microglial activation state.* PLoS One, 2012. **7**(2): p. e30832.
201. Strickland, I.T., et al., *Axotomy-induced miR-21 promotes axon growth in adult dorsal root ganglion neurons.* PLoS One, 2011. **6**(8): p. e23423.
202. Montalban, E., et al., *MiR-21 is an Ngf-modulated microRNA that supports Ngf signaling and regulates neuronal degeneration in PC12 cells.* Neuromolecular medicine, 2014. **16**(2): p. 415-430.
203. Sayed, D., et al., *MicroRNA-21 targets Sprouty2 and promotes cellular outgrowths.* Molecular biology of the cell, 2008. **19**(8): p. 3272-3282.

204. Izumi, B., et al., *MicroRNA-223 expression in neutrophils in the early phase of secondary damage after spinal cord injury.* Neuroscience letters, 2011. **492**(2): p. 114-118.
205. Carlos, T., et al., *Expression of endothelial adhesion molecules and recruitment of neutrophils after traumatic brain injury in rats.* Journal of leukocyte biology, 1997. **61**(3): p. 279-285.
206. Wang, P., et al., *Inducible microRNA-155 feedback promotes type I IFN signaling in antiviral innate immunity by targeting suppressor of cytokine signaling 1.* J Immunol, 2010. **185**(10): p. 6226-33.
207. Zhou, H., et al., *miR-155 and its star-form partner miR-155* cooperatively regulate type I interferon production by human plasmacytoid dendritic cells.* Blood, 2010. **116**(26): p. 5885-94.
208. Dufour, J.H., et al., *IFN-γ-inducible protein 10 (IP-10; CXCL10)-deficient mice reveal a role for IP-10 in effector T cell generation and trafficking.* The Journal of Immunology, 2002. **168**(7): p. 3195-3204.
209. Nakagawa, R., et al., *SOCS-1 participates in negative regulation of LPS responses.* Immunity, 2002. **17**(5): p. 677-87.
210. Cardoso, A.L., et al., *miR-155 modulates microglia-mediated immune response by down-regulating SOCS-1 and promoting cytokine and nitric oxide production.* Immunology, 2012. **135**(1): p. 73-88.
211. Guedes, J.R., et al., *Early miR-155 upregulation contributes to neuroinflammation in Alzheimer's disease triple transgenic mouse model.* Hum Mol Genet, 2014.
212. Butovsky, O., et al., *Targeting miR-155 restores dysfunctional microglia and ameliorates disease in the SOD1 model of ALS.* Int J Dev Neurosci, 2015. **47**(Pt A): p. 5.
213. Woodbury, M.E., et al., *miR-155 Is Essential for Inflammation-Induced Hippocampal Neurogenic Dysfunction.* J Neurosci, 2015. **35**(26): p. 9764-81.
214. Takagi, Y., et al., *STAT1 is activated in neurons after ischemia and contributes to ischemic brain injury.* J Cereb Blood Flow Metab, 2002. **22**(11): p. 1311-8.
215. Klein, R.S., et al., *Neuronal CXCL10 directs CD8+ T-cell recruitment and control of West Nile virus encephalitis.* Journal of virology, 2005. **79**(17): p. 11457-11466.
216. Sui, Y., et al., *Neuronal apoptosis is mediated by CXCL10 overexpression in simian human immunodeficiency virus encephalitis.* The American journal of pathology, 2004. **164**(5): p. 1557-1566.
217. Nelson, T.E. and D.L. Gruol, *The chemokine CXCL10 modulates excitatory activity and intracellular calcium signaling in cultured hippocampal neurons.* Journal of neuroimmunology, 2004. **156**(1): p. 74-87.
218. Hall, E.D., et al., *Evolution of post-traumatic neurodegeneration after controlled cortical impact traumatic brain injury in mice and rats as assessed by the de Olmos silver and fluorojade staining methods.* Journal of neurotrauma, 2008. **25**(3): p. 235-247.
219. Antunes, M. and G. Biala, *The novel object recognition memory: neurobiology, test procedure, and its modifications.* Cogn Process, 2012. **13**(2): p. 93-110.

220. Siopi, E., et al., *Evaluation of late cognitive impairment and anxiety states following traumatic brain injury in mice: the effect of minocycline.* Neuroscience letters, 2012. **511**(2): p. 110-115.
221. Fromm, L., et al., *Magnesium attenuates post-traumatic depression/anxiety following diffuse traumatic brain injury in rats.* Journal of the American College of Nutrition, 2004. **23**(5): p. 529S-533S.
222. Kalueff, A.V. and P. Tuohimaa, *Experimental modeling of anxiety and depression.* Acta Neurobiol Exp (Wars), 2004. **64**(4): p. 439-48.
223. Varendi, K., et al., *miR-1, miR-10b, miR-155, and miR-191 are novel regulators of BDNF.* Cellular and Molecular Life Sciences, 2014. **71**(22): p. 4443-4456.
224. Alexander, W.S., et al., *SOCS1 is a critical inhibitor of interferon gamma signaling and prevents the potentially fatal neonatal actions of this cytokine.* Cell, 1999. **98**(5): p. 597-608.
225. Lopez-Ramirez, M.A., et al., *MicroRNA-155 negatively affects blood–brain barrier function during neuroinflammation.* The FASEB Journal, 2014. **28**(6): p. 2551-2565.
226. Israelsson, C., et al., *Appearance of Cxcl10 – expressing cell clusters is common for traumatic brain injury and neurodegenerative disorders.* European Journal of Neuroscience, 2010. **31**(5): p. 852-863.
227. Steffensen, M.A., et al., *Suppressors of cytokine signaling 1 and 3 are upregulated in brain resident cells in response to virus-induced inflammation of the central nervous system via at least two distinctive pathways.* J Virol, 2014. **88**(24): p. 14090-104.
228. Fonken, L.K., et al., *MicroRNA-155 deletion reduces anxiety-and depressive-like behaviors in mice.* Psychoneuroendocrinology, 2016. **63**: p. 362-369.
229. Valentine, A.D., et al. *Mood and cognitive side effects of interferon-alpha therapy*. in *Seminars in oncology*. 1998.
230. Bianchi, M.E., *DAMPs, PAMPs and alarmins: all we need to know about danger.* Journal of leukocyte biology, 2007. **81**(1): p. 1-5.
231. Yelamanchili, S.V., et al., *MicroRNA-21 dysregulates the expression of MEF2C in neurons in monkey and human SIV/HIV neurological disease.* Cell Death Dis, 2010. **1**: p. e77.
232. Li, M., et al., *Generation of purified neural precursors from embryonic stem cells by lineage selection.* Current biology, 1998. **8**(17): p. 971-S2.
233. Sakai, A. and H. Suzuki, *Nerve injury-induced upregulation of miR-21 in the primary sensory neurons contributes to neuropathic pain in rats.* Biochem Biophys Res Commun, 2013. **435**(2): p. 176-81.
234. Strickland, I.T., et al., *Axotomy-induced miR-21 promotes axon growth in adult dorsal root ganglion neurons.* PLoS One, 2011. **6**(8): p. e23423.
235. Bellingham, S.A., B.M. Coleman, and A.F. Hill, *Small RNA deep sequencing reveals a distinct miRNA signature released in exosomes from prion-infected neuronal cells.* Nucleic Acids Res, 2012. **40**(21): p. 10937-49.
236. Ziu, M., et al., *Temporal differences in microRNA expression patterns in astrocytes and neurons after ischemic injury.* PLoS One, 2011. **6**(2): p. e14724.

237. Buller, B., et al., *MicroRNA-21 protects neurons from ischemic death.* FEBS J, 2010. **277**(20): p. 4299-307.
238. Zhang, L., et al., *miR-21 represses FasL in microglia and protects against microglia-mediated neuronal cell death following hypoxia/ischemia.* Glia, 2012. **60**(12): p. 1888-95.
239. Liu, F.J., et al., *microRNAs Involved in Regulating Spontaneous Recovery in Embolic Stroke Model.* PLoS One, 2013. **8**(6): p. e66393.
240. Deng, X., et al., *MiR-21 involve in ERK-mediated upregulation of MMP9 in the rat hippocampus following cerebral ischemia.* Brain Res Bull, 2013. **94**: p. 56-62.
241. Shi, Y., et al., *MiR-21 is continually elevated long-term in the brain after exposure to ionizing radiation.* Radiat Res, 2012. **177**(1): p. 124-8.
242. Redell, J.B., J. Zhao, and P.K. Dash, *Altered expression of miRNA-21 and its targets in the hippocampus after traumatic brain injury.* J Neurosci Res, 2011. **89**(2): p. 212-21.
243. Peng, J., et al., *Expression patterns of miR-124, miR-134, miR-132, and miR-21 in an immature rat model and children with mesial temporal lobe epilepsy.* J Mol Neurosci, 2013. **50**(2): p. 291-7.
244. Lescher, J., et al., *MicroRNA regulation in experimental autoimmune encephalomyelitis in mice and marmosets resembles regulation in human multiple sclerosis lesions.* J Neuroimmunol, 2012. **246**(1-2): p. 27-33.
245. Patterson, P.H., *The emerging neuropoietic cytokine family: first CDF/LIF, CNTF and IL-6; next ONC, MGF, GCSF?* Current opinion in neurobiology, 1992. **2**(1): p. 94-97.
246. Group, A.C.T.S., *A double‐blind placebo‐controlled clinical trial of subcutaneous recombinant human ciliary neurotrophic factor (rHCNTF) in amyotrophic lateral sclerosis.* Neurology, 1996. **46**(5): p. 1244-1244.
247. Yokogami, K., et al., *Serine phosphorylation and maximal activation of STAT3 during CNTF signaling is mediated by the rapamycin target mTOR.* Current Biology, 2000. **10**(1): p. 47-50.
248. Nakajima, K., et al., *A central role for Stat3 in IL-6-induced regulation of growth and differentiation in M1 leukemia cells.* The EMBO journal, 1996. **15**(14): p. 3651.
249. Hirota, H., et al., *Accelerated Nerve Regeneration in Mice by upregulated expression of interleukin (IL) 6 and IL-6 receptor after trauma.* The Journal of experimental medicine, 1996. **183**(6): p. 2627-2634.
250. Cui, Q., et al., *CNTF, not other trophic factors, promotes axonal regeneration of axotomized retinal ganglion cells in adult hamsters.* Investigative ophthalmology & visual science, 1999. **40**(3): p. 760-766.
251. Thier, M., et al., *Interleukin‐6 (IL‐6) and its soluble receptor support survival of sensory neurons.* Journal of neuroscience research, 1999. **55**(4): p. 411-422.
252. Sawada, M., et al., *Expression of cytokine receptors in cultured neuronal and glial cells.* Neuroscience letters, 1993. **160**(2): p. 131-134.

253. Numakawa, T., et al., *BDNF function and intracellular signaling in neurons.* Histol Histopathol, 2010. **25**(2): p. 237-58.
254. Schust, J., et al., *Stattic: a small-molecule inhibitor of STAT3 activation and dimerization.* Chemistry & biology, 2006. **13**(11): p. 1235-1242.
255. Zhang, J.G., et al., *MicroRNA-21 (miR-21) represses tumor suppressor PTEN and promotes growth and invasion in non-small cell lung cancer (NSCLC).* Clin Chim Acta, 2010. **411**(11-12): p. 846-52.
256. Sperow, M., et al., *Phosphatase and tensin homologue (PTEN) regulates synaptic plasticity independently of its effect on neuronal morphology and migration.* J Physiol, 2012. **590**(Pt 4): p. 777-92.
257. Backman, S.A., et al., *Deletion of Pten in mouse brain causes seizures, ataxia and defects in soma size resembling Lhermitte-Duclos disease.* Nature genetics, 2001. **29**(4): p. 396-403.
258. Han, Z., et al., *miR-21 alleviated apoptosis of cortical neurons through promoting PTEN-Akt signaling pathway in vitro after experimental traumatic brain injury.* Brain Res, 2014.
259. Montalban, E., et al., *MiR-21 is an Ngf-modulated microRNA that supports Ngf signaling and regulates neuronal degeneration in PC12 cells.* Neuromolecular Med, 2014. **16**(2): p. 415-30.
260. Doble, A., *The role of excitotoxicity in neurodegenerative disease: implications for therapy.* Pharmacology & therapeutics, 1999. **81**(3): p. 163-221.
261. White, M.J., M.J. DiCaprio, and D.A. Greenberg, *Assessment of neuronal viability with Alamar blue in cortical and granule cell cultures.* Journal of neuroscience methods, 1996. **70**(2): p. 195-200.
262. Kang, S.S., et al., *Loss of neuron-astroglial interaction rapidly induces protective CNTF expression after stroke in mice.* J Neurosci, 2012. **32**(27): p. 9277-87.
263. Park, C.Y., et al., *A resource for the conditional ablation of microRNAs in the mouse.* Cell reports, 2012. **1**(4): p. 385-391.
264. Calvo-Garrido, J., et al., *Vacuole membrane protein 1 is an endoplasmic reticulum protein required for organelle biogenesis, protein secretion, and development.* Mol Biol Cell, 2008. **19**(8): p. 3442-53.
265. Hirasawa, M., et al., *Neuron-specific expression of Cre recombinase during the late phase of brain development.* Neuroscience research, 2001. **40**(2): p. 125-132.
266. Dubois, N.C., et al., *Nestin‐Cre transgenic mouse line Nes‐Cre1 mediates highly efficient Cre/loxP mediated recombination in the nervous system, kidney, and somite‐derived tissues.* Genesis, 2006. **44**(8): p. 355-360.
267. Rohlmann, A., et al., *Sustained somatic gene inactivation by viral transfer of Cre recombinase.* Nature biotechnology, 1996. **14**(11): p. 1562-1565.
268. Patrick, D.M., et al., *Stress-dependent cardiac remodeling occurs in the absence of microRNA-21 in mice.* J Clin Invest, 2010. **120**(11): p. 3912-6.
269. Cheng, Y. and C. Zhang, *MicroRNA-21 in cardiovascular disease.* Journal of cardiovascular translational research, 2010. **3**(3): p. 251-255.

270. Brem, G. and B.H. Thoenen, *Disruption of the CNTF gene results in motor neuron degeneration.* Nature, 1993. **365**: p. 2.
271. Leaver, S.G., et al., *AAV-mediated expression of CNTF promotes long-term survival and regeneration of adult rat retinal ganglion cells.* Gene therapy, 2006. **13**(18): p. 1328-1341.
272. Kauper, K., et al., *Two-year intraocular delivery of ciliary neurotrophic factor by encapsulated cell technology implants in patients with chronic retinal degenerative diseases.* Invest Ophthalmol Vis Sci, 2012. **53**(12): p. 7484-91.
273. Woodcock, T. and M.C. Morganti-Kossmann, *The role of markers of inflammation in traumatic brain injury.* Front Neurol, 2013. **4**: p. 18.
274. Mittelbrunn, M., et al., *Unidirectional transfer of microRNA-loaded exosomes from T cells to antigen-presenting cells.* Nat Commun, 2011. **2**: p. 282.
275. Montecalvo, A., et al., *Mechanism of transfer of functional microRNAs between mouse dendritic cells via exosomes.* Blood, 2012. **119**(3): p. 756-66.
276. Fabbri, M., et al., *MicroRNAs bind to Toll-like receptors to induce prometastatic inflammatory response.* Proc Natl Acad Sci U S A, 2012. **109**(31): p. E2110-6.
277. Thery, C., M. Ostrowski, and E. Segura, *Membrane vesicles as conveyors of immune responses.* Nat Rev Immunol, 2009. **9**(8): p. 581-93.
278. Valadi, H., et al., *Exosome-mediated transfer of mRNAs and microRNAs is a novel mechanism of genetic exchange between cells.* Nat Cell Biol, 2007. **9**(6): p. 654-9.
279. Faden, A.I., et al., *Progressive inflammation-mediated neurodegeneration after traumatic brain or spinal cord injury.* Br J Pharmacol, 2016. **173**(4): p. 681-91.
280. Lehmann, S.M., et al., *An unconventional role for miRNA: let-7 activates Toll-like receptor 7 and causes neurodegeneration.* Nat Neurosci, 2012. **15**(6): p. 827-35.
281. Liu, H.Y., et al., *The microRNAs Let7c and miR21 are recognized by neuronal Toll-like receptor 7 to restrict dendritic growth of neurons.* Exp Neurol, 2015. **269**: p. 202-12.
282. Forsbach, A., et al., *Identification of RNA sequence motifs stimulating sequence-specific TLR8-dependent immune responses.* J Immunol, 2008. **180**(6): p. 3729-38.
283. Sandhir, R., E. Gregory, and N.E. Berman, *Differential response of miRNA-21 and its targets after traumatic brain injury in aging mice.* Neurochem Int, 2014.
284. Han, Z., et al., *miR-21 alleviated apoptosis of cortical neurons through promoting PTEN-Akt signaling pathway in vitro after experimental traumatic brain injury.* Brain Res, 2014. **1582**: p. 12-20.
285. Bhalala, O.G., M. Srikanth, and J.A. Kessler, *The emerging roles of microRNAs in CNS injuries.* Nat Rev Neurol, 2013. **9**(6): p. 328-39.
286. Patz, S., et al., *More than cell dust: microparticles isolated from cerebrospinal fluid of brain injured patients are messengers carrying mRNAs, miRNAs, and proteins.* J Neurotrauma, 2013. **30**(14): p. 1232-42.
287. Kraft-Terry, S.D., et al., *A coat of many colors: neuroimmune crosstalk in human immunodeficiency virus infection.* Neuron, 2009. **64**(1): p. 133-145.

288. Hu, G., et al., *Exosome-mediated shuttling of microRNA-29 regulates HIV Tat and morphine-mediated neuronal dysfunction.* Cell Death Dis, 2012. **3**: p. e381.
289. Crozat, K. and B. Beutler, *TLR7: A new sensor of viral infection.* Proc Natl Acad Sci U S A, 2004. **101**(18): p. 6835-6.
290. Taganov, K.D., et al., *NF-kappaB-dependent induction of microRNA miR-146, an inhibitor targeted to signaling proteins of innate immune responses.* Proc Natl Acad Sci U S A, 2006. **103**(33): p. 12481-6.
291. Boldin, M.P., et al., *miR-146a is a significant brake on autoimmunity, myeloproliferation, and cancer in mice.* J Exp Med, 2011. **208**(6): p. 1189-201.
292. Alexander, M., et al., *Exosome-delivered microRNAs modulate the inflammatory response to endotoxin.* Nat Commun, 2015. **6**: p. 7321.
293. Choi, D.C., et al., *MicroRNA-7 protects against 1-methyl-4-phenylpyridinium-induced cell death by targeting RelA.* J Neurosci, 2014. **34**(38): p. 12725-37.
294. Choudhury, N.R., et al., *Tissue-specific control of brain-enriched miR-7 biogenesis.* Genes Dev, 2013. **27**(1): p. 24-38.
295. Wanet, A., et al., *miR-212/132 expression and functions: within and beyond the neuronal compartment.* Nucleic Acids Res, 2012. **40**(11): p. 4742-53.
296. Zhang, Z., et al., *MicroRNAs: potential regulators involved in human anencephaly.* Int J Biochem Cell Biol, 2010. **42**(2): p. 367-74.
297. Kim, A.H., et al., *MicroRNA expression profiling in the prefrontal cortex of individuals affected with schizophrenia and bipolar disorders.* Schizophr Res, 2010. **124**(1-3): p. 183-91.
298. Wang, W.X., et al., *Patterns of microRNA expression in normal and early Alzheimer's disease human temporal cortex: white matter versus gray matter.* Acta Neuropathol, 2011. **121**(2): p. 193-205.
299. Zhao, Z., et al., *Comparing the predictive value of multiple cognitive, affective, and motor tasks after rodent traumatic brain injury.* J Neurotrauma, 2012. **29**(15): p. 2475-89.
300. Tong, J., et al., *Inhibition of Nogo-66 receptor 1 enhances recovery of cognitive function after traumatic brain injury in mice.* J Neurotrauma, 2013. **30**(4): p. 247-58.
301. Carola, V., et al., *Evaluation of the elevated plus-maze and open-field tests for the assessment of anxiety-related behaviour in inbred mice.* Behav Brain Res, 2002. **134**(1-2): p. 49-57.
302. Kulkarni, S.K., K. Singh, and M. Bishnoi, *Elevated zero maze: a paradigm to evaluate antianxiety effects of drugs.* Methods Find Exp Clin Pharmacol, 2007. **29**(5): p. 343-8.
303. Cryan, J.F., C. Mombereau, and A. Vassout, *The tail suspension test as a model for assessing antidepressant activity: review of pharmacological and genetic studies in mice.* Neurosci Biobehav Rev, 2005. **29**(4-5): p. 571-625.
304. Steru, L., et al., *The tail suspension test: a new method for screening antidepressants in mice.* Psychopharmacology (Berl), 1985. **85**(3): p. 367-70.
305. Kaidanovich-Beilin, O., et al., *Assessment of social interaction behaviors.* J Vis Exp, 2011(48).

306. Hsieh, C.L., et al., *CCR2 deficiency impairs macrophage infiltration and improves cognitive function after traumatic brain injury.* J Neurotrauma, 2014. **31**(20): p. 1677-88.
307. Homsi, S., et al., *Blockade of acute microglial activation by minocycline promotes neuroprotection and reduces locomotor hyperactivity after closed head injury in mice: a twelve-week follow-up study.* J Neurotrauma, 2010. **27**(5): p. 911-21.
308. Siopi, E., et al., *Etazolate, an alpha-secretase activator, reduces neuroinflammation and offers persistent neuroprotection following traumatic brain injury in mice.* Neuropharmacology, 2013. **67**: p. 183-92.
309. Luo, J., et al., *Long-term cognitive impairments and pathological alterations in a mouse model of repetitive mild traumatic brain injury.* Front Neurol, 2014. **5**: p. 12.
310. Elliott, M.B., et al., *Acute effects of a selective cannabinoid-2 receptor agonist on neuroinflammation in a model of traumatic brain injury.* J Neurotrauma, 2011. **28**(6): p. 973-81.
311. Starkstein, S.E. and R.G. Robinson, *Mechanism of disinhibition after brain lesions.* J Nerv Ment Dis, 1997. **185**(2): p. 108-14.
312. Crane, A.T., K.D. Fink, and J.S. Smith, *The effects of acute voluntary wheel running on recovery of function following medial frontal cortical contusions in rats.* Restor Neurol Neurosci, 2012. **30**(4): p. 325-33.
313. Bondi, C.O., et al., *Old dog, new tricks: the attentional set-shifting test as a novel cognitive behavioral task after controlled cortical impact injury.* J Neurotrauma, 2014. **31**(10): p. 926-37.
314. Malkesman, O., et al., *Traumatic brain injury - modeling neuropsychiatric symptoms in rodents.* Front Neurol, 2013. **4**: p. 157.
315. Siopi, E., et al., *Evaluation of late cognitive impairment and anxiety states following traumatic brain injury in mice: the effect of minocycline.* Neurosci Lett, 2012. **511**(2): p. 110-5.
316. Shultz, S.R., et al., *Repeated mild lateral fluid percussion brain injury in the rat causes cumulative long-term behavioral impairments, neuroinflammation, and cortical loss in an animal model of repeated concussion.* J Neurotrauma, 2012. **29**(2): p. 281-94.
317. Semple, B.D., S.A. Canchola, and L.J. Noble-Haeusslein, *Deficits in social behavior emerge during development after pediatric traumatic brain injury in mice.* J Neurotrauma, 2012. **29**(17): p. 2672-83.
318. Konigs, M., et al., *Pediatric Traumatic Brain Injury and Attention Deficit.* Pediatrics, 2015.
319. Thounaojam, M.C., D.K. Kaushik, and A. Basu, *MicroRNAs in the brain: it's regulatory role in neuroinflammation.* Mol Neurobiol, 2013. **47**(3): p. 1034-44.
320. Khudayberdiev, S.A., et al., *A comprehensive characterization of the nuclear microRNA repertoire of post-mitotic neurons.* Front Mol Neurosci, 2013. **6**: p. 43.
321. Bhalala, O.G., M. Srikanth, and J.A. Kessler, *The emerging roles of microRNAs in CNS injuries.* Nature Reviews Neurology, 2013. **9**(6): p. 328-339.

322. Deb, S., et al., *Rate of psychiatric illness 1 year after traumatic brain injury.* Am J Psychiatry, 1999. **156**(3): p. 374-8.
323. Fann, J.R., et al., *Psychiatric illness following traumatic brain injury in an adult health maintenance organization population.* Arch Gen Psychiatry, 2004. **61**(1): p. 53-61.
324. DeNardo, L.A., et al., *Connectivity of mouse somatosensory and prefrontal cortex examined with trans-synaptic tracing.* Nat Neurosci, 2015. **18**(11): p. 1687-97.